2015

Numerical Investigation of Steady-State and Transient Operations of a Turbocharged SI Engine with Electric Supercharger

Ivan Filidoro
University of Windsor

Numerical Investigation of Steady-State and Transient Operations of a Turbocharged SI Engine with Electric Supercharger

By

Ivan Filidoro

A Thesis
Submitted to the Faculty of Graduate Studies
through the Department of Mechanical, Automotive & Materials Engineering
in Partial Fulfillment of the Requirements for
the Degree of Master of Applied Science
at the University of Windsor

Windsor, Ontario, Canada

2015

Numerical Investigation of Steady-State and Transient Operations of a Turbocharged SI Engine with Electric Supercharger

by

Ivan Filidoro

APPROVED BY:

_____

Dr. R. Balachandar
Department of Civil and Environmental Engineering

_____

Dr. D. Ting
Department of Mechanical, Automotive & Materials Engineering

_____

Dr. A. Sobiesiak, Advisor
Department of Mechanical, Automotive & Materials Engineering

July 28, 2015

DECLARATION OF ORIGINALITY

I hereby certify that I am the sole author of this thesis and that no part of this thesis has been published or submitted for publication.

I certify that, to the best of my knowledge, my thesis does not infringe upon anyone's copyright nor violate any proprietary rights and that any ideas, techniques, quotations, or any other material from the work of other people included in my thesis, published or otherwise, are fully acknowledged in accordance with the standard referencing practices. Furthermore, to the extent that I have included copyrighted material that surpasses the bounds of fair dealing within the meaning of the Canada Copyright Act, I certify that I have obtained a written permission from the copyright owner(s) to include such material(s) in my thesis and have included copies of such copyright clearances to my appendix.

I declare that this is a true copy of my thesis, including any final revisions, as approved by my thesis committee and the Graduate Studies office, and that this thesis has not been submitted for a higher degree to any other University or Institution.

ABSTRACT

Gasoline engine downsizing, associated with turbocharging, has proved to be one of the most effective ways to reduce specific fuel consumption of the internal combustion engine. This tendency introduces a number of technical challenges, such as reduced steady-state low speed torque, delay in transient response caused by the turbocharger, combustion limitations due to propensity to knock. Advanced boosting systems can succeed in overcoming these issues; of particular interest is the solution featuring a second, electrically-driven, compressor in series with the turbocharger compressor. The engine considered in this work is a four-cylinder inline, turbocharged and electrically supercharged engine by FCA. In this work a 1D simulation of the mentioned engine is performed with and without the use of the electric supercharger in order to analyze its effect on steady-state and transient performance. The exploited software is GT-Power Version 7.4, by Gamma Technologies.

DEDICATION

To my parents, Maria Pia and Peppe

ACKNOWLEDGEMENTS

This thesis is the culmination of a two year Double Degree Master program that was possible only thanks to the collaboration and organization efforts of two universities, University of Windsor and Politecnico di Torino, and a leading group in the automotive sector, Fiat Chrysler Automobiles.
Therefore I would like to express my deepest appreciation to the persons who representing the aforementioned institutions played a very important role in coordinating this ambitious program, Dr. Andrzej Sobiesiak from University of Windsor, Prof. Giovanni Belingardi from Politecnico di Torino, Edoardo Rabino from FCA Italy and Mohammed Malik and Ishika Towfic from FCA Canada.

I offer my sincere gratitude to my academic advisors Dr. Andrzej Sobiesiak, Prof. Daniela Misul and Prof. Ezio Spessa that have supervised my activities and offered their support throughout my thesis project, while allowing me to make my own choices.
I wish also to express my gratitude to my industrial supervisors for the assistance they gave me; Andrea Gerini and Vittorio Doria from Centro Ricerche Fiat, Ron Reese, Saad Umer and Bo Yang from Chrysler Technical Center.

I am profoundly thankful to my parents; they have always morally supported me and economically sustained me throughout my studies. Moreover, without their education, I would never have achieved my academic successes.
I want to reserve the most important thanks to my big sister, Maura. She always encouraged me to pursue the most ambitious goals.
Finally, special thanks goes to my colleagues, housemates and friends who shared with me this unique experience, Biagio, Fabio, Francesco and Sergio.

TABLE OF CONTENTS

LIST OF TABLES

LIST OF FIGURES

LIST OF ABBREVIATIONS

Abbreviations

0D	Zero dimensional
1D	Mono dimensional
2D	Two dimensional
3D	Three dimensional
BDC	Bottom Dead Center
BMEP	Brake Mean Effective Pressure
BSFC	Brake Specific Fuel Consumption
CA	Crank Angle
CAD	Computer Aided Design
CAI	Controlled Auto Ignition
cc	Cubic centimeters
CFD	Computational Fluid Dynamics
CI	Compression Ignition
CO	Carbon monoxide
CO_2	Carbon dioxide
CPU	Central Processing Unit
CR	Compression Ratio
CTC	Chrysler Technical Center
EGR	Exhaust Gas Recirculation
EIVC	Early Intake Valve Closing
EPA	Environmental Protection Agency
ES	Electric Supercharger
EU	European Union
EV	Electric vehicle
FCA	Fiat Chrysler Automobiles
FMEP	Friction Mean Effective Pressure
GDI	Gasoline Direct Injection
GT	Gamma Technologies
h	Hour
H_2O	Water
HC	Hydrocarbon
HCCI	Homogeneous Charge Compression Ignition
HEV	Hybrid electric vehicle
HP	Horsepower
IMEP	Indicated Mean Effective Pressure
J	Joule

K	Kelvin
kg	Kilograms
l	Liter
LIVC	Late Intake Valve Closing
LP	Low Pressure
m	Meter
min	Minute
mpg	Miles Per Gallon
NA	Naturally Aspirated
NEDC	New European Driving Cycle
NO_X	Nitrogen Oxides
O_2	Oxygen
Pa	Pascal
PID	Proportional Integral Derivative
PM	Particulate Matter
ppm	Part Per Million
P-V	Pressure-volume
RPM	Revolution Per Minute
SC	Supercharger
SI	Spark Ignition
TC	Turbocharger
TDC	Top Dead Center
TVO	Throttle Valve Opening
UC	Ultra Capacitors
VVA	Variable Valve Actuation
VVT	Variable Valve Timing
W	Watt
WG	Wastegate valve
WOT	Wide Open Throttle

NOMENCLATURE

Symbols

A_e	Flame area
$BMEP_{max,EB}$	Maximum BMEP when electric supercharger is active
$BMEP_{max,NO\ EB}$	Maximum BMEP without electric supercharger
$BMEP_{MT}$	BMEP level for maximum throttle opening
CA50	50% burned crank angle
c_p	Specific heat at constant pressure
ECL	Exhaust valve lift peak position
h	Enthalpy
I	Knock model induction time integral
ICL	Intake valve lift peak position
I_t	Turbocharger moment of inertia
M_1	Knock Induction Time Multiplier
M_2	Activation Energy Multiplier
M_b	Burned mass
M_e	Entrained mass
ON	Octane Number
p	Instantaneous cylinder pressure
PR	Pressure ratio
S_L	Laminar flame speed
S_T	Turbulent flame speed
t	Time
T	Air temperature
$T_{compressor}$	Compressor torque
$T_{friction}$	Friction torque
t_{resp}	Response time to 90% of BMEPmax,NO EB
$t_{resp,EB}$	Response time to 90% of BMEPmax,EB
t_{start}	Time of electric supercharger activation
T_{total}	Total air temperature
$T_{turbine}$	Turbine torque
T_u	Instantaneous unburned gas temperature
u	Velocity

Greek Symbols

α	Crank Angle
γ	Specific heat ratio
η	Isentropic efficiency
λ	Taylor microscale
ρu	Unburned mixture density
τ	Combustion model time constant
τi	Knock model induction time
ω	Engine speed
ωt	Turbocharger speed

1 INTRODUCTION

1.1 Problem Statement

One of the main issues that car industry has to face is to meet fuel consumption and emission regulations, which are getting increasingly stringent. The combustion of hydrocarbons in combustion engines, even if ideally considered as complete, removes O_2 from the atmosphere and produces water and carbon dioxide. Carbon dioxide is one of the main contributors to the greenhouse effect, together with methane and nitrous oxide. In 2010, for instance, the global transport sector was responsible for almost a quarter of all anthropogenic CO_2 emissions [1]. In order to help mitigate the environmental effects associated with CO_2 production and to reduce the petroleum demand, many governments have developed policies to improve the environmental and energy performance of vehicles and fuels.

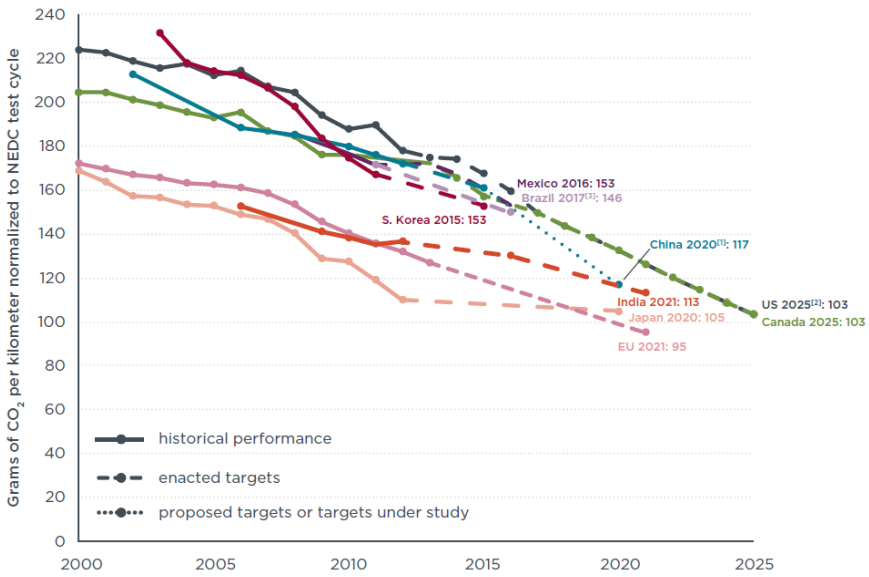

Figure 1-1: Global comparison of passenger car efficiency standards [1]

Emissions of CO_2 were chosen as a regulation parameter because the amount of carbon dioxide in exhaust is directly proportional to the fuel consumption; as a consequence, the only way to reduce this amount is to reduce the amount of fuel needed by the vehicle.

In order to reach the future targets in terms of fuel consumption, all the areas of the vehicle must be optimized so that less fuel must be burned for a determined mission of the car; some of the main ways that have been followed are reported below:

- aerodynamic drag reduction;
- vehicle mass reduction;
- tire and rolling resistance reduction;
- internal combustion engine efficiency improvement;
- electrical power losses reduction.

As far as the engine efficiency is concerned, studies indicate that there is still significant potential for increasing the efficiency of both diesel and gasoline fueled powertrains. In particular, the relative advantage of CI engines in terms of efficiency with respect to SI engines is likely to be reduced [2].

In order to increase the efficiency of the internal combustion engines many different technologies have been developed in recent years; some of the most significant techniques, referred in particular to spark ignited engines, are:

- GDI – gasoline direct injection, homogeneous and stratified;
- EGR – exhaust gas recirculation;
- Variable valve lift and timing;
- Gasoline engine downsizing;
- Turbocharging and supercharging;
- Mechanical friction reduction;
- CAI (Controlled Auto-Ignition) or HCCI (Homogeneous Charge Compression Ignition);
- Advanced thermal control.

Gasoline engine downsizing, associated with turbocharging, has proved to be one of the most effective ways to reduce the specific fuel consumption of the engine. Several car makers have shown interest in it and have replaced engines of big displacement with turbocharged smaller engines. The main advantage of downsized engines is represented by the higher specific load (BMEP) at which they work, which results in reduced friction and pumping losses, hence improved efficiency.

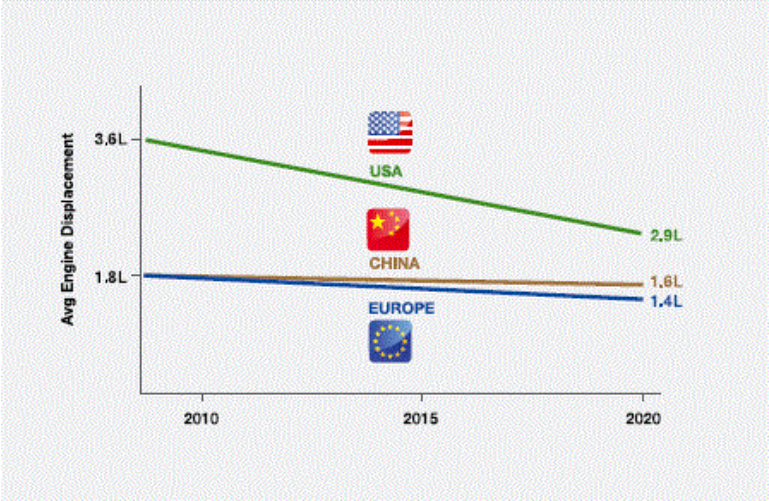

Figure 1-2: Engine downsizing trend in Europe, China, U.S.A. [3]

On the other hand, downsizing and turbocharging a SI engine presents many technical challenges; the three main limitations historically encountered are:

- Reduced steady-state low speed torque;
- Delay in transient response caused by the turbocharger;
- Combustion limitations due to propensity to knock.

As a consequence, the tendency to downsize gasoline engine would be even stronger if a means of overcoming these limitations, or at least some of them, was available. Boosting systems are critical components in order to face the aforementioned technical challenges. Traditional turbocharged engines cannot in most cases overcome these issues, even if modern technologies such as variable valve timing and direct injection are applied simultaneously. Advanced supercharging systems can succeed in matching or exceeding the performance target while retaining the advantage in terms of fuel consumption. In the last years several types of advanced boosting systems have been investigated, some of the most interesting technologies are:

- Two stage turbocharging;
- Mechanical supercharging in combination with conventional turbocharging;
- Turbo-compounding;

- Electrical compressor supercharging in combination with conventional turbocharging.

Of particular interest is the solution featuring a second, electrically-driven, compressor in series with the turbocharger compressor: the steady-state low end torque deficit and the slower transient response with respect to naturally aspirated engines can be reduced (or potentially cancelled).

1.2 Objectives

As previously said, in the last years a tendency to downsize and turbocharge gasoline engines has been shown by car makers. Provided that this policy is introducing fuel consumption benefits in most cases, other technical issues have to be faced when the downsizing level of an engine is to be increased. In particular, the drivability of the engine may be worsen due to the slower transient response and lower torque at low speeds of a turbocharged engine with respect to a naturally aspirated one with comparable maximum power. In this work the possibility to increase low speed and transient performance of a turbocharged engine by using an electrical supercharger (placed upstream of the turbocharger compressor) is investigated. The considered engine is a four-cylinder inline, four valves per cylinder engine by FCA. The aim of the work is to predict the improvement in steady-state and transient performance due to the contribution of the electric supercharger. A 1D simulation of the mentioned engine is performed with and without the use of the electric supercharger in order to quantify its effect on engine operations. The exploited software is GT-Power Version 7.4, by Gamma Technologies. In particular, for what concerns the steady state torque, the maximum BMEP obtainable for both boosting conditions will be evaluated in the low speed range. As far as the transient response of the engine is concerned, the time for the torque to build up at fixed speed is evaluated for both boosting conditions. The effect of different control strategies for the electric supercharger will be also assessed.

1.3 Methodologies

The advantage of the 1D simulation is to provide answers which, otherwise, should come from very expensive and time demanding testing. Thus, the model should strictly behave like the real engine, within a given range of accuracy. As a consequence, after the model is created, some experimental measurements are necessary to have real data to compare with the output of the software: with those data the model is tweaked until it describes the characteristics of the real engine. This step is called model correlation or calibration. Once the model is correlated it is a powerful tool available to predict the effect of modifications without doing costly testing activity. In this case, the model of the engine was given to the author by FCA and most of the calibration work was already done, thus the present work starts from the model validation. Since the interest for both steady state and transient performance is related to the low speed range, the operating points for the model validation were chosen at 1500 rpm and 2000 rpm from minimum to maximum load. After the model validation is obtained, some steady state runs are performed at engine speeds between 1000 to 3000 rpm at maximum load to evaluate the BMEP improvement provided by the electric supercharger. The last part of the work is represented by the setup of the model to run a transient load step at fixed speed and evaluate the potential of the electric supercharger in reducing the transient response time of the engine.

1.4 Thesis Organization

The remaining part of the present work is organized in the following chapters:

- Chapter 2: this chapter presents all the literature review performed by the author in the early stage of the project. In the first part of the chapter the main feature of the engine such us turbocharger, electrical supercharger, cooled EGR and variable valve timing are treated in order to give to the reader a better understanding of the design choices for this engine; in the second part of the chapter some of the

advantages and issues of 1D engine modelling are presented with special focus on transient simulation.

- Chapter 3: the engine main features are reported and the most important model components are described;
- Chapter 4: the simulation procedure for steady-state and transient conditions is reported, the choice of the selected input parameters and the results that will be presented in Chapter 5 is explained;
- Chapter 5: in this chapter the results of the simulations for the model validation, maximum steady-state BMEP and transient response estimation phases are provided; the results are discussed and the influence of the different parameters on the engine performance, focusing on transient conditions, is evaluated;
- Chapter 6: conclusion and recommendations.

2 LITERATURE REVIEW

2.1 Gasoline Engine Downsizing

The internal combustion engine represents the major source of power for cars, and will still represent it for several years, despite the spread of EVs and HEVs predicted for the following years.

Today's engine efficiency is limited to only 30-35% for a SI engines and 35-40% for a CI engine; this means that improvements are still possible. Studies into the development of future powertrains report that spark ignition engines have more potential improvement than compression ignition engines, and predict that the relative advantage of diesel over gasoline engine is going to be reduced [2].

As previously stated, many different technologies have been developed for SI gasoline engines in order to reduce fuel economy. Among those, gasoline engine downsizing (along with turbocharging) has been shown to be one of the most effective improvements in the short-medium term, claiming up to 20% improvement in fuel economy for a 40% downsized engine [4], as shown in Figure 2-1.

As a consequence, many companies started to investigate the possibility to substitute current engines with downsized ones [5]- [6] and numerous turbocharged engines were introduced into production [7]- [8], initially in Europe. Research work is continuing in this area in order to understand advantages and limitations of further level of downsizing [9]- [10]- [11]. To provide the same peak power output of larger displacement engines, downsizing comes usually together with turbocharging, sometimes with other forms of supercharging.

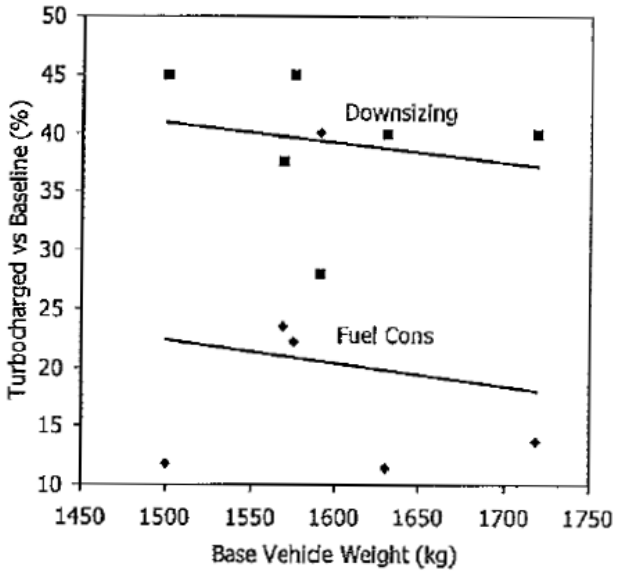

Figure 2-1: Downsizing level and fuel consumption reduction in 2009 model year production vehicles [4]

The main advantage of downsized engines is represented by the higher specific load (BMEP) at which they work compared to naturally aspirated engines, which results in reduced friction and pumping losses, hence improved efficiency. Since most of the operating points required from driving cycles are located in the low load region of conventional internal combustion engines, shifting this region towards higher specific loads should theoretically results in reduced fuel consumption.

On the other hand, downsizing and turbocharging a SI engine presents many technical challenges; three main issues need to be faced:

- Steady-state low speed torque – with increased downsizing, low speed BMEP requirement increases to maintain acceptable performance. Turbocharged downsized engines can match the torque of NA engines very well at medium and high engine speed but they show usually a torque deficit at low engine speed because of the reduced displacement and the low flow rate through the turbocharger;
- Transient performance – engine response to load transient needs to be maintained with increased low speed torque requirement. The transient response of a turbocharged engine is limited by the inertia of the turbine, compressor and turbocharger shaft, i.e. when the engine load is increased part of the energy is

used to accelerate the mentioned rotating parts and it is not available as power output. In order to reduce the driver perception of the lag in transient response in some case it is chosen to change the gear ratios to work at higher engine speeds where the transient response is better, wasting some of the fuel consumption advantage of the downsized engine. Another option is the application of advanced supercharging systems, such us multiple stage boosting, as proposed in this work.

- Combustion limitations – propensity to knock of turbocharged engines leads to reduced compression ratio and retarded spark timing, hence lower efficiency at equal engine speed and BMEP. Furthermore, the retarded spark timing causes higher exhaust temperature at high loads; measures must be taken so that excessive over-fueling is not needed to lower that temperature, because that would cause a penalty in both fuel consumption and emissions.

As shown in Figure 2-2, the conventional turbocharged engine has lower fuel consumption at low outputs, but the fuel consumption benefit is cancelled at higher loads due to need for spark retarding and mixture enrichment.

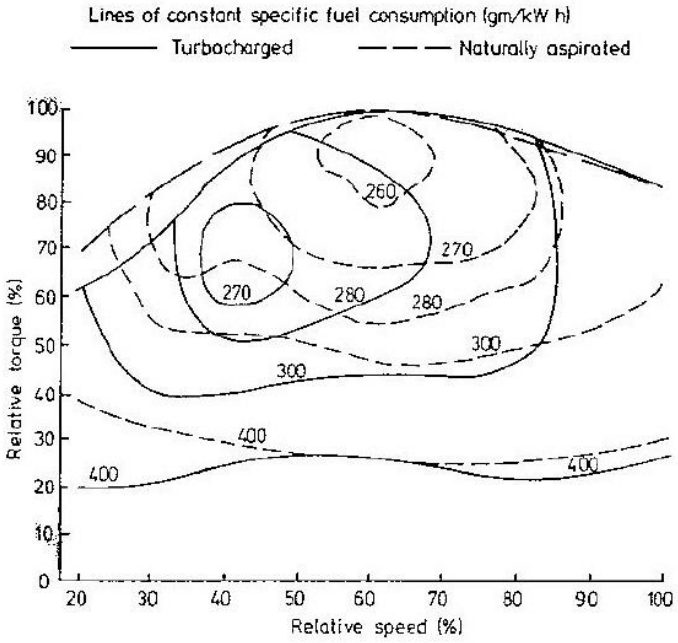

Figure 2-2: Comparative specific fuel consumption of a turbocharged and naturally aspirated engine scaled for the same maximum torque [12]

Boosting systems are critical components in order to face the aforementioned technical challenges, thus their characteristics and choice, together with the application of other technologies aimed at reducing fuel consumption, will be discussed in the following paragraph.

2.2 Boosting Systems

The maximum amount of fuel that can be burned in an engine cylinder each cycle depends on the quantity of air that is introduced in the cylinder. In order to burn more fuel, thus obtain more power, the air can be compressed to a density higher than atmospheric. The term supercharging refers to increasing the air (or mixture) density by increasing its pressure before induction, and its primary purpose is to increase the power output of a given engine [13]. There are different methods used to accomplish this, the following two are the most common:

- Mechanical supercharging - a separate blower or compressor, usually driven by power taken from the engine, compresses the inlet air.
- Turbocharging - a turbocharger (a compressor and a turbine on a single shaft) is used to boost the inlet air (or mixture) pressure. Energy available in the engine exhaust is used to drive the turbine which in turn drives the compressor which raises the inlet fluid density prior to entry engine cylinders.

Supercharging is used in four-stroke cycle engines to boost the power per unit displaced volume, which usually results in higher efficiency since mechanical losses in the engine are not solely dependent on the power output. Whether or not there is an improvement in efficiency ultimately depends on the efficiency and matching of the turbocharger or supercharger [12].

2.2.1 Turbocharging

In a turbocharger, a turbine wheel – (4) in Figure 2-4 - is driven by the 'waste' exhaust gases. The turbine drives the compressor wheel through the shaft. Air drawn from the

external environment is led to the compressor inlet – (1) in Figure 2-3 - after passing through the air filter, and as it passes through the compressor its pressure is increased. Since with the rise in pressure is associated a rise in temperature, the compressed air is sometimes cooled in a charge air cooler – (3) in Figure 2-3 - in order to decrease its density and increase volumetric efficiency.

Compressors of axial and radial type can most appropriately be driven by a turbine (which again can be of an axial or radial flow type). Dynamic (not positive displacement) compressors work by accelerating the flow in a rotor (rise in total pressure) and then decelerating the flow in a diffuser to produce a static pressure rise. Radial compressors are more tolerant of different flow conditions and therefore more suitable to be matched with internal combustion engines. Furthermore radial compressor can achieve much higher pressure ratios in a single stage. The most common arrangement involves, indeed, a centrifugal compressor driven by a centripetal turbine, as shown in Figure 2-3. It means the air is entering in the compressor along the direction of its axis of revolution and is expelled radially. On the contrary, the exhaust gases enter the turbine from the external scroll and are expelled along the axis.

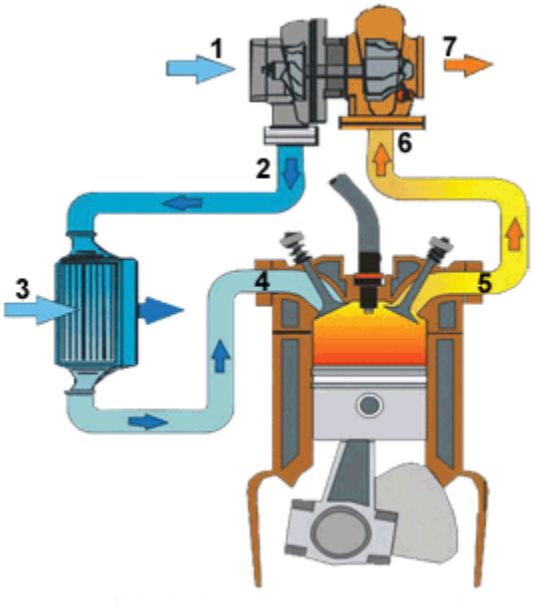

Figure 2-3: Schematic of a conventional turbocharger [14]

The flow from an engine is unsteady, owing to the pulses associated with the exhaust from each cylinder, yet turbines are most efficient with a steady flow. If the exhaust flow is smoothed by using a plenum chamber, then some of the energy associated with the pulses is lost. The usual practice is to design a turbine for pulsed flow and to accept the lower turbine efficiency. For four-stroke engines no more than three cylinders should feed the same turbine inlet. Otherwise there will be interactions between cylinders exhausting at the same time. For a four-cylinder engine a turbine with two inlets should be used. Double entry turbines in series production today are almost exclusively designed as twin scroll turbines, i.e. the scrolls are divided circumferentially, as shown in Figure 2-4.

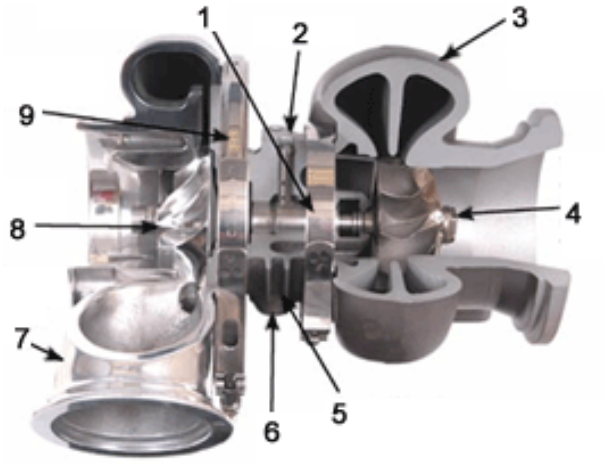

Figure 2-4: Twin scroll turbochargers main components [14]

Double entry turbines feature lower peak efficiencies compared to conventional mono scroll turbines (see Figure 2-5) as a result of inherent friction losses on the separation wall of the turbine housing – (3) in Figure 2-4. Despite this drawback, double entry turbines are an alternative to complex charging systems on four-cylinder engines for achieving satisfying low-end-torque combined with high specific power.

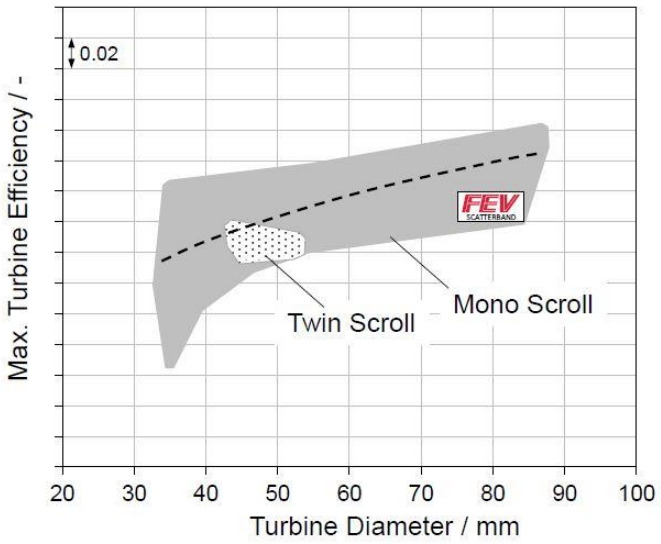

Figure 2-5: Twin scroll – Mono scroll peak efficiency comparison [15]

Some of the main advantages of twin-scroll turbines are the followings:

- Higher turbine efficiency considering the pulsating nature of the exhaust gas
- Possible application of longer intake valve event length at part load with corresponding reduction in part load fuel consumption

Whereas the main disadvantages can be identified as:

- Lower peak efficiencies
- Higher level of complexity
- Complicated casting process and high thermo-mechanical load.

An example of twin-scroll turbocharger application [7] is represented by the BMW 2.0-l four-cylinder engine. The twin scroll turbine provides a very fast torque transient with respect to the engine equipped with a mono-scroll turbine: after a load step engine achieves maximum torque more than 40%. It is also of particular note that the maximum torque of 350 Nm is available at the very low engine speed of 1250 rpm, as shown in Figure 2-7.

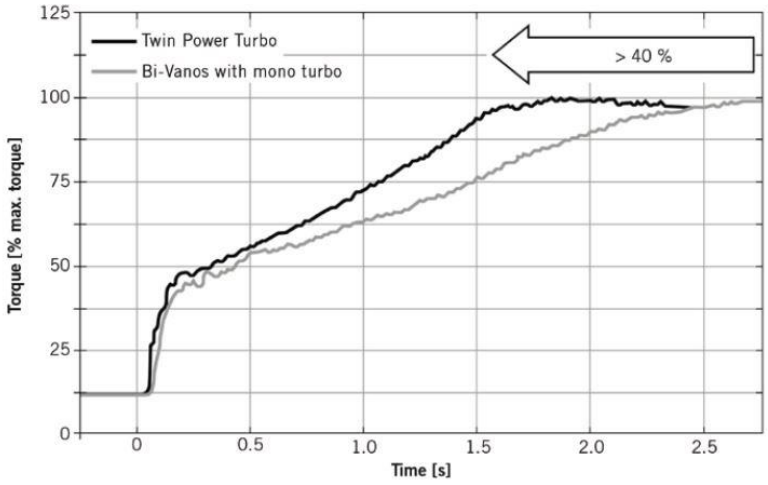

Figure 2-6: Advantage in transient response of the twin scroll turbocharged engine at 1500 rpm [7]

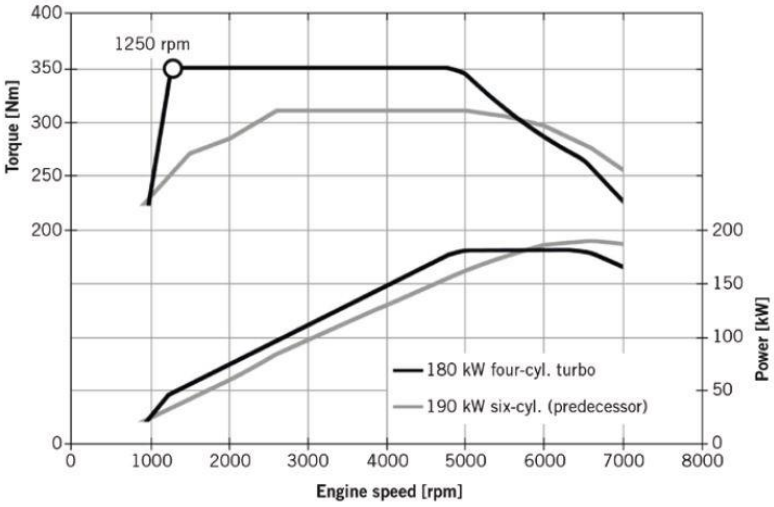

Figure 2-7: Torque and power of the BMW 2.0l four-cylinder in comparison with the older six-cylinder NA engine [7]

2.2.2 Electric supercharger

Since conventional boosting devices, both turbochargers and mechanical superchargers, are subject to different physical constraints (e.g. turbolag), the electrically-driven supercharger is emerging as an interesting approach to increase charge air density. This kind of supercharger, as opposed to the mechanical one, is usually of centrifugal type, the same preferred for the turbo compressor.

The electrical supercharger has the following advantages:

- It is able to increase the air charge with no significant delay in boosting effect during engine load transients, especially at low engine speeds;
- No mechanical connections are required with the engine, which means no increase in friction losses of the engine. Moreover it allows to provide engine charging only when required;
- Because it is not coupled to the engine directly via exhaust or mechanical link, it is easier to design a control algorithm without too many adverse impacts on the engine performance;
- The electrical power necessary to drive the electric supercharger could be provided by any energy recovery system, such us kinetic energy recover system under braking condition.

Pallotti et al. have shown [16] the potential advantages of the application of electrical supercharging to a SI engine. In their work a 1.4 dm^3, inline, 4 cylinders, 16 valves gasoline engine equipped with an electric centrifugal compressor is compared with the baseline engine (1.6 dm^3, inline, 4 cylinders, 16 valves) with which the normal production C-segment vehicle is equipped. The centrifugal compressor is driven by an electrical motor and it is used to increase the engine torque under full load conditions; in order to ensure minimum pressure losses when the engine is running under naturally aspirated conditions the air is delivered to the engine through a by-pass when the compressor is not required. The system described is indeed an on-demand booster which increases the torque only when a full acceleration is required by the driver, thus the compressor only operates for a limited amount of time. The main characteristic of the electrical boosting system are as follows:

- Motor maximum rotational speed – 70000 rpm
- Motor maximum continuous current – 200 A
- Battery capacity – 42 Ah, Low impedance
- Alternator – 115 A

A 12% improvement in NEDC fuel economy was achieved by the downsized electrically supercharged engine w.r.t. the baseline engine, through the increase in specific torque output and re-optimization of the transmission gearing.

Electric supercharging of diesel engines has also been investigated, due to its potential ability to overcome some of the limitations of conventional turbocharged CI engines, such us poor transient performance, especially when accelerating from low speeds. The solution proposed by Divekar et al. features an electric supercharging in coordination with a turbo-generation in order to decouple the air compression and exhaust energy recovery functions [17]. The proposed system is evaluated, by means of a simulation model, on standard test cycles and it is compared with the conventional turbocharger. The electrically supercharged system responds faster to large demanded speed changes and virtually eliminates the turbo-lag. Furthermore, over the EPA urban driving cycle an improvement in fuel consumption of nearly 7% is obtained with respect to a similar engine fitted with a conventional turbocharger. The improvement is, however, absent over the EPA highway cycle due to the mostly steady-state operations.

The most interesting application for the electric supercharger though is represented by its application in series with a conventional turbocharger, as will be discussed later. Research work indeed has been done in this direction in the last years, and some of the obtained results will be analyzed in the followings. One of the car makers that showed interest in this technology is Audi, which has already proven the potential of a car featuring an electric compressor placed between induction system and intercooler of a turbodiesel engine [18]. The RS5 concept uses a separate 48V system from the car's regular electrics to spin-up the small compressor. The e-booster takes only 250 ms to reach its maximum revs, and provide 7 kW (9 hp) of power. The RS5 TDI Concept is meant to deliver power with no detectable lag even at low engine speeds; problem which is nowadays more and more related to gasoline engines as well because of the trend to downsize and turbocharge engines of the latest years. The energy needed by the compressor, moreover, is mostly recuperated energy, stored in a lithium-ion battery in the trunk. The decision to use a 48-V sub-system means it can also support other applications in order to provide different type of electrification across the production range.

2.3 Advanced boosting systems for gasoline engines

In order to maintain low speed torque and transient response, the choice of the boosting system for downsized engine is critical. Currently single turbocharger systems are predominantly used in gasoline engines, combined in some applications with GDI and VVT. This has enabled acceptable performance to be achieved, with specific power outputs up to 80 kW/l [9]. However, in order to obtain high levels of downsizing, additional boosting technology is required: single turbocharger performance is going to be always limited by the energy available in exhaust at low engine speed.

Different options for advanced boosting systems can be:

- 2-stage turbocharging – Utilizes a small high pressure turbo for low speed in series with a large low pressure turbo for high speed. It must be possible to by-pass the high-P turbo to prevent over-speed.
- Supercharger and Turbocharger – Features a mechanical supercharger (typically roots type) in series with a larger turbocharger. Supercharger must be used at low speed and bypassed as speed increases; it needs a drive system with clutch.
- Electrical Supercharger and Turbocharger – combines an electrically driven compressor installed upstream or downstream of a turbocharger compressor. The electric one is used at low engine speed in series with the main compressor and then is bypassed once the main one has spooled up.
- Turbo-compounding – use of exhaust gas driven turbine directly geared to the engine drive shaft in order to increase engine power. Sometimes, typically in hybrid applications, the turbine does not directly increase the engine power but is geared to an electric generator; the produced power is then used to supply an electric motor or other utilities.

2.3.1 Combination of electrical supercharging and turbocharging

The relative performance of some of the different aforementioned advanced boosting systems was evaluated by testing in both steady-state and transient conditions of the same downsized engine by Mahle Powertrain [9]. In particular the two-stage turbocharger was compared to a system featuring an electric centrifugal compressor located upstream of the turbo compressor (the low pressure stage of the two-stage turbocharger). As far as the steady state torque is concerned, the best result was obtained with the two-stage turbocharger, which was shown to be able to exceed the target. However, both the systems showed an improvement in low end torque with respect to a single-stage turbocharger.

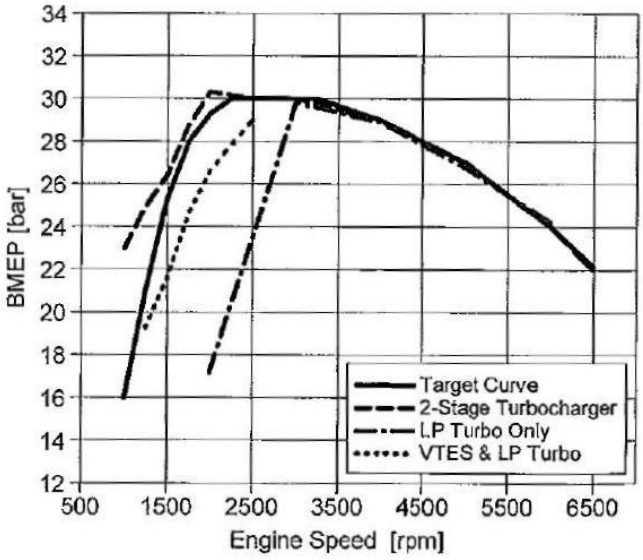

Figure 2-8: Steady state full load curve with different boosting systems [9]

In terms of transient response, the ES and Turbo configuration was shown to provide the faster response to a load step from a 2 bar BMEP to wide open throttle. In a real world application though, the improved transient could compensate for the lack of steady state torque.

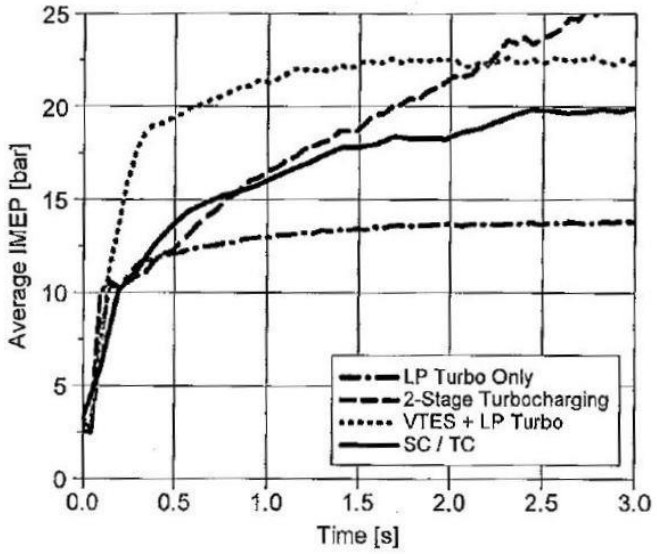

Figure 2-9: Transient load step comparison at 1250 rpm for different boosting systems [9]

Furthermore, the ES is much simpler to package than either the 2-stage turbo or the supercharger-turbocharger combination, since the electrical compressor can be packaged in any suitable location in the inlet system. The biggest challenge is identified in the paper [9] as the appropriate matching of the vehicle electrical system to the transient energy requirements of the supercharger. To satisfy this requirement the ES must be coupled with an appropriate battery system or an ultracapacitors based storage system.

The advantages of the combined action of a conventional turbocharger and an electric supercharger have also been shown by An et al. which carried out both simulation and testing [19]. The mentioned supercharger is powered by a motor with 12 V supply which reaches a power output of 2.4 kW and gains boost pressure ratio of 1.6 in 0.7 s, as shown in Figure 2-10.

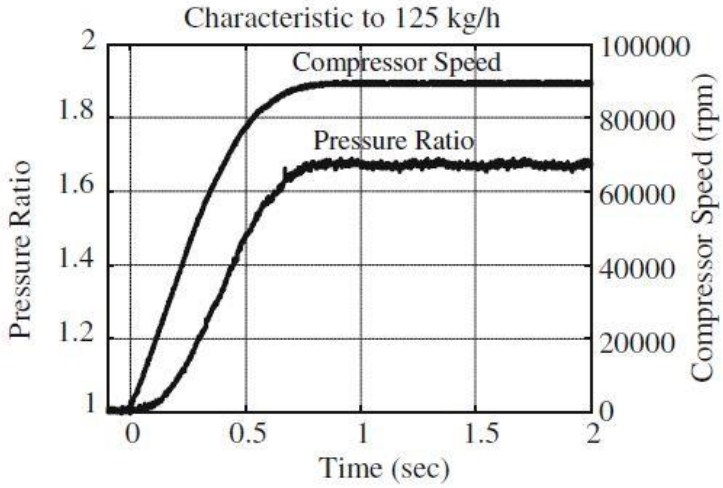

Figure 2-10: Response time of the electric supercharger [19]

In the investigated configuration the electrical supercharger was located downstream of the compressor of a normal turbocharger with waste-gate valve, see Figure 2-11.

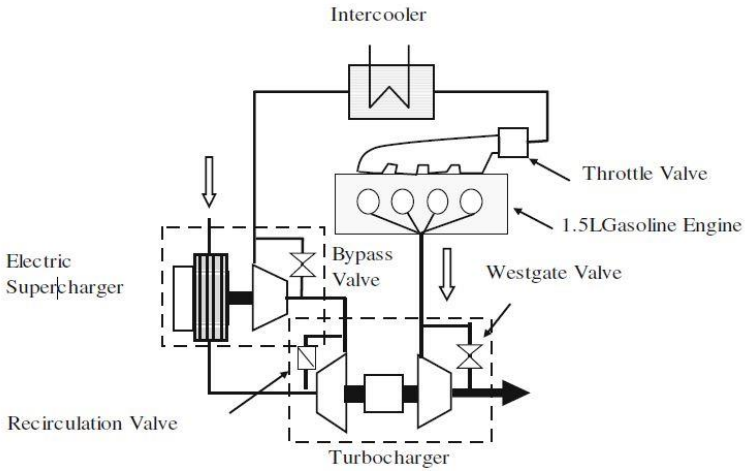

Figure 2-11: Schematic of the two-stage supercharging system [19]

Simulations results clearly highlighted that, with the mentioned arrangement, turbolag is dramatically reduced and peak low-end torque are achieved in around 1.0 s at 1500 and 1750 rpm. Engine test results showed that, using a 1.5 L gasoline engine, the electric two-stage turbocharger shows a 43% improvement in a response time at 1500 rpm as compared with two-stage turbocharger.

Another research work which proposes the application of electric supercharger combined with conventional turbocharging is represented by the HyBoost project developed by Ricardo [20]. A modified Ford 1.0-l 3-cylinder turbo GDI EcoBoost engine is compared to a Ford 2.0L Duratec (Naturally Aspirated) in terms of torque curve. It is found that the downsized engine is superior in peak torque to the baseline even without the electric supercharger; only when the latter is added though the brake torque is higher even in the low speed range.

Preliminary transient testing shows that the ES is capable of achieving maximum speed greater than 60000 rpm in less than 200 ms and maximum pressure ratio of 1.6 bar. The time to reach the peak boost pressure is found to be halved by the action of the ES (operated for two seconds) during the transient load step at fixed speed.

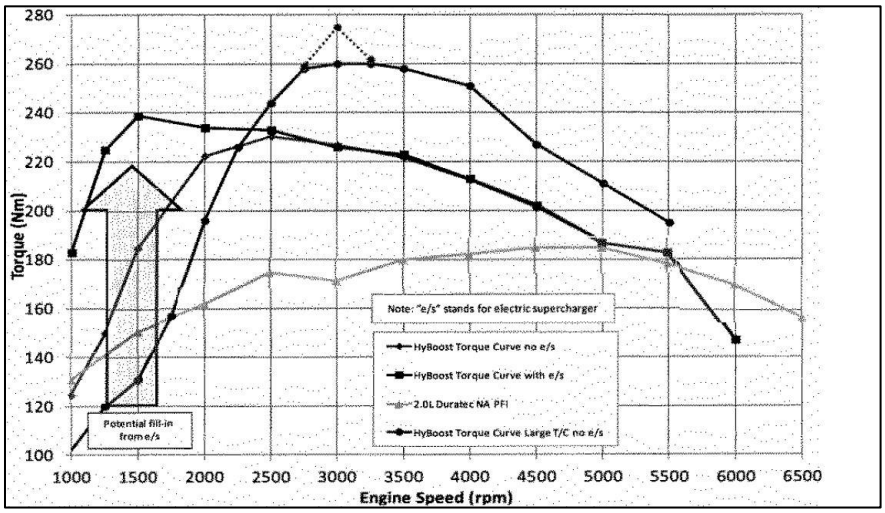

Figure 2-12: Ford 2.0L Duratec vs Hyboost torque curves comparison [20]

The latest car maker group to investigate the potential of e-boosting is Volvo. Its advanced boosting system features a bi-turbo configuration supported by an electrically-driven compressor, meant to ensure high power output and linear torque delivery [21]. Volvo refers to the engine simply as "triple boost technology", but the development of this system is part of a larger policy towards engine downsizing and emissions reduction. This system consists of two turbochargers which are connected in parallel and an electrically-powered compressor which is linked to them in order speed them up in the lower rpm range, thus virtually eliminating lag. The technology is meant to be applied in

the future to both gasoline and diesel powertrains; in the SI version a 2.0-L four-cylinder engine produces a claimed 450HP (331 kW), fuel being provided by a fuel pump working at a high 250 bar. Such an engine would have a huge power density which in turns would allow for compact package size and reduced weight. Furthermore, when compared to an engine of six or eight cylinders, it would improve weight balance and allow a lower center of gravity.

2.4 Part load efficiency improvements

Downsized engines improve fuel economy by shifting the operating points to more efficient locations, increasing the specific loading and thus reducing pumping losses. When compared to naturally aspirated engines of higher capacity and similar power output, also usually achieve a reduction in friction losses. This is due to reduction in cylinder number, thus lower number of bearings, springs and other additional components, even if they might be of increased size.

The fuel consumption at low load, though, can get worse than in naturally aspirated engines, mainly because of the reduced compression ratio in turbocharged engines and the pumping work required given the more sophisticated intake and exhaust systems.

In order to achieve good part load fuel consumption different strategies are applied.

One of the most implemented solutions is variable valve timing: it can achieve reduction in fuel consumption by partially de-throttling the engine at part load and thus reducing pumping losses. Combining variable valve timing and lift with GDI could lead to a further improvement in fuel consumption, mainly due to the possibility to run under lean stratified conditions. Charge stratification is obtained by injecting the fuel during the compression stroke, so that in the region close to the spark plug a flammable (close to stoichiometric) mixture is formed, yet the overall equivalence ratio is lower than one. However, charge stratification must be applied carefully in order to achieve very low NO_x emissions, since the three-way catalyst will operate in oxidation mode only. Another advantage of GDI is the avoiding of wall wetting by the injected fuel and no build-up of fuel films inside the intake ports; this leads to formation of a better mixture and a faster

combustion process, which determine lower HC and CO emissions especially during warm-up and transient phases.

Other technologies can be applied to improve part load BSFC of downsized gasoline engines, such as variable compression ratio and Miller cycle. Both of these technologies can be used to vary the (geometric or effective respectively) compression ratio with engine load. Higher compression ratio can be used at part load to increase efficiency, lower CR at higher loads in order to reduce knock sensitivity and allow for combustion phasing advancing.

2.4.1 Variable valve timing

Conventional valve trains feature fixed intake and exhaust valve timings and valve lifts over the whole operating range of a given engine. Since optimum valve events are strongly dependent on engine speed and load, this conventional strategy results in a compromise in engine performance almost at any operating point. An available alternative to reduce these compromises and improve engine performance over the entire operating range is the implementation of a variable valve train. The very large number of patent applications concerning VVA and VVT systems in the past decades confirms the great effort made in this area within the automotive industry [22].

Simpler variable valve event strategies focus on the variation of timing only and for just one of the valves; in particular the late or early intake valve closing can be used to control engine load reducing, or even avoiding, the throttling. The possibility of eliminating the throttle valve and associated pumping losses was subject of many researches; it was shown ever since the eighties [23] by Elrod and Nelson that improvements in fuel consumption, especially at low speed and light loads can be achieved. One of the first practical applications is represented by the system that was developed by Mercedes-Benz [24], in which the intake valve timing is adjusted (in dependence to load and engine speed) by turning the intake camshaft using a hydraulic-mechanically acting camshaft adjuster.

Another approach to variable valve trains is to switch between two different cam profiles, featuring two different maximum lifts; in this case a so called VVA (Variable Valve

Actuation) system is implemented. The profile with a lower lift can be used at low loads for some of the intake valves in order to reduce pumping losses. The high lift profile can be independently optimized for peak power at rated engine speed, thus improving the classic tradeoff between the two load conditions. Among the several options for variable valve train, the use of the two step profile switching VVA system is one of the most attractive to engine manufacturers; it is indeed relatively simple, low cost and easy to package on new and existing engines. Moreover, it can be configured for a variety of different engine strategies using a common architecture and thus can be tuned and adapted for different vehicle missions, from high fuel economy to high performance.

However the profile switching has limited benefits with respect to a fully variable VVA system (such as BMW's Valvetronic [25]). These systems can continuously vary the valve lift and timing over the operating range and most of them use the Early Intake Valve Closing (EIVC) as the primary strategy to reduce pumping work and improve fuel economy through a very limited intake system throttling for engine load regulation.

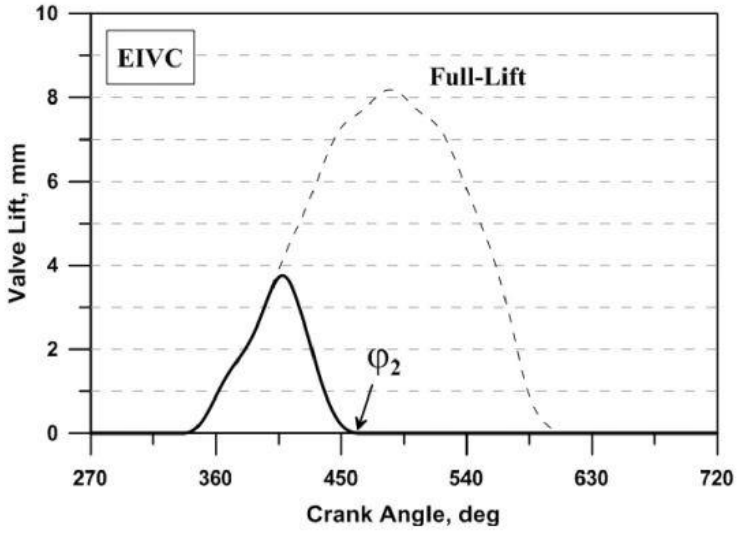

Figure 2-13: Example of EIVC valve lift profile featuring reduced lift [26]

As shown in Figure 2-13, the EIVC and the reduced lift are used in combination in order to control the load without increasing the throttling; thanks to this strategy the fuel consumption levels can be kept low and only increase at very low loads [26]. Moreover, reduced friction work is achieved on account of reduced part-load intake valve lift.

2.4.2 Miller Cycle

A particular application of the variable valve timing is the so called Miller cycle: shortening compression stroke relative to expansion stroke is effective to reduce the temperature and pressure at the end of compression stroke, and therefore suppress knock. Miller cycle can be realized by either early or late intake valve closing (EIVC or LIVC). Moreover, as already mentioned above, the part-load fuel consumption can be potentially reduced thanks to unthrottled operation of the engine.

Part-load and high-load evaluations have been conducted by Tie Li et al. on a boosted direct injection SI 2.0L four-cylinder engine [27] by comparing the performance obtained applying EIVC and LIVC with a high compression ratio of 12.0.

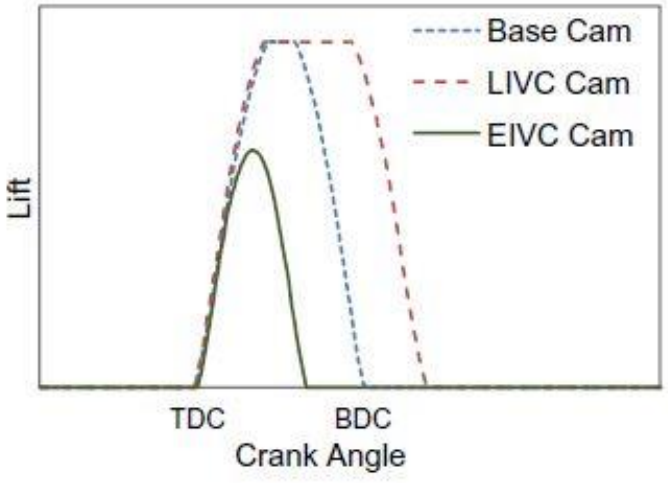

Figure 2-14: Schematic of the different valve lift profiles [27]

By only increasing the compression ratio from 9.3 to 12 a fuel consumption improvement is achieved at part load; however, at high load the higher CR increases knock tendency and the fuel consumption deteriorates.

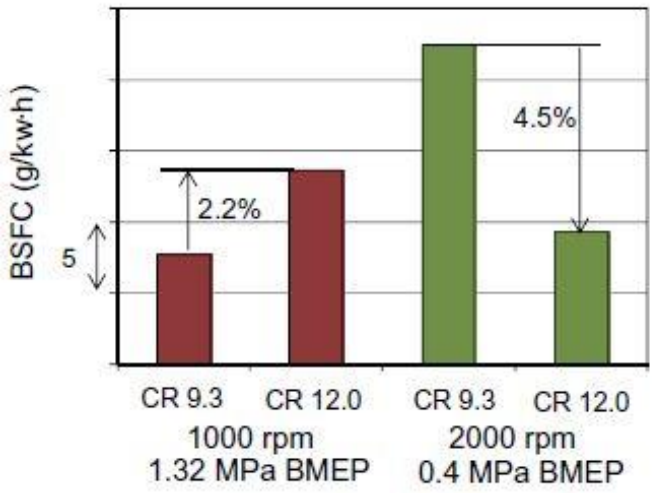

Figure 2-15: Effect of the higher compression ratio (CR) on the brake specific fuel consumption (BSFC) at the high and low load operating conditions [27]

Anti-knock performance is improved by applying either EIVC or LIVC strategies for the higher compression ratio engine; with LIVC (advantageous over EIVC at high load) and high compression ratio combination fuel economy is even better than for the case of CR 9.3 and base valve timing.

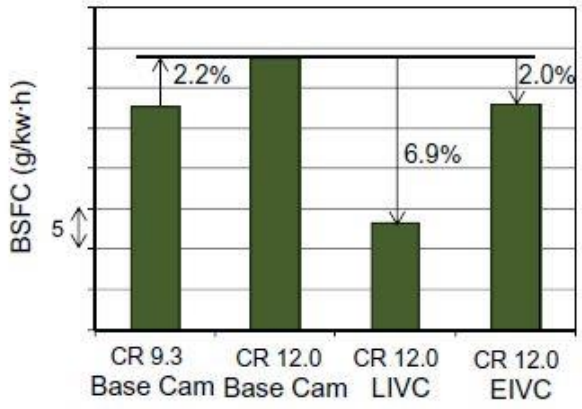

Figure 2-16: Effects of EIVC and LIVC on improving BSFC at the knock limited point under the high load condition (1000 rpm, 1.32 MPa BMEP) [27]

At low load the fuel economy is improved by either EIVC or LIVC, primary owing to reduction in pumping losses; EIVC achieves an improvement of up to 2.9% with respect to CR 12 and base camshaft and up to 7.4% with respect to CR 9.3.

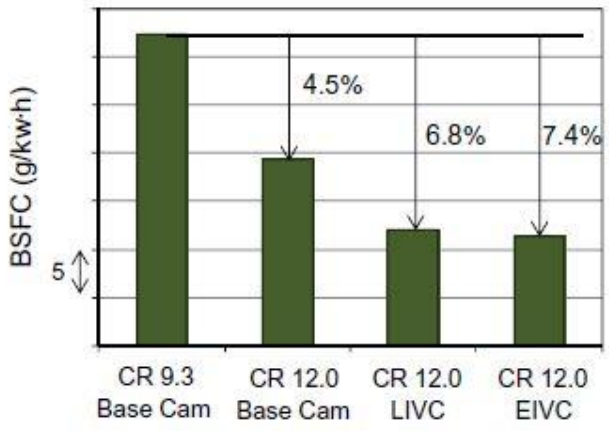

Figure 2-17: Effects of EIVC and LIVC on improving BSFC at the MBT point under the low load condition (2000 rpm, 0.4 MPa BMEP) [27]

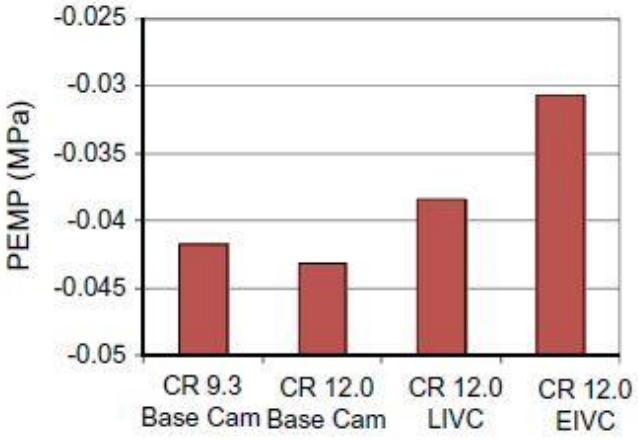

Figure 2-18: Effects of EIVC and LIVC on pumping work at the MBT point under the low load condition (2000 rpm, 0.4 MPa BMEP) [27]

2.5 External EGR

The application of cooled EGR system to downsized turbocharged engines has been studied and introduced by several companies in the last years, because of the need to improve fuel economy in the turbocharged region.

EGR was originally used in Diesel engines as a means for the reduction of NO_x emissions; this is obtained thanks to the reduction of burnt gases temperature produced by the fresh charge dilution with a percentage of exhaust gas reintroduced at engine intake. For NO_x to form two main conditions must be satisfied: presence of nitrogen and oxygen in the mixture and high temperature; the lower combustion chamber temperatures caused by EGR reduces the amount of NO_x generated during the combustion. In stoichiometrically-operated gasoline engines the NO_x-reducing effect of EGR is even more evident because the increase in heat capacity of the mixture is achieved without affecting the stoichiometry, while in CI engines the mixture is richened by reducing the oxygen amount.

Beside the benefits in terms of NO_x emissions, the use of a cooled EGR system affects the combustion, hence the fuel economy, in several other ways by lowering the combustion temperature:

- Allows a better knocking suppression, giving the possibility to advance ignition timing;
- By lowering the exhaust gas temperature reduces the need for mixture enrichment in high load region;
- Reduces cooling losses;
- Increases the specific heat ratio which in turn improves ideal thermal efficiency.

Furthermore the use of EGR in throttled engines is used to reduce the part-load fuel consumption. This is obtained because EGR leads to a reduction in the throttling losses: to admit the same quantity of air in the engine, the throttle has to be more fully open. The reduction in the pressure drop across the throttle also reduces the loss of work caused by the flow restriction.

Naturally, EGR produces also deterioration in engine performance since the volumetric efficiency decreases (part of the displaced volume is occupied by recirculated exhaust gas instead of combustible mixture); therefore the value of torque delivered is reduced. In addition, large amounts of recycled gases could significantly slow down the flame development, thus instable combustion could occur producing large cyclic variations, deterioration in car drivability and an increase in pollutant levels [28].

Different types of EGR system can be distinguished depending on the positions where exhaust gas is extracted and reintroduced:

- Low Pressure loop EGR system: exhaust gas extracted downstream of the turbine and introduced upstream of the compressor
- High Pressure loop EGR system: exhaust gas extracted upstream of the turbine and introduced downstream of the compressor
- Mixed Pressure loop EGR system: exhaust gas extracted upstream of the turbine and introduced upstream of the compressor

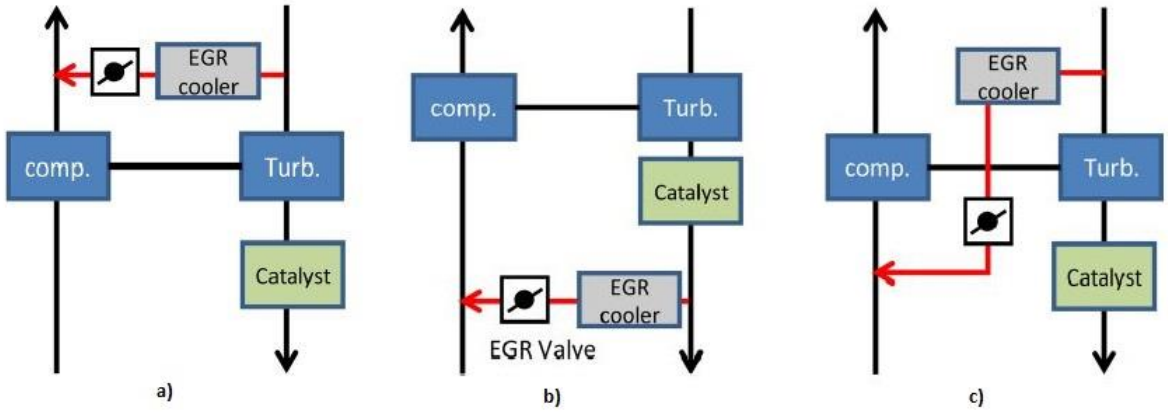

Figure 2-19: Three different EGR system configurations: a) High Pressure Loop EGR (HP EGR), b) Low Pressure Loop EGR (LP EGR), c) Mixed Pressure Loop EGR (Mixed EGR). Adapted from [29]

In order to provide the required amount of EGR, a positive differential pressure must be ensured at all operating conditions. Differential pressure in the EGR system refers to the pressure difference between the EGR gas extraction point and the supply port. Low pressure loop EGR is easily achievable because a positive differential pressure, even if low, between the turbine outlet and compressor inlet is generally available. Furthermore,

tailpipe pressure can be elevated by partial throttling that ensures sufficient driving pressure for the EGR flow if necessary. HP EGR is only applicable when the pressure upstream the turbine is sufficiently higher than the boost pressure. In some cases the intake air pressure is higher than the exhaust gas pressure so that fresh air flows into the exhaust pipe if the EGR valve is open. This problem is not encountered with Mixed Pressure loop EGR which is clearly characterized by the highest differential pressure among the three systems. However, the mixed loop, by extracting the exhaust gas upstream of the turbine, inhibits the transfer of exhaust gas dynamic pressure to the latter and causes turbocharging efficiency to decline (whereas no decline occurs with the LP-EGR system). This means that the Mixed-EGR system cannot generate enough torque in the low speed condition while the differential pressure on the EGR system is large [29].

It has already been mentioned that knocking is suppressed by the introduction of cooled EGR [30], [31]. On the other hand, the recirculation of exhaust causes various components contained in the gas to be reintroduced into the combustion chamber: they will in turns influence the combustion process. Among the various chemical species present in the exhaust, it has been reported that nitrogen oxides (NO_x) in particular tend to promote auto-ignition of the combustible mixture [32]. As a consequence, it has been shown that reducing the NO_x concentration in the EGR gas is effective in strengthening the effect of cooled EGR on suppressing knocking and thus that extracting EGR gas downstream of the 3-way catalyst increased the knock suppression effect of exhaust recirculation [29]; this is possible only with a LP loop EGR.

It is well known [30], [31] and it has already been mentioned that the exhaust gas temperature is reduced by the introduction of cooled EGR. As a consequence, the area of stoichiometric combustion can be extended towards the high load region, and improvement of fuel economy can be expected. This benefit it is given by all of the mentioned systems; however, given the advantages of the Low Pressure EGR in terms of broader load range of application and better knocking suppression, the LP-EGR system can be expected to reduce the exhaust gas temperature more effectively than the High Pressure and Mixed Pressure loop EGR [29].

From the point of view of mechanical components design, it must be considered that with the Low Pressure loop configuration the compressor and intercooler must be designed to

tolerate the higher temperature and the presence of other species in exhaust. High pressure loop EGR, on the other hand, does not expose compressor and intercooler to the engine exhaust gases. It should be noted though, that in this case the EGR loop components - ducts and valves - need to withstand the higher pressure due to the boosting system [33].

2.5.1 Low pressure EGR control issues

An important characteristic of LP-EGR is the low differential pressure between the exhaust gas extraction and EGR supply ports with respect to the other systems. This is a factor that could impede the stable supply of EGR gas, since it flows according to this differential pressure. This parameter in the EGR system is determined according to the intake air flow rate of the engine: higher intake air flow rate causes a higher differential pressure. As a consequence, for a fixed EGR valve opening diameter the EGR flow rate increases with intake air flow rate, thus the EGR fraction in the intake will remain constant. Therefore, as shown in Figure 2-20, EGR rate can be effectively controlled by varying the valve opening [29], even if a certain degree of variability can be introduced by different designs of the intake and exhaust systems.

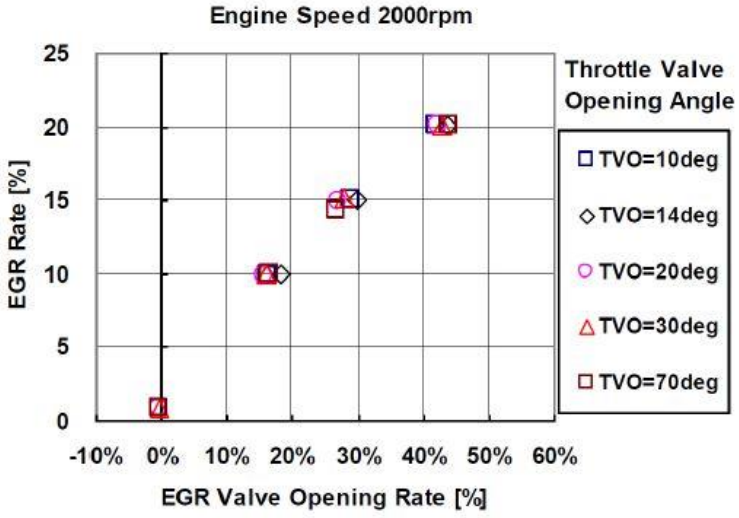

Figure 2-20: EGR rate vs EGR valve opening area in several throttle valve opening conditions [29]

The only limitation is encountered on the low-load side, where the pulsating nature of the exhaust flow combined with the low differential pressure could impede a correct EGR control. Further limitations to this simple control strategy can be encountered under transient conditions. The variation of the pressure at the extraction port can indeed show a delay with respect to the variation of the intake flow.

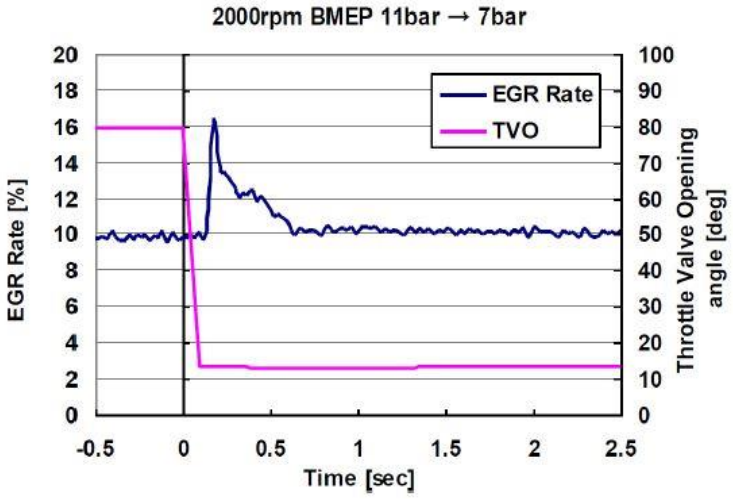

Figure 2-21: EGR rate motion during sharp decrease of engine load for a fixed EGR valve opening [29]

However, it was shown [29] that a control procedure for compensating this effect can be implemented by varying the EGR valve opening in transient operations during the response delay, in order to obtain stable EGR rate even if the differential pressure and the intake air flow rate are not varying simultaneously.

2.6 Engine modelling applications in engine development

It would be clearly an advantage if engine performance could be predicted without the need of physically building the engine in order to test it. Engine modelling can help saving both time and money with respect to conventional testing and this is the reason why is increasingly integrated in the engine design and development phases by many engine manufacturers. Unfortunately most of processes occurring in engines are very complex and it is impossible to model them without the aid of experimental data, used to

correlate the model or to provide it with look-up tables. For example, the turbocharger performance and the valve flow characteristics can be determined from steady-flow tests, and look-up tables can be built into the engine model, along with appropriate interpolation routines. Nevertheless, engine (and vehicle) simulation is one of the most effective ways to predict the results and reduce the amount of experimental tests needed to evaluate the effectiveness of a given design solution. As a matter of fact, it offers the possibility to save money (given its low cost when compared to testing) during the engine control design process.

Mainly three types of modelling levels are used for engine simulation [34].

- The most accurate modelling method is the CFD 2D/3D simulation. It is dedicated to local studies such as the turbulent combustion simulation which permits to finely capture the small scale in-cylinder phenomena.
- At a lower level of accuracy is located the engine system modelling. This approach involves phenomenological or empirical models and allows representing the complete engine with a characteristic timescale lower than 1 crankshaft angle degree. The equations of the flow are usually solved in one dimension (1D models), which means that all quantities are averages across the flow direction. Codes of this kind can be, in some applications, optimized to limit the CPU time cost: the engine system model allows reproducing accurately the behavior of the engine even during transients such as driving cycles, and is able to reach the real time in certain conditions. Therefore, this approach is well adapted to be used as a support tool for engine control design from the control development to the hardware-in-the-loop validation.
- The simplest modelling approach consists in representing the engine with operating condition look-up tables. This level achieves CPU time lower than real time and is mainly used to run standard driving cycle with vehicle simulators. The characteristic timescale of vehicle simulation is to the order of 0.1 second.

The application of engine modelling and simulation methodology in engine development goes back to the late 1970's. At that time, because of limitation of computing power, modelling was usually consisted of simple 0D models. Today, increasingly, the industry

is moving toward a larger use of simulation results, by limiting the reliance on dynamometer testing to support engine development. Especially when dealing with innovative downsizing approach which combines direct injection, variable valve timing and turbocharging, 1D codes were demonstrated to be a useful and efficient tool during all steps of the engine design and control development process [35]. The predictive ability of these models is used to guide dynamometer tests in order to find target points quickly and reduce test points, cost and development time [36]. Depending on the intended application of the model, the simulator has to reach accuracy targets that have to be taken into account when choosing the type of modelling. It is usually not possible to address all the performance targets in a single simulator. For instance, if the model is going to be used for the development of the control of the air path, it will need an accurate modelling of the different components of the air circuit (the turbocharger, the EGR loop, the heat exchanger, etc.); on the other hand it will not require the same accuracy for the combustion process or pollutant emissions (as it would if it was intended for investigating combustion control issues). Computational time considerations also play an important role in the choice of the model accuracy level. Simulation speed is of primary importance when running long transients such as a driving cycle (used to compare several different configurations for the engine or for the whole vehicle) or for control design application when Hardware-in-the-Loop platforms are used and thus real time speed is required. Detailed engine models may require execution times up to two orders of magnitude slower than real time, depending on CPU capabilities; a simplified or Fast Running Model can be derived from the detailed one by using a coarser discretization of the flow path but still maintaining the advantage in terms of prediction accuracy of a physics based model. A detailed engine model can be reduced to a faster running model basically joining volumes together, thereby reducing their total number, increasing the discretization length and as a consequence reducing the computational time. At least in certain conditions, this kind of simplified models can reach real time speed; if the computational time reduction is not adequate, the aforementioned map based models must be used.

Another aspect to be taken into account when choosing the simulator type is available data. Indeed, to build a very sophisticated model when very few data are available is a non-sense because the calibration level will not be sufficient to obtain a valid model.

2.6.1 Model correlation and validation

After an engine model is created, independently on the software used, the simulator has to be calibrated on different operating conditions; in order to achieve the required simulator accuracy. Different strategies can be applied to achieve the calibration in a complete way. The best methodology would be to try to separate the different component calibrations in order to limit the interactions between them, since those can induce mistakes [34]. Ideally each component should be isolated in order to obtain precise calibration of a given submodel. With this approach, boundary conditions have to be imposed by the user for each component or submodel so that the calibration is not disturbed by the environment. Nevertheless, the application of this methodology to a whole engine is very time consuming and an accurate boundary condition determination is difficult for all the components. Furthermore, the amount of experimental data necessary to an accurate calibration process is very large and such an amount is usually not available in real world applications.

As a consequence, an alternative is to successively calibrate the different components of the complete engine simulator by choosing operating conditions that minimize the component interactions. For instance, in the first stage of the process the focus can be placed on the operating points with a closed EGR valve in order to minimize the interactions between the exhaust and the intake lines.

The calibration methods can be also distinguished on the base of the type of control used for the actuators. The so called open loop methodology is the most accurate and the most difficult to implement. It consists in imposing in the actuators submodels the values measured during experimental testing. The different models are then tweaked in order to obtain the same outcomes reported for the engine on test bench. The main difficulty introduced by this method is that an actuator modelling defect may induce significant errors on the calibration. The so called closed loop method consists in imposing

controllable variables like the intake pressure and the air fuel ratio; the actuator regulation will be then imposed by the model in order to obtain the desired values for the given operating variables. Any defect in the actuator modelling does not induce error anymore by applying this strategy and the component calibration can be achieved in an easier way.

The validity of the model calibration in steady state conditions is usually proved on several steady state set points covering a large range of engine speeds and loads representative of the whole engine application field. For each operating condition chosen, the simulator results are compared to test bed results and the accuracy of the model is evaluated.

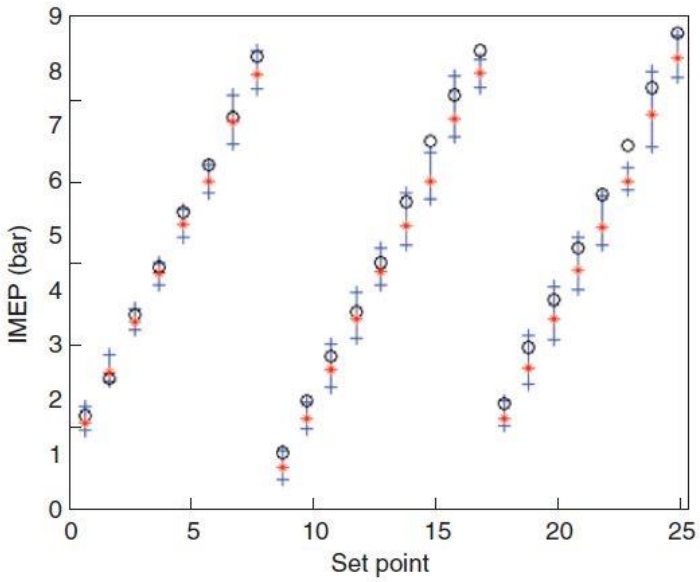

Figure 2-22: Comparison between model (circle) and bench (star) for the IMEP on the 25 operating set points (standard deviation range in solid line) [34]

The choice of the operating points also depends on the use that will be done of the model; in any case is better to prove the validity of the model on the whole range of speeds and loads of interest, if not on the complete engine operating range.

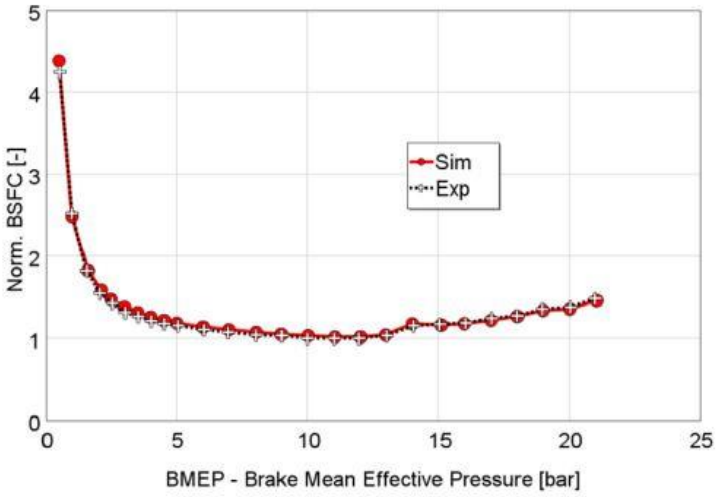

Figure 2-23: Normalized Brake Specific Fuel Consumption at 2000 rpm part load: simulated (red solid line) and experimental (black dashed line). The match between the simulation results and the measurements is quite good and can be considered as satisfactory [37]

2.6.2 Simulation in transient conditions

An automotive engine is working in transient conditions most of the time. Hence, both in test and simulation it is of paramount importance not to limit performance assessment to the steady state operations; this is especially true for turbocharged engines, characterized by phenomena such as the so called turbolag. The usefulness of engine simulation in transient conditions is even more evident than in steady state conditions, since the physical testing is very time demanding and expensive. Different methods can be used to evaluate dynamic performance of an engine, depending of the objectives of the test. A first distinction of the type of simulation can be made as follows:

- Vehicle level simulation: outcome of the simulation is vehicle performance over time, i.e. instantaneous vehicle acceleration and velocity or fuel consumption and pollutant emissions on a given driving cycle. This kind of simulation is useful in order to evaluate, for instance, the performance of different engines on the same vehicle. On the other hand it has several drawbacks. It requires, indeed, modeling a gear box and a vehicle characteristic and the extension of the model, besides being time demanding, could introduce errors not dependent on the engine model.

- Engine level simulation: the engine operating condition is varied over a period of time and the results are limited to variation of engine parameters, such as engine speed, IMEP, BMEP, turbocharger speed.

Besides this distinction, different type of transient operating conditions can be simulated. Some among the most common types are described below.

Simulation of a load step: this type of simulation consists in simulating a step opening of the throttle and the subsequent increase in the engine load. It can be chosen to simulate the engine at a fixed speed (chosen for this work and described in details in the next paragraph) or to simulate a so called tip-in maneuver. In the latter case an abrupt opening of the throttle body and the subsequent acceleration of the vehicle is simulated; this second case obviously requires a vehicle and transmission model.

Simulation of a complete driving cycle: it consists in imposing the vehicle speed (if a vehicle model is considered) or the engine load (if the engine only is simulated) over a longer cycle during which engine speed and load will increase and decrease multiple times to reproduce real world conditions. It is very useful, for instance, in evaluating the effect of different parameters on the fuel consumption on a given driving cycle. The length of the cycle can be in order of magnitude of minutes in real time, as a consequent a model which runs much slower than real time is not suitable for this kind of simulations; a fast running or map based model is generally preferred.

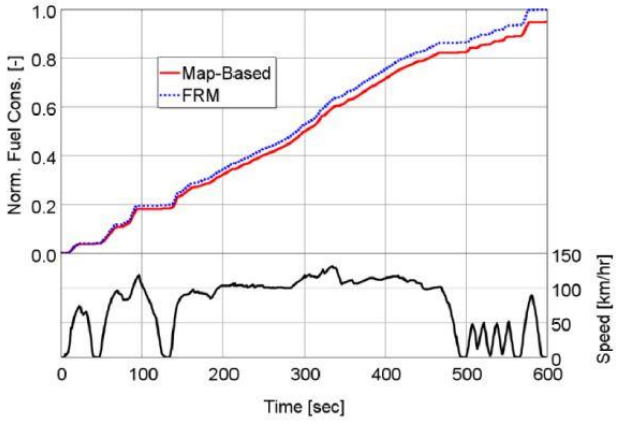

Figure 2-24: Integral of fuel consumption (normalized) over an US06 simulation, Map-Based (red solid line) and FRM (blue dashed line) [37]

2.6.3 Load step at fixed engine speed

One of the main issues for turbocharged SI engines is represented by the turbolag during load transient, as a consequence the simulation of this kind of condition is very useful in order to optimize control strategies and obtain the best possible response time. The 1-D compressible flow formulation used by software such us GT-Power in steady-state conditions is relevant also in transient conditions, hence many authors have used this kind of tool to compare different technical solutions, at least in a relative way. To ensure that model predictions are quantitatively significant a validation versus experimental results would be necessary. Especially if the combustion is modelled by imposing a combustion profile or a Wiebe function, these models should be calibrated thanks to experimental data obtained in transient conditions [38].

The procedure implemented to simulate the load transient is the following. The speed is fixed for the whole transient simulation and usually a value between 1000 and 2000 rpm is chosen [38]- [39]. At the beginning of the simulation a steady-state condition must be reached for a very low load, e.g. 2 bar BMEP. The transient is started by suddenly opening the throttle: a realistic value for the throttle opening duration is between 0.15 and 0.3 seconds, but depending on the accuracy needed even an instantaneous throttle opening can be simulated. The increase in BMEP over time up to the maximum load is predicted together with the evolution of other engine variables.

When a turbocharged engine is object of the simulation or testing, two phases of the transient can be identified. At the beginning of the load change (up to about 0.5 seconds) the engine runs like a naturally aspirated engine. During this first phase the increase in engine load is very fast, as well as the increase in intake pressure. This phases ends when the intake pressure reaches the atmospheric one, i.e. the action of the compressor is necessary to further increase this pressure. During the second phase, the boost pressure is increasing slowly: the main part of the energy is exploited to overcome the inertia of the turbocharger and accelerate its rotating components.

When a second, electrically driven compressor, is placed in series with the main compressor a third phase can be in some cases identified during the transient [40]. At first, as in the case of the turbocharged engine, for a very short time (less than a half

second) the engine runs almost as a naturally aspirated engine and the intake pressure rapidly builds up to a value around 1 bar. In the second phase, both the electric and the main compressor are accelerating. The BMEP increase is faster than it would without electric boost but still slower than during the first phase. During the third phase (which starts when the E-Boost has reached the maximum speed) the load keeps increasing due to the action of the turbo compressor only, up to its maximum value.

The relative length of phase 2 and 3 is dependent on the characteristics of the boosting systems. In particular, if the electric supercharger was large enough it would be possible to have the load increasing very fast almost up to the maximum value.

The main objective of this type of simulation is the evaluation of the response time. The latter is usually defined as the time needed to reach the 90% of the maximum torque value (see Figure 2-25).

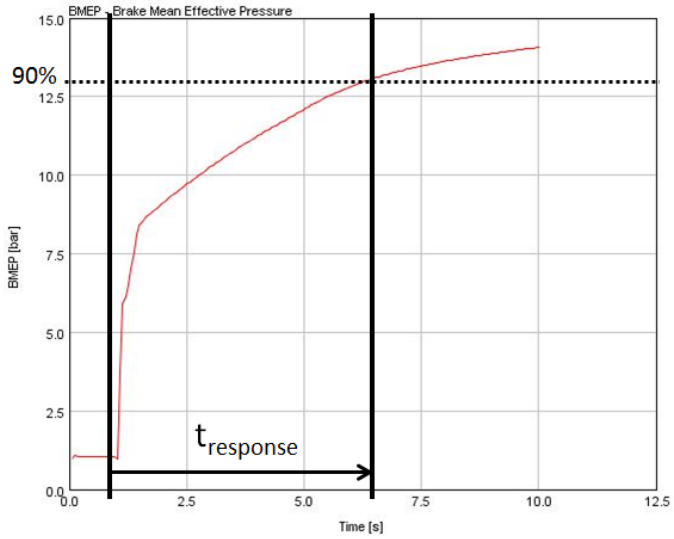

Figure 2-25: Definition of response time - required to reach 90% of max BMEP. Picture adapted from [41], the values of BMEP and time do not refer to the engine considered in this work

If an electrical boost (or any other device able to increase the maximum BMEP) is applied, it is also useful to define a 'relative response time': the time needed to reach 90% of the maximum torque value reached without the electrical supercharger. Comparing such a parameter with the response time of the base turbocharged engine gives a direct assessment of the electric supercharger contribution.

3 ENGINE AND MODEL DESCRIPTION

3.1 Engine General Specifications

The engine considered for the simulation activity is a research engine by FCA. The engine was being tested at CTC, Auburn Hills, MI before and during the timeframe of this project; the engine is not yet introduced in any production vehicle. As a consequence, some limitations applied to the engine data that were provided to the author in the first phase of this work and some data will be reported in a non-dimensional form in the following chapters for confidentiality reasons. The main engine specifications are reported in the table below.

Engine type	4 cylinder inline, SI, supercharged
Valve System	4 valves per cylinder, VVT with independent cam phasing
Fuel delivery	Sequential Port Injection
Induction system	Turbocharger (twin-scroll with wastegate valve), Electrically driven supercharger
EGR System	Low pressure cooled EGR

Table 3-1: Engine specifications

In Figure 3-1 the configuration of the engine is shown, including the intake and exhaust systems. The intake system features an electrical supercharger located upstream of the turbocharger compressor which can be bypassed when its contribution is not needed. This configuration certainly causes less packaging issues than it would if the position of the two compressors was inverted. The electric compressor can indeed be added along the intake system with no need to separate the turbocharger from the engine and fewer restrictions apply to design of the bypass channel. Furthermore, the fact that the turbine is still located close to the exhaust valves (as it would be in a production turbocharged engine), is an advantage because less exhaust enthalpy is wasted as heat transfer during the path to the turbine inlet. The turbine is a conventional twin-scroll controlled by a

wastegate valve. The EGR system is of the Low Pressure Loop type: the exhaust gas is extracted downstream of the turbine and reintroduced in the intake system upstream of both the compressors. The characteristics and advantages of this type of system were already discussed in the paragraph of literature review about external EGR. The throttle valve is located downstream of the turbocharger compressor, the intake gases, after flowing through the throttle have to pass through the charge air cooler and then finally to the 4-cylinder engine. The fuel is injected in the intake ports; the engine does not feature a direct injection system and as a consequence cannot be run in stratified mode. It is, on the contrary, meant to be operated always in stoichiometric conditions without the need for mixture enrichment in most cases.

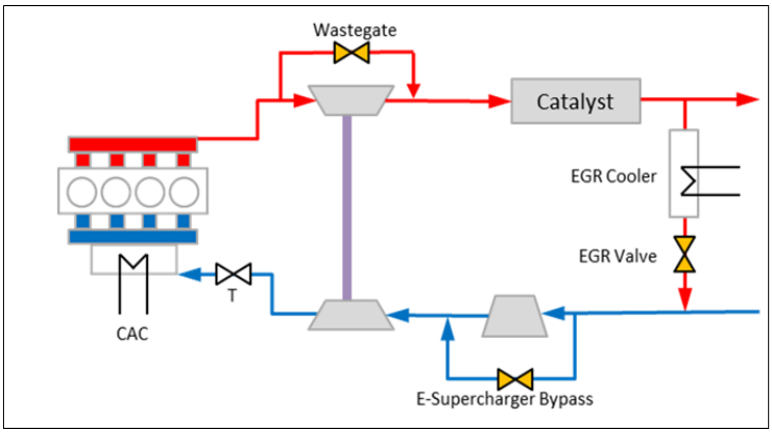

Figure 3-1: Engine system schematics

3.2 GT-POWER Model Description

GT-Power is the leading engine simulation software used by the majority of car makers and engine manufacturers to simulate the performance of internal combustion engines during design and development phases. It is a 1D simulation tool for computational fluid dynamic (CFD); it is a licensed product from the package GT-SUITE, provided by the company Gamma Technologies.

The software is based on one-dimensional fluid dynamics, which is used to represent the flow and heat transfer in the flow components of an engine system. In addition to the fluid flow modelling, the code contains many other specialized sub-models required for

system analysis. GT-SUITE features an object-based code; its structure consists of a three-level hierarchy: templates, objects, parts (these three terms will be used in the following paragraphs to describe the elements in the considered model). Templates are provided in libraries, they contain the unfilled attributes needed by the various sub-models. Objects are templates in which all the values of the attributes are specified; when components and connections objects are placed on the project map they become parts and inherit their values from their parent objects.

With the use of the model the author simulated the behavior of the considered engine in both steady-state and transient conditions. The exact procedures used for the different type of simulations will be explained in the next chapter; in the following paragraphs the working principle of the model is explained and the main modelling choices are reported and justified.

3.2.1 Fluid Dynamics

Fluids behavior in the modeled internal combustion engine (intake air, fuel, combustion products, etc.) is predicted by solving the Navier-Stokes equations, i.e. conservation of continuity, momentum and energy equations. In GT-Power, the solutions are based on one-dimensional fluid dynamics: the equations used to describe the behavior of the fluids are resolved in one dimension, which basically means that all the quantities are averages through the direction of the flow. In order to be simulated with GT-Power the whole system needs to be discretized, i.e. split in smaller volumes. Each pipe is divided into one or more volumes and each ‘flowsplit’ is represented by a single volume, as shown in Figure 3-2.

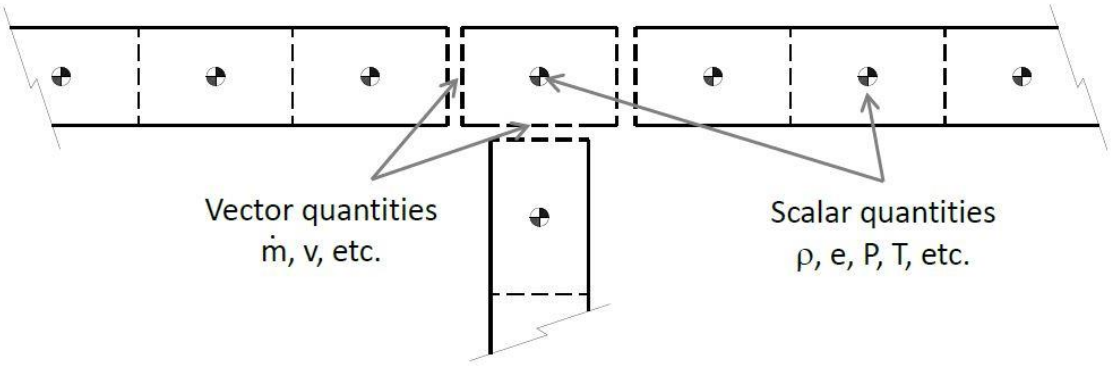

Figure 3-2: Schematic of flowsplit and adjacent pipes discretization in GT-Power [42]

For each of the small sub-volumes, the software computes the scalar variables (like pressure, temperature, density, internal energy, etc.) at the centroid; these are indeed supposed to be uniform in the considered sub-volume. The vector quantities (like mass flux and velocity) are instead computed at the boundary of each sub-volume.

This means that large volumes will badly describe the real behavior of the fluid because only one value for scalar quantities is considered and the small variations are not caught by the system. On the other hand, if the discretization is small the computational time will increase; the trade-off between longer simulation time and increased accuracy must be carefully considered.

There are two choices for the time integration method in GT-Power: it is possible to select an explicit or an implicit integrator. The primary solution variables in the explicit method are mass flow, density and internal energy. The primary solution variables in the implicit method are mass flow, pressure and total enthalpy. The explicit method is recommended for the large majority of GT-POWER simulations [42] and it is utilized in the considered model. It is undesirable only for simulations that are relatively long (on the order of minutes in real time) because of the small time step required, which would cause very long simulation times. The relation between the time step and the discretization length is determined by the Courant condition, smaller discretization length will mean smaller time steps and longer simulation duration. According to GT-Power manual, a discretization length of approximately 0.4 times the cylinder bore diameter is recommended for the intake system and 0.55 times the bore is recommended for the exhaust system. The difference in the recommendation for intake and exhaust

discretization is the result of differences in the speed of sound due to the different temperature. The conservation equations used to calculate the values of mass flow, density and internal energy (the primary solution variables) can be found in the GT-Power Flow Theory Manual [42], as well as the procedure used by the model to derive from them also pressure and temperature at each time step. This is done knowing the mass in each volume and calculating the density first; afterwards, from the equations of state for each species, pressure and temperature are calculated as a function of density and energy.

Pipes and flowsplits wall temperatures are also calculated by the model, the temperature solvers take into account the internal heat transfer, the external heat transfer, the thermal capacitance of the walls, and the initial wall temperature entered by the user. The wall temperature may be solved in both a steady-state or transient simulation. If a steady-state simulation is selected, the software tries to reach the final steady-state wall temperatures as quickly as possible so that a fully-warmed system may be simulated in only a few cycles [42] , i.e. lower weight is given to the thermal capacitance of the walls.

3.2.2 In-cylinder flow and heat transfer

The same type of flow modelling cannot be applied to the flow inside engine cylinders, since it is not possible to accurately represent them with 1D elements. The in-cylinder flow model breaks the cylinder into multiple regions: the central core region, the squish region, the head recess region, and the piston cup region. At each time step in each region, the mean radial velocity, axial velocity, and swirl velocity are calculated taking into account the cylinder chamber geometry, the piston motion, and the flow rates of the incoming and exiting gases through the valves [43]. The flow model also contains single zone turbulence and tumble models. The turbulence model solves the turbulence kinetic energy equation and the turbulence dissipation rate equation; from those the instantaneous mean turbulence intensity and turbulence length scale are calculated. These turbulence values are used in the predictive combustion model and the heat transfer models.

Among the various available in-cylinder heat transfer model, the 'WoschniGT' type was selected. The in-cylinder heat transfer is then calculated by a formula which closely emulates the classical Woschni correlation (reported also by Heywood [13]) without swirl [43]. A convection multiplier is available in this sub-model to tune the heat transfer intensity on the basis of experimental data or 3D CFD simulations. No modifications to this multiplier were implemented by the author.

3.2.3 Predictive combustion model

The selected GT-Power combustion model is called Spark-Ignition Turbulent Flame Model ('EngCylCombSITurb'). This model predicts the burn rate for homogeneous charge, spark-ignition engines. This prediction takes into account cylinder geometry, spark locations and timing, air motion, and fuel properties. The mass entrainment rate into the flame front and the burn rate are governed by the following three equations, reported from GT-SUITE Engine Performance Application Manual [43]:

$$\frac{dM_e}{dt} = \rho_u A_e (S_T + S_L) \tag{3.1}$$

$$\frac{dM_b}{dt} = \frac{(M_e - M_b)}{\tau} \tag{3.2}$$

$$\tau = \frac{\lambda}{S_L} \tag{3.3}$$

These equations state that the unburned mixture of fuel and air is entrained into the flame front through the flame area (A_e) at a rate proportional to the sum of the turbulent and laminar flame speeds (S_T and S_L respectively). The burn rate is proportional to the amount of unburned mixture behind the flame front ($M_e - M_b$) divided by a time constant (τ). The time constant is calculated by dividing the Taylor microscale (λ) by the laminar flame speed. Turbulence intensity (turbulent flame speed) and length scale will be provided by the in-cylinder flow model.

In order to calibrate the combustion model with experiment, one can adjust the effects of turbulence intensity and length scale on the calculation of turbulent flame speed and the Taylor microscale length using the multipliers available in the template, i.e. Flame Kernel Growth Multiplier, Turbulent Flame Speed Multiplier, Taylor Length Scale Multiplier. In the considered model for the first two multipliers an increasing trend with engine load was already defined in the model given to the author, the latter was adjusted to give the best possible agreement of the combustion phasing with experimental data; the parameter used to validate the model was the 50% burned fraction crank angle (CA50). It was avoided an excessive modification of this multiplier since that would imply that the latter is probably used to compensate some other inaccuracies of the model. GT-SUITE manual [43] suggests that usually a value of 2 must not be exceeded for this kind of multipliers. The effective trend of the mentioned multipliers will be shown in the results chapter.

3.2.4 Knock model

The 'EngCylKnock' object may optionally be activated in combustion reference objects to make phenomenological predictions of knock or pre-ignition tendencies in spark-ignited combustion. This object allows the user to choose between different knock prediction models; in this case the 'Douaud&Eyzat' knock model is used. The latter uses the method described by A. M. Douaud and P. Eyzat [44].

The occurrence of knock is predicted based on empirical induction time correlations. The following equation [45] defines the induction time integral or so-called "state of pre-reactions":

$$I(t) = \int_0^t \frac{1}{\tau_i} dt \tag{3.4}$$

The empirical correlation for the induction time integral can be written in terms of crank angle as:

$$I(\alpha) = \frac{1}{6(\omega)} \int_{-100}^{\alpha} \frac{1}{M_1 C_1 \left(\frac{ON}{100}\right)^{C_2} p^{-C_3} exp\left(\frac{C_4}{M_2 T_u}\right)} d\alpha \tag{3.5}$$

In the model of Douaud and Eyzat, knock is predicted to occur at the crank angle at which the induction time integral (for any end gas zone) attains a value of 1.0.

The formula above is influenced by instantaneous pressure and temperature and by the fuel properties (octane number, coefficients from C_1 to C_4); on the other hand, it has no direct dependence on air/fuel ratio or on EGR fraction even though knock occurrence is influenced by both. Therefore, it is likely that the Knock Induction Time Multiplier (M_1) and Activation Energy Multiplier (M_2) should be modified from their default values when the air/fuel ratio is not stoichiometric or if EGR is present in significant amounts. Specifically, EGR is expected to make the mixture more knock resistant than a baseline mixture without EGR, therefore increasing the induction time. In the model used for this project, the influence of EGR is taken into account for; in particular the Induction Time Multiplier is calculated, from case to case, as a polynomial function of the EGR fraction.

It must be noted, though, that the dependency on EGR (and in general the knock model) has not been precisely calibrated using experimental data aimed at helping in the knock model development. As a consequence, the prediction of knocking by the model will not be considered quantitatively precise in this work. As far as the transient run are concerned, for instance, even a value of the induction time integral up to 1.2-1.3 will be considered acceptable.

3.2.5 Turbine and compressors modelling

Turbine and compressor modelling is not based on direct CFD analysis, performance of these elements is modeled in GT-SUITE using performance maps that are provided by the user to the software. Both compressor and turbine maps can be summarized as a series of performance data points, each of which describes the operating condition by specifying speed, pressure ratio, mass flow rate, and thermodynamic efficiency. The

maps are supplied by the turbomachinery manufacturers. The data provided to the model for each turbine/compressor must be organized as several different speed lines; in the considered model, for instance, eight speed lines are provided for each compressor. Each speed line is made of several sets of the remaining three variables. The raw data given as an input to the model is extrapolated and interpolated during a preprocessing phase to create maps that define the performance of the component even outside of the input data range. In GT-Power the pressure ratio is predicted together with the turbocharger speed at each time step and the other two variables are looked up in the map. The mass flow rate from the map, which may be damped in case of extreme fluctuations, is then imposed as a boundary condition for the flow of the adjacent elements. Knowing the efficiency (η, from the map) also the outlet enthalpy can be calculated (equations reported below). Turbine/compressor outlet temperature and power are then evaluated from the outlet enthalpy.

Compressor:
$$\Delta h_s = c_p T_{total,in}\left(PR^{\frac{\gamma-1}{\gamma}} - 1\right) \tag{3.6}$$

$$h_{out} = h_{in} + \Delta h_s \eta \tag{3.7}$$

Turbine:
$$\Delta h_s = c_p T_{total,in}\left(1 - PR^{\frac{1-\gamma}{\gamma}}\right) \tag{3.8}$$

$$h_{out} = h_{in} - \Delta h_s \eta \tag{3.9}$$

where
$$T_{total,in} = T_{in} + \frac{u_{in}^2}{2c_p} \tag{3.10}$$

Turbine/Compressor:
$$P = \dot{m}(h_{in} - h_{out}) \tag{3.11}$$

The modelling approach for the twin entry turbine consists in treating both scrolls as completely separated turbines. Each of them is modeled by placing a turbine part in the engine map. In each of the turbine parts more than one turbine map are specified, and this is done exploiting the template available in GT-SUITE for variable geometry turbines.

The different maps, instead of being associated to different rack positions (as for actual variable geometry turbines), are meant to model the different behavior of the turbine depending on equal admission or admission in only one of the two scrolls. The interaction between the two scrolls is accounted for by integrating an orifice between the inlets of the two scrolls. It is common practice to calibrate the cross sectional area of the orifice depending on the operating point to match measured engine data. In the considered model the orifice diameter varies (increases) with engine speed.

The wastegate valve is modelled by means of an external wastegate flow path. The valve is represented by an orifice, which diameter can be imposed as a fixed value by the user or changed by a controller during the simulation. GT-SUITE provides a built in controller for the wastegate diameter, which automatically calculates the desired wastegate diameter to obtain a given target for a specified quantity; this type of controller is used in this work (for steady state simulations) and the target quantity is the engine BMEP.

The turbine/compressor torque associated to the power is used by the software to calculate the turbocharger speed (ω_t) at the end of the simulation time step; the moment of inertia of the turbocharger (I_t) must be provided. The latter is specified in the 'ShaftTurbo' element, which is used to connect the turbine to the compressor and make the turbocharger. In the same template also an 'Inertia Multiplier' attribute is available; this is often used in steady state simulations to keep the inertia very high for the first part of a simulation so that the shaft does not slow down while the system is building up its initial pressure and velocity.

The formula used to compute the change in turbo speed, from the GT-Power manual [43], is reported in Equation 3.12.

$$\Delta\omega_t = \frac{\Delta t\left(T_{turbine} - T_{compressor} - T_{friction}\right)}{I_t} \tag{3.12}$$

This formula includes also a friction component ($T_{friction}$) of the torque; the latter is part of the computation only when the friction is represented by the use of the 'Friction Mechanical Efficiency' attribute in the 'Shaft' part that connects the compressor and

turbine. However, in the model used in this work, as in many cases, the bearing losses are included in the turbine efficiency in the map data. Most suppliers of turbochargers, indeed, measure the turbine efficiency in such a way that the bearing friction is combined into that efficiency; in most cases this is an acceptable approximation.

For what concerns the electrically driven compressor, a ‘Shaft’ part is not included in the model. The compressor is just connected to a ‘SpeedBoundaryRot’ object, which can be used to prescribe a constant or variable angular velocity on 1-D rotational parts. The imposed rotational speed will be, obviously, constant during steady-state simulations; on the other hand a time varying profile will be imposed during transient simulations.

4 SIMULATION PROCEDURES

4.1 Steady-State Simulations

The model described in the previous chapter was, at first, used for simulations of engine performance in steady-state conditions. As previously stated, the model was provided to the author at the beginning of the project; as a consequence, in the first phase of this work an analysis of the model and a refinement of the latter in order to be fitted for the objectives of this research were conducted. Even if the model was already working and most of the calibration work of the various sub-models had already been conducted, some minor modifications were made to the model (as explained during the previous section) in order to obtain its validation versus experimental data, necessary step to assume the meaningfulness of the results obtain in the following phases of the project. The aforementioned experimental data was provided by FCA to the author partially at the beginning of the research project and the partially during the time frame of this work. The procedure to obtain validation of the model is basically very simple: set in the model the same input as for experimental conditions; run the model; check that the results are in agreement with experimental data within a given range of accuracy. Not all of the possible engine data were available though and, as mentioned in the description, the model has the capability to control autonomously some of the engine operating parameters; the exact procedure chosen to run the model is explained below.

The parameters which were chosen to be imposed by the user, considering they were available from experimental data, are reported below.

- Engine speed
- Air-Fuel ratio: imposed in the 'InjAFSeqConn' part, which is used in GT-POWER to model a sequential injector with imposed A/F ratio for port injected engines. The name of the part which will sense the air mass flow rate for the Fuel Ratio calculation is specified in the part, the resultant injection pulse width is calculated for each injection event.

- Intake valve timing: a fixed valve lift can be shifted earlier or later during the cycle by specifying a single parameter which defines the position of the valve event with respect to the firing TDC.
- Exhaust valve timing: controlled using the same method as for the intake valve timing.
- Spark timing
- Ambient pressure and temperature: considered fixed and independent from the operating condition. T_{amb}=298.15 K; p_{amb}=0.98 bar.
- Electric supercharger Speed (if different from 0 rpm)
- Electric supercharger by-pass valve position

The following parameters were chosen to be imposed as a target to be achieved by the model as explained below:

- BMEP: the two operating variables affecting the engine load (considering the variables mentioned above as fixed) are the throttle valve angle and the wastegate valve opening, and those are actuated by two controllers which are targeting the imposed value for the engine BMEP. Two different types of operating conditions must be distinguished for this engine depending on the load. If the BMEP target is lower than a certain value (which will be called $BMEP_{MT}$ – maximum throttle - and is in the medium load range) the two controllers act simultaneously in the model. It must be noted that in this condition is the throttle which is mainly controlling the load, since the intake pressure is kept below atmospheric by the restriction in the intake flow. The wastegate control is active but in general it will leave the valve in the position of maximum opening, since no boost pressure is needed to achieve the required load. If the BMEP target is higher than $BMEP_{MT}$ than the throttle will be imposed to be fully open and the load will be mainly controlled by the wastegate valve.
- EGR: exhaust gas recirculation valve is reproduced in the model by an orifice with variable diameter. The diameter is varied during the simulation by the EGR controller, which is a part derived from the so called 'ControllerEGRValve' template. This template contains a model-based controller used to target EGR rate

by controlling throttle angle or an orifice diameter (this second option is selected in this case). This built-in controller is a useful tool in order not to have to design a PID controller which would require significant effort to determine gains for this particular application.

When the simulation is run, after some start-up cycles, the input values are imposed and the controllers are activated. The model then runs until the controllers have achieved their targets (if possible) and the convergence to a stable condition is reached by the system. In order for the simulation to be considered converged and to be automatically shut-off, several conditions must be verified:

- Convergence of the wastegate controller: a maximum error of 2% must be verified over a cycle. The condition must be verified for two consecutive cycles.
- Cycle to cycle convergence of BMEP: at the end of each cycle the value of the variable is checked, the fractional variation with respect to the previous cycle must be lower than 0.001. The condition must be verified for 4 consecutive cycles.
- Cycle to cycle convergence of CA50: at the end of each cycle the value of the variable is checked in a given cylinder, the fractional variation with respect to the previous cycle must be lower than 0.0002. The condition must be verified for 3 consecutive cycles.
- Cycle to cycle convergence of EGR fraction: at the end of each cycle the value of the variable is checked, the fractional variation with respect to the previous cycle must be lower than 0.0001. The condition must be verified for 2 consecutive cycles.
- Convergence for torque on mechanical parts with rotational degree of freedom: the torque imbalance is checked and compared with a tolerance value at the end of each cycle. The default value, used in this model, is 0.002 (fraction). Considering that the speed of the crankshaft and electric compressor are imposed, the only rotational part for which torque balance must be checked is the turbocharger shaft.

When all of the mentioned conditions are verified, the simulation is automatically stopped and the results are available for analysis through GT-POST (the graphical interface that enables viewing and manipulating of the data collected from the simulation).

4.1.1 Model Validation

In the first part of this work the validation of the model was obtained by comparing the model results with experimental data obtained and provided to the author by FCA.
The engine values that were chosen to be used for comparison with experimental data are:

- Engine BMEP [bar]: since it was imposed as a target, a value very close to the experimental one is expected; it is necessary to check anyway, at least in cases of maximum load, to ensure the engine is capable to reach the target.
- BSFC (Brake specific fuel consumption) [g/kW h]: it is a direct measure of how much fuel is needed to produce a given power output. It is a macro engine variable which gives important evidence that the model is correctly predicting the engine behavior. Furthermore, a typical application of engine models is to help during control design, in order to optimize some parameters to get the best fuel consumption; thus, a correct prediction of the fuel consumption is very important.
- Air mass flow rate [g/s]: the amount of air flowing through the engine intake per second is a fundamental variable to determine if the simulated operating condition is close to the experimental one.
- Intake manifold pressure [bar]: it is an important variable to be checked because it is related to the effect of the turbocharger and electrical compressor.
- CA50 [crank angle degrees]: it is the only combustion variable that was chosen to be compared for model validation. Obviously it does not insure that the burn rate and heat release rate are matching exactly the experimental trends, but it is a very powerful tool to get a first approximation of the combustion phasing, given that the spark timing from experimental data is imposed.

The choice of the set of operating conditions to be simulated in order to obtain the model validation was based on two main factors: the first is the availability of experimental data; the second is the range of loads and speeds of interest for the next steps of this work.

Two different speeds were selected, both in the low speed range because this is the area of interest of this research: 1500 and 2000 rpm. For each speed 8 different operating points were simulated, from very low to maximum load. Figure 4-1 and Table 4-1 sum up the operating conditions chosen for model validation. The engine load is expressed as the BMEP normalized to the value of the highest load condition at 1500 rpm when the electric supercharger is not applied (condition characterized by a value equal to 100% in Table 4-1). The absolute values are not shown because this information is FCA confidential.

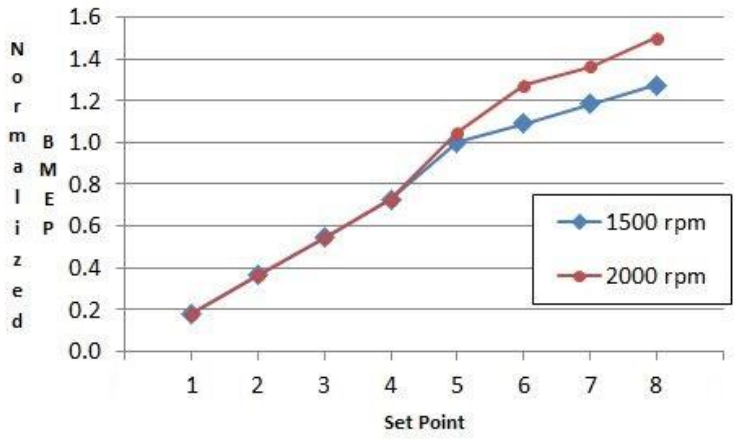

Figure 4-1: Normalized BMEP for model validation set points

The three operating points characterized by the highest BMEP, for the two speeds, refer to conditions in which the electric supercharger is active; as a consequence they are highlighted in Table 4-1.

		Engine Speed [rpm]	
		1500	**2000**
Normalized BMEP [-]	Turbo Only	19%	19%
		36%	36%
		55%	55%
		73%	73%
		100%	105%
	Turbo and Electric Supercharger	109%	127%
		118%	136%
		127%	150%

Table 4-1: Set of steady-state operating points for model validation

4.1.2 Remarks about engine operating conditions

The operating points simulated for the model validation phase were imposed by the experimental conditions selected in FCA when the testing was conducted. Even though the author didn't take part in the setup of the testing, some of the trends in the input variables will be discussed and explained in this paragraph for clarity and in order to highlight their impact on engine performance.

Among the input parameters, an important role in defining engine performance is played by the spark timing. The latter is progressively retarded while the load is increasing, both at 1500 and 2000 rpm, up to extreme cases at very high loads in which the spark is fired around or after TDC, as shown in Figure 4-2. The reason is the need to avoid knock occurrence while the load is increasing: higher load causes higher temperature and pressure inside the engine cylinders, hence knock is more likely to occur for a given spark timing. The trend is not linear in the high load region because other factors, mainly EGR fraction, influence the combustion.

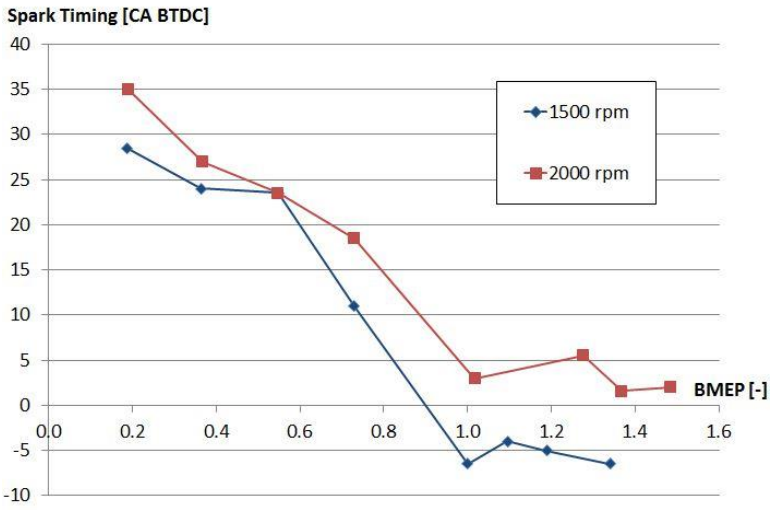

Figure 4-2: Spark timing (expressed in crank angle degree before TDC) of model validation set points

Very retarded spark timing will cause in-cylinder pressure behavior throughout the cycle to be pretty different from what expected for a conventional SI engine, as shown in Figure 4-3.

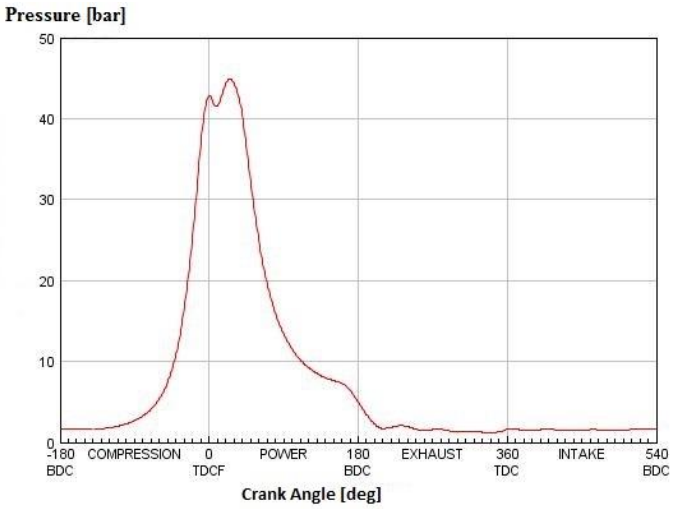

Figure 4-3: Example of in-cylinder pressure trace for retarded spark firing from GT-POWER simulation

Also the timing of the valves events has a strong effect on the performance of the engine. In particular, late intake valve timing is used at some operating points in order to obtain a

reduction of the effective compression ratio. An extremely retarded intake valve closure is applied at low loads, for instance, in order to reduce the pumping losses.

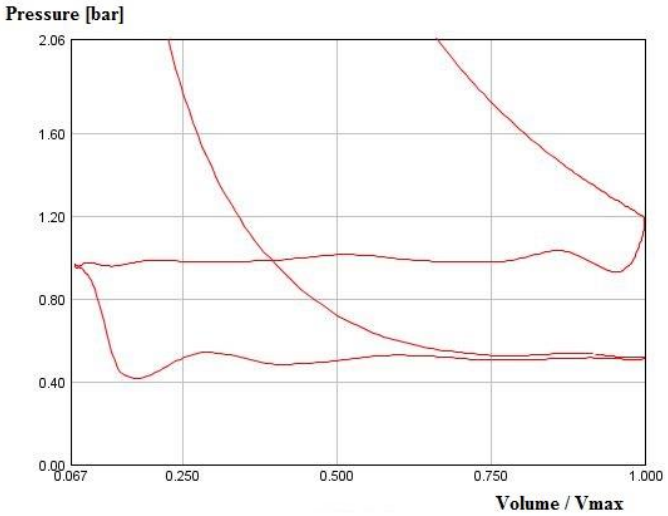

Figure 4-4: Pumping loop p-V diagram from GT-POWER simulation with LIVC at minimum load (1500 rpm)

As can be seen in Figure 4-4, in such a case the in-cylinder pressure does not start rising with respect to the intake pressure (in this case around 0.5 bar) until the in-cylinder volume is reduced by one quarter of the displacement volume by the cylinder motion. This causes the area of the pumping loop to be reduced; hence the pumping losses are reduced, since that is an area of negative work made by the piston on the in-cylinder gases. The VVT system of the considered engine allows only the shift of the given intake and exhaust lifts earlier or later during the cycle; the maximum lift is fixed. As a consequence, the position of the intake valve event can be specified by using a single parameter; the same stands for the exhaust valve event. Those two parameters will be indicated respectively as ICL and ECL and define the position of the lift peak with respect to the firing TDC. Their variation over the load range of the engine is shown in Figure 4-5 and Figure 4-6 respectively. In both cases a positive variation refers to a retarded event and a negative variation to an advanced event with respect to the reference position.

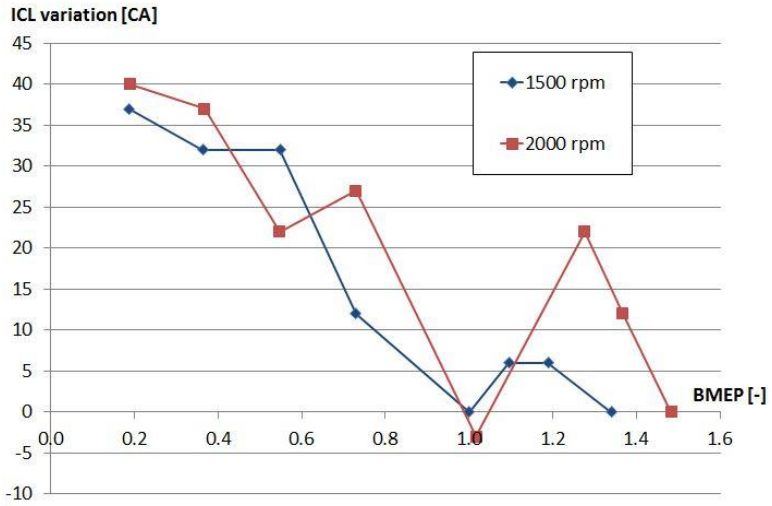

Figure 4-5: ICL variation with respect to value adopted at maximum load, all model validation set points are shown

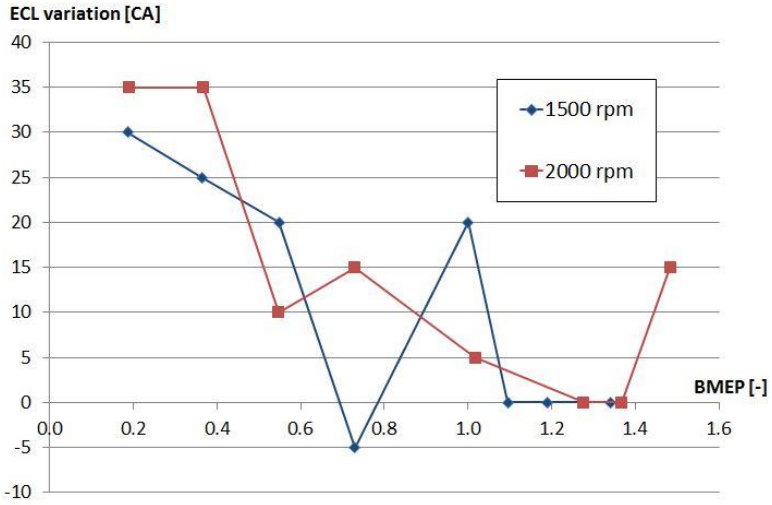

Figure 4-6: ECL variation with respect to value adopted at maximum load (1500 rpm), all model validation set points are shown

The reported trend clearly shows the choice to retard the intake event at low loads in order to obtain the mentioned pumping losses reduction. While the load increases the intake valve event is generally retarded and the exhaust valve event tends to follow the intake one. The exhaust is advanced slightly less than the intake, causing (in most cases) an increase in the overlap while the load is increasing.

The pumping loop on the p-V diagram at medium and high load is then more similar to that of a conventional turbocharged SI engine.

The air-fuel ratio was kept almost stoichiometric over the whole simulated range, as shown in Figure 4-7. Only in the high load region slightly richer air fuel ratio is sometimes used, as happens for conventional SI engines.

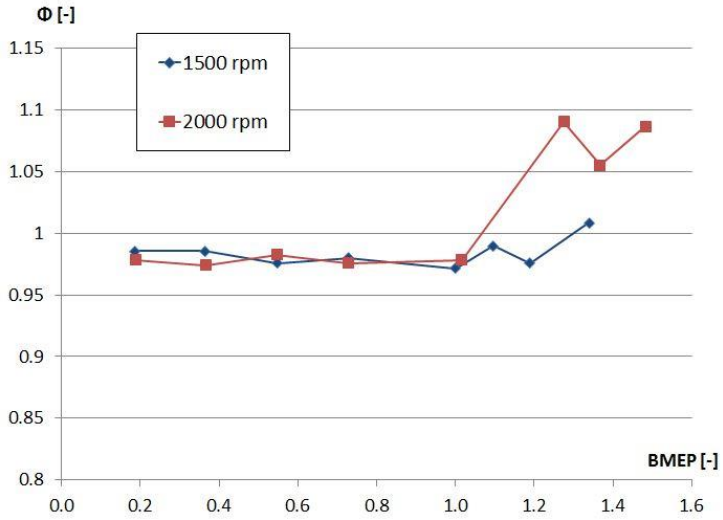

Figure 4-7: Equivalence ratio as a function of normalized BMEP for model validation set points

4.1.3 Steady-state simulations for low end torque improvement estimation

Once the model validation was obtained, steady-state simulation was used to quantify the steady state torque improvement at low speed produced by the contribution of the electric supercharger. In order to do that, a series of simulation was run to estimate the maximum BMEP that the engine could reach (with no knock occurrence predicted by the model) for different engine speeds. The obtained results are meant to be then compared with the torque curves showed in the figure. This represents the torque target that was extrapolated by FCA material provided for the engine considered in this work. The BMEP is in this case normalized to the absolute maximum value for the engine, which is supposed to be obtained for both boosting conditions at engine speeds between 3000 and 5000 rpm.

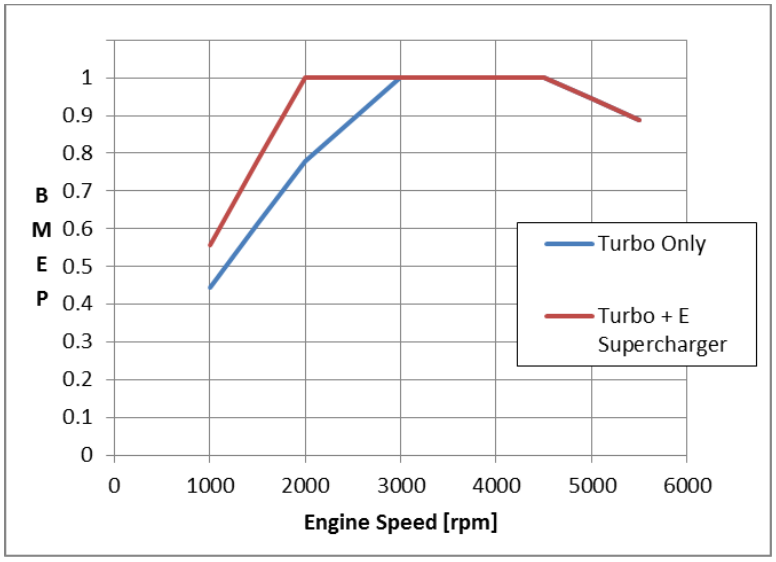

Figure 4-8: Normalized BMEP target vs Engine speed

As can be noticed from the figure, the area characterized by the improvement of the engine torque by the electric supercharger is supposed to be limited to a maximum engine speed of 3000rpm. The aim of this section, more than exactly estimate the maximum load reached by the engine, is indeed to show the contribution of the electric supercharger within this area and to show its decreasing effect as the engine speed is increasing. As a consequence two operating points (the first with active electric supercharger and the second with turbocharged only engine) were simulated for each of the following engine speeds: 1000, 1500, 2000, 2500, 3000 rpm. As far as the choice of the other operating parameters (spark timing, valve timing, EGR fraction, etc.) is concerned, their selection was based on the knowledge of the strategies used in the experimental testing at the operating points considered for validation; their values were maintained as close as possible to the ones used in those cases.

The exact matrix of speed and load conditions imposed to the model for this second phase of the steady-state simulations are summed up in Table 4-2. Note that the load is again normalized because the exact values are not to be disclosed since they are FCA confidential data. The value chosen to normalize the BMEP in this case is the absolute maximum, same as in Figure 4-8. Once again, it is possible to notice how, with the

addition of the second supercharger, the engine is supposed to reach the maximum load at lower speed.

		Engine Speed [rpm]				
		1000	**1500**	**2000**	**2500**	**3000**
Normalized Engine Load BMEP [-]	Turbo Only	44.4 %	61.1 %	77.8 %	88.9 %	100 %
	Turbo + Electric Supercharger	55.6 %	77.8 %	100.0 %	100.0 %	100.0 %

Table 4-2: Engine speed [rpm] and Normalized BMEP target [-] imposed to the model for the operating points used in steady-state simulations

4.2 Transient Simulations

In the last phase of this work the model was used to simulate engine performance in transient conditions. It was necessary to perform some modifications in the model in order to achieve better results; the procedure suggested in the section about transient modelling of the GT-SUITE Manual [43] was followed as closely as possible and the main setting modifications that have been made are reported below.

As far as the turbocharger modelling is concerned, the maps in the software can be used also for transient simulations; what becomes an essential parameter is the moment of inertia of the turbocharger, which must be specified in the 'ShaftTurbo' element as explained in section 3.2.5.

From the point of view of the thermal behavior, it is necessary to set the operating modes of the wall temperature solvers (that must be specified in all the pipes and in the cylinders) to 'transient'; this is necessary so that the temperature solver will calculate the instantaneous temperatures, taking into account also the effect of the thermal capacitance.

The transient simulation type selected for this work is a load step at constant engine speed, as it was described in section of the literature review dedicated to transient simulation (2.6.3). The engine speed selected for this simulation is 1500 rpm. As highlighted in the mentioned section the first step is represented by the simulation of a steady state case at very low load that can be then used as a starting operating point for the transient.

The choice was to run the model with the same procedure as explained for steady-state and to target a value for the BMEP close to the one of minimum load among the operating points used for model validation, i.e. 18% of the maximum load obtainable with no electric supercharger at 1500 rpm. Among the three controllers active during steady-state simulations only the throttle controller is working in these simulations, while the position of EGR and wastegate valve are imposed.

Depending on the position of these two actuators different starting conditions for the transient were simulated:

- No EGR, closed wastegate valve
- No EGR, open wastegate valve
- 5% EGR, closed wastegate valve
- 5% EGR, open wastegate valve
- 10% EGR, closed wastegate valve
- 10% EGR, open wastegate valve

The electric supercharger was always considered to be by-passed in these simulations: its speed set to 0 rpm and the diameter of the by-pass set to the maximum. The valve timings were imposed to be equal to the condition of minimum load at 1500 rpm considered for model validation. The air fuel ratio was set to stoichiometric (Φ=1).

The simulated steady-state conditions were then used as an input for the initialization of the transient cases; this can be done in GT-POWER by specifying the name of the output file of the steady-state case in the transient case.

At the beginning of the transient simulation, the system is kept in steady-state conditions for 1 second in order to ensure that the system is actually stable at the beginning of the

transient. From now on, though, the time of the load step beginning (opening of the throttle) will be referred to as t=0 s.

Once again, to run the transient cases the input variables must be redefined, as explained below.

The throttle controller is not needed for this type of simulation since the throttle opening is now imposed over time, using the 'ProfileTransient' template of GT-SUITE, as shown in Figure 4-9. The time needed to open the throttle from minimum to maximum was chosen to be 0.3 seconds, which is a realistic value according to the literature [35].

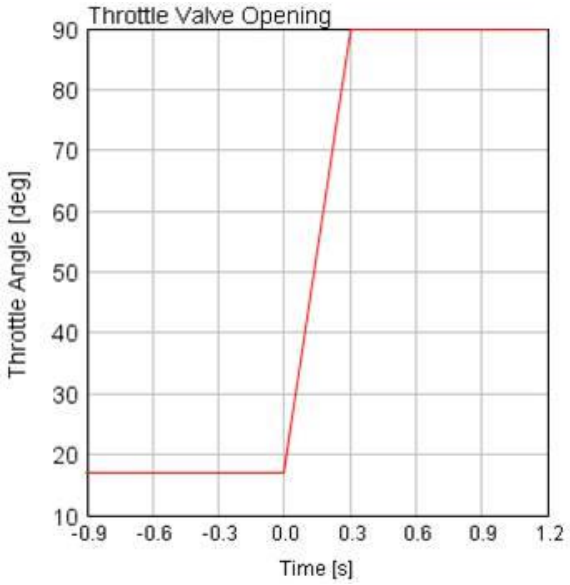

Figure 4-9: Throttle opening step defined in a 'ProfileTransient' template in GT-SUITE

The wastegate valve opening can be controlled by imposing the value of the diameter over time, in order to ensure that the latter is kept equal to 0 mm until the BMEP is closely approaching the target value. This option also permits to simulate a realistic behavior of the wastegate valve. If the latter is open at low loads and needs to be closed during the transient run, indeed, in real application a small amount of time (in the order of magnitude of milliseconds) is needed for the wastegate to be closed after the throttle starts opening. As a consequence, for 150 ms the wastegate will be kept open and then it will be closed in 300 ms. The influence on the response of this realistic actuation strategy

for the wastegate valve, with respect to the idealized case in which the valve is closed for the whole transient, will be shown in the next chapter.

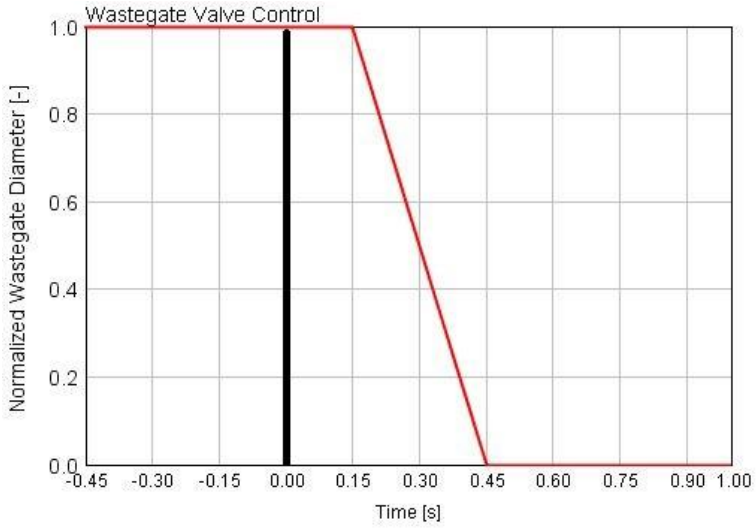

Figure 4-10: Wastegate valve position during the load step

The EGR valve opening also can be imposed over time during the transient run. Different simulations were run in order to find the influence of different EGR valve opening during the load step; the results will be shown in the next chapter.

A stoichiometric air fuel ratio is imposed as for steady-state simulation. Due to the very fast change in the intake air flow rate, the air fuel ratio is expected to slightly detach from the imposed value during the first part of the load step and then to stabilize again.

As far as the spark timing is concerned, it needs to be changed during the transient as the engine load is increasing. Some steady-state simulations were run in order to evaluate the correct spark-timing depending on the load and on the EGR level. A control sub-model, developed by FCA specifically for this engine model, was used to determine the spark (see Table 4-3). This sub-model takes into account several factors such as the BMEP level to be reached and the engine knocking in order to evaluate the correct spark timing; a detailed description of the mentioned element is not provided since it was not developed by the author.

Considering the very fast transient condition simulated, it is likely that a further retarding of the spark will be needed during the load step in order to avoid knocking. In order to

figure out the best spark timing during the transient, the CA at which the spark is fired has been then imposed over time during the simulation (see results chapter) instead of only as look-up table from BMEP.

Normalized BMEP [-]	Spark Timing [CA ATDC]	Spark Timing [CA ATDC]	Spark Timing [CA ATDC]
	0% EGR	5% EGR	10% EGR
0.18	-25.3	-29.7	-36.4
0.36	-18.7	-21.4	-25.0
0.73	-3.1	-6.9	-10.9
1.00	4.0	0.3	-2.8
1.27 (electric supercharger)	8.3	4.4	1.0

Table 4-3: Spark timing as a function of BMEP and EGR to be used as input for the transient simulation

Also the behavior of the electric compressor during the transient must be defined. As previously mentioned, before the load step, the compressor speed is 0 rpm and the bypass channel is open.

At the beginning of the transient the increase in the electric supercharger speed and the closure of the valve must be imposed. The electric supercharger speed is imposed to change as a function of time, linearly increasing from 0 rpm to the maximum speed of 65000 rpm in 0.5 s, as shown in Figure 4-11.

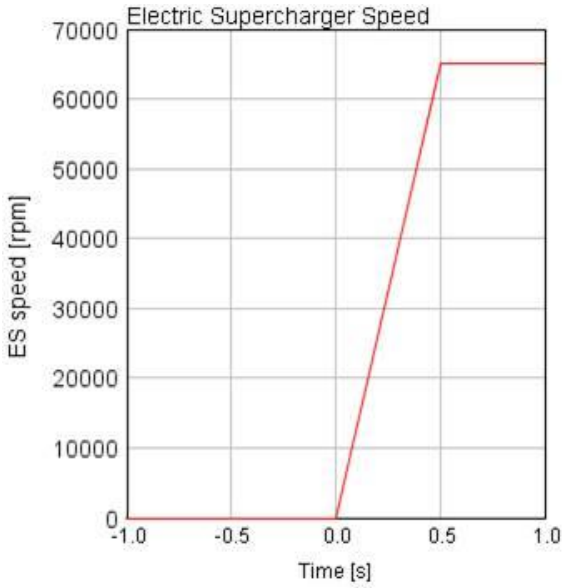

Figure 4-11: Electric supercharger speed during the load step

Such a value for the duration of the electric supercharger transient, besides being realistic according to the literature, was suggested by FCA considering the specification of the compressor and the preliminary testing.

The bypass channel closure is simulated by imposing the diameter of the channel over time: as for the throttle and wastegate valve, a transient duration of 0.3 s from fully open to fully close is assumed.

The influence of some control parameters on the transient response has been also evaluated. In particular, the maximum electric supercharger speed and the time instant at which the acceleration of the compressor starts were separately varied in order to quantify their effect on the transient response. Three different values of the maximum supercharger speed have been chosen, as shown in Table 4-4.

Maximum ES Speed [rpm]	65000	50000	40000

Table 4-4: Values of the maximum electric supercharger speed imposed in different cases in load step simulations

The simulation of different time instant for the activation of the electric supercharger is motivated by the need to reproduce a possible delay in the activation of the electric compressor with respect to throttle opening. The time values chosen roughly correspond to the instant in which 40% and 60% of the maximum load is reached by the turbocharged-only engine.

Time for ES activation [s]	0	0.3	0.5

Table 4-5: Time instant at which the electric supercharger is activated in different cases in load step simulations

5 RESULTS AND DISCUSSION

5.1 Model Validation

Before its use for prediction of engine performance, an engine model has to be validated. This is achieved by comparing computation results with experimental measurements. As previously explained, the test results needed were provided to the author by FCA at the beginning of the project. Experimental acquisitions provided data on a wide set of operating points, only some of them were used to validate the model. The operating points for model validation were selected in the range of interest for the following phases of this project, i.e. low engine speed from minimum to maximum load. From experimental measurements, in general, many mean engine values and instantaneous pressures can be used to calibrate and validate a model. To show that the model is validated, in this case, some mean engine values were selected as explained in Chapter 4.

5.1.1 Load variation at 1500 rpm

The model has been tested with 8 steady-state load points. The load will be expressed in terms of BMEP Normalized to the maximum value without electric supercharger (same notation as in Table 4-1) and it goes from 0.19 to 1.27. The engine load is imposed to the model as a target that must be reached during the simulation by acting on two controllers: throttle angle and diameter of the wastegate ‘orifice’, as explained in Chapter 4. As highlighted in Figure 5-1, the target is always reached with 1% or less error; only for the sixth point the BMEP obtained by the model is slightly lower than the target: the deviation from the experimental value is still only 2.85%. From Figure 5-2 can be noticed that the sixth set point refers to a condition in which the electric supercharger is active; the supercharger speed, though, is not the maximum one but is limited in this case to 45000 rpm.

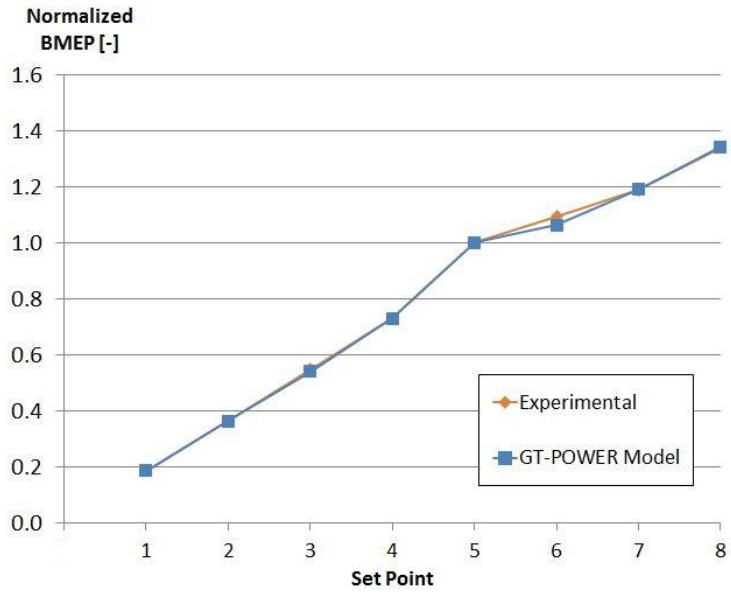

Figure 5-1: Experimental - Model comparison for Normalized BMEP at 1500 rpm

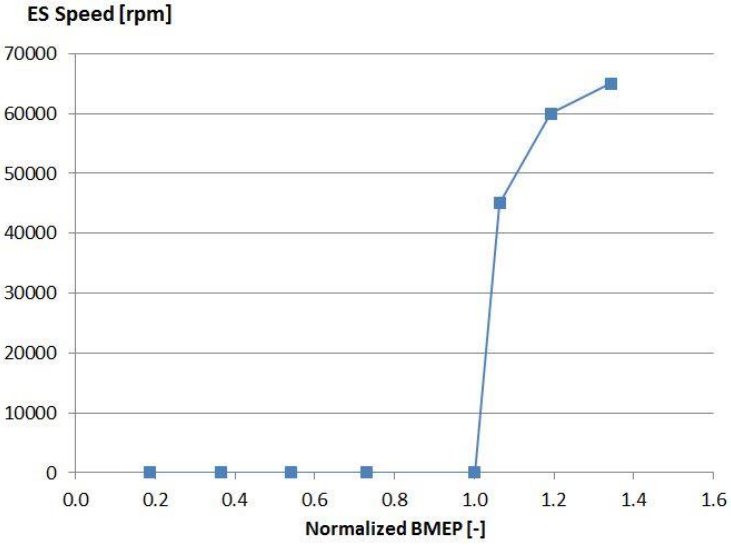

Figure 5-2: Imposed Electric Supercharger Speed [rpm] for the model validation set points

In Figure 5-3, the output of the throttle controller, which is influencing the engine load, is shown. As far as the sixth point is concerned, it is possible to notice how the throttle is imposed to be fully open (being the target BMEP higher than $BMEP_{MT}$ – defined in 4.1); the wastegate valve at the same time is fully closed. The engine is then working at the

maximum possible load given the valve timing, spark timing and electric supercharger speed imposed from experimental data.

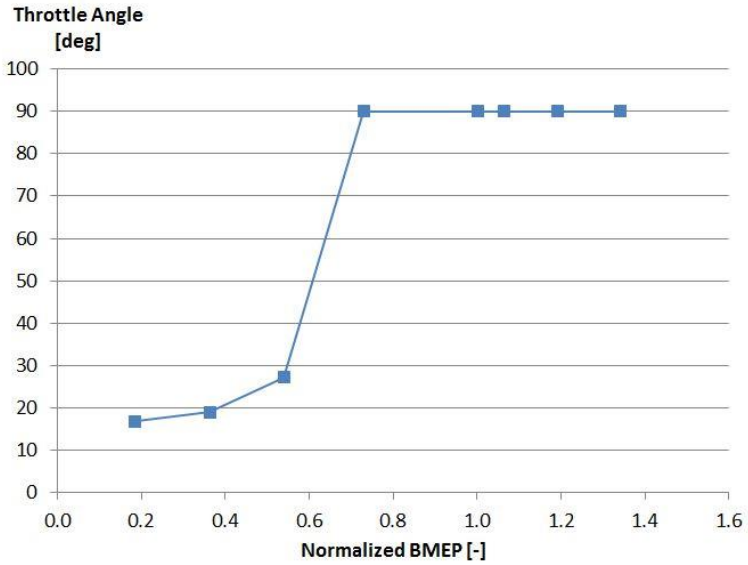

Figure 5-3: Throttle Angle imposed by the model to obtain the required BMEP target (1500 rpm set points)

The BMEP is very close to the expected one: it is possible to assume that the simulated operating condition is close enough to the experimental one, as will be confirmed by the further comparison of the other engine variables selected for the model validation.

The trend for the wastegate diameter is opposite to the trend shown by the throttle valve angle. The first three load points have a wastegate valve completely open; they indeed refer to conditions in which the throttle is not completely open: the intake pressure, and consequently the load, will be just regulated by the throttle angle and the contribution of the turbine to increase the intake pressure is not needed. In the other points the throttle is completely open and the wastegate diameter is generally pretty low because the turbocharger needs to increase the intake pressure to get the desired load. The wastegate diameter though is not showing a linear trend while the load is increasing because there are other factors influencing the engine load: mainly the electric supercharger contribution (it is active only in the last three cases and its speed is increasing while the load is increasing) and the valve timing, which is not constant over the eight load points (as highlighted in Chapter 4).

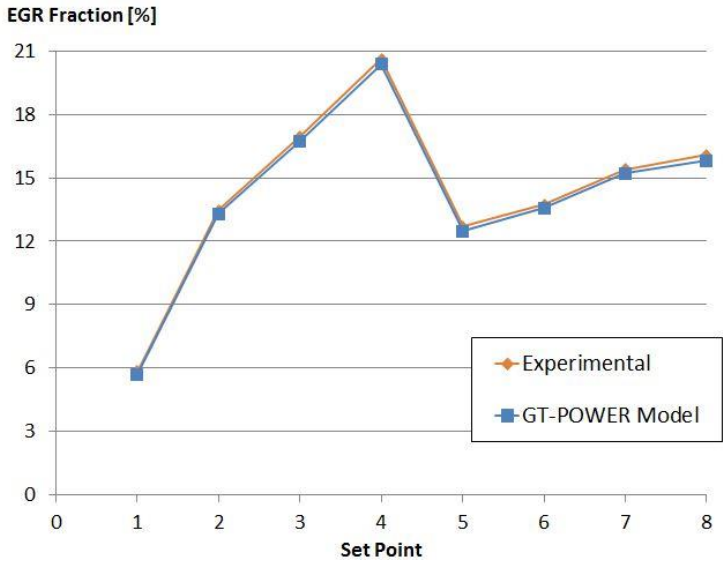

Figure 5-4: Experimental - Model comparison for EGR Fraction at 1500 rpm

Also the EGR Fraction is imposed as a target, which is reached by the model controlling the EGR valve diameter. As for the valve timing and spark timing the EGR fraction is varying with the set point. The relative deviation of the reached value with respect to the imposed target is never higher than 2% for the considered 8 load points, as shown in Figure 5-4.

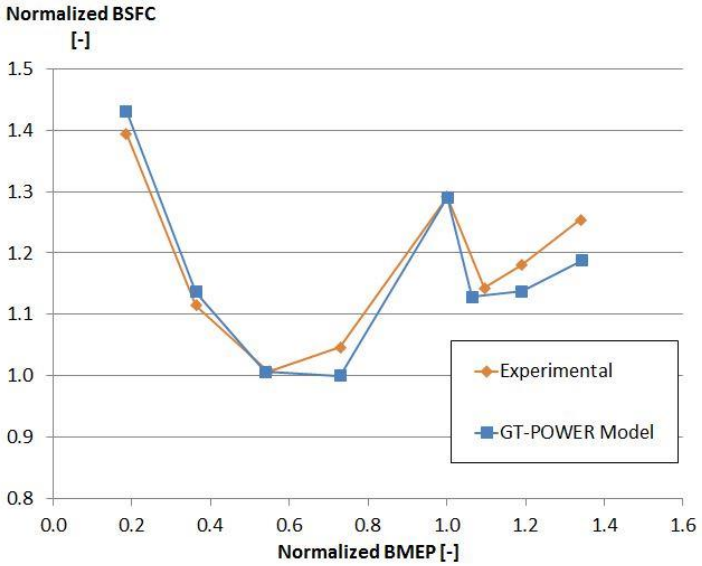

Figure 5-5: Experimental - Model comparison for Normalized Brake Specific Fuel Consumption at 1500 rpm

Figure 5-5 presents normalized BSFC comparison at 1500 rpm. In general the comparison shows good agreement between experimental and model results. The maximum relative deviation is 5.4% at the maximum load point. It must be noted that the BSFC has a minimum at medium load, as expected; the last 3 points show a lower fuel consumption value due to the effect of the electric supercharger. The latter is not connected to the engine: the power required for its rotation is assumed to be externally provided and this power commutes in engine power (by increasing the charge air density) with no need for more fuel to be burned, lowering the BSFC.

The comparison between experimental and model results for the engine air mass flow rate and the pressure at the inlet of the intake manifold is presented in Figure 5-6 and Figure 5-7 respectively.

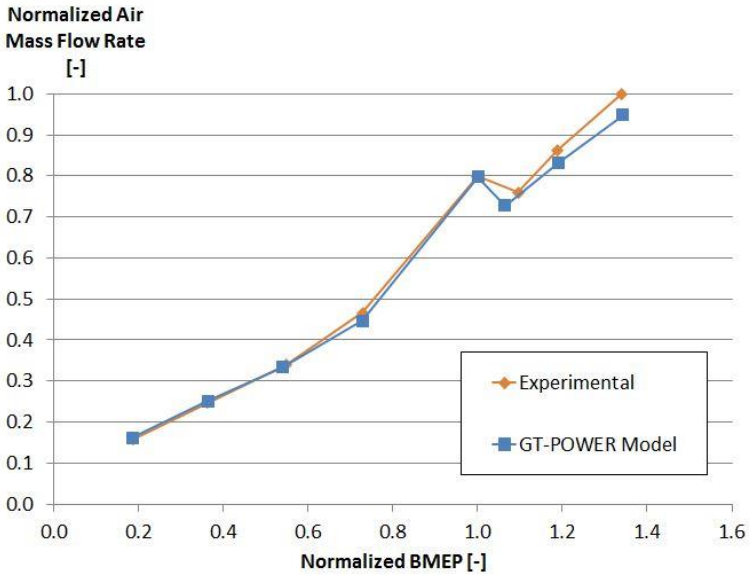

Figure 5-6: Experimental - Model comparison for Normalized Air Mass Flow Rate at 1500 rpm

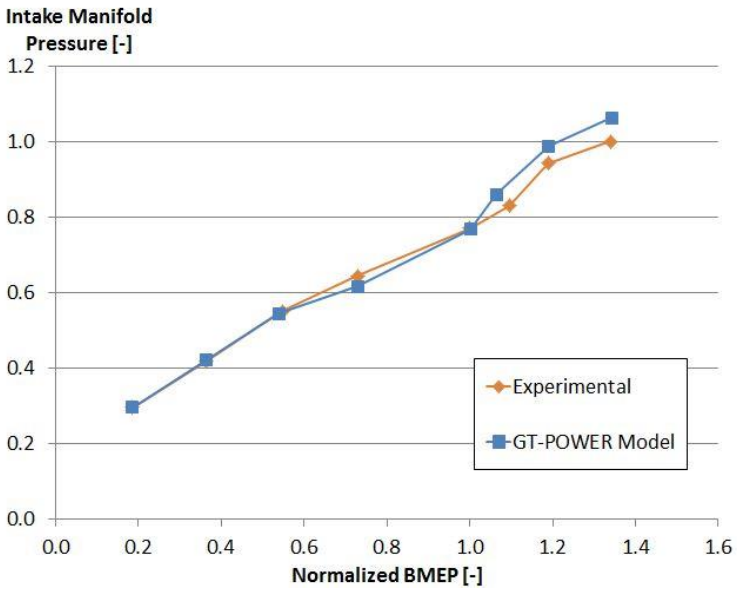

Figure 5-7: Experimental - Model comparison for Normalized Intake Manifold Pressure at 1500 rpm

In both cases the two curves show good agreement and for both variables the highest deviation is encountered at maximum load. The maximum relative deviation between the value given by the model and the measured one is 5.2% for the air flow rate and 6.3% for the pressure measured at the inlet of the intake manifold.

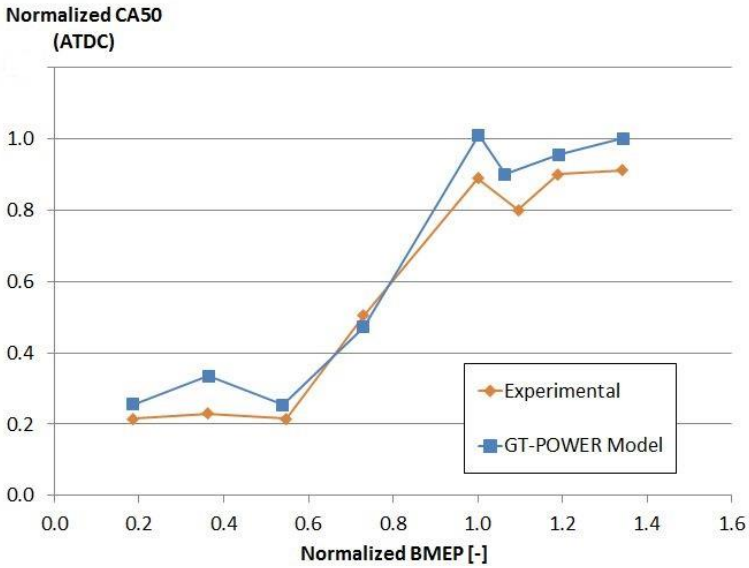

Figure 5-8: Experimental - Model comparison for 50% Burned Crank Angle (after TDC) normalized to the maximum value at 1500 rpm

Figure 5-8 shows the comparison for CA50 for the eight load points at 1500rpm: the two curves show the same trend even if, especially in the high load region, the combustion phasing predicted by the model seems to be slightly retarded. The maximum deviation of the model results with respect to the experimental one is encountered for the fifth load point and is about 4.5 crank angle degrees. Considering how many factors are influencing the combustion model, which was not developed by the author as explained in Chapter 4, and considering the good agreement shown by the other mean engine values taken into account this level of accuracy will be considered sufficient. The only modification made by the author to the model is represented by an adjustment of the Turbulent Flame Speed Multiplier variation with load. In order to reduce the delay of the CA50 at high loads the value of multiplier was increased, never exceeding a value of 1.5 in order not to fall in a misuse of this parameter to balance for other issues. The trend imposed to the multiplier is shown in a normalized form in Figure 5-9.

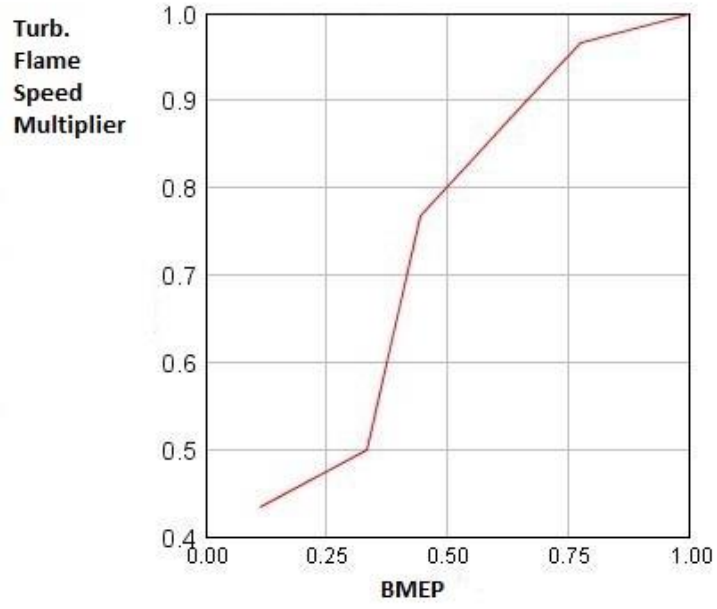

Figure 5-9: Normalized Turbulent Flame Speed Multiplier vs Normalized BMEP imposed in the model at 1500rpm

5.1.2 Load variation at 2000 rpm

Also for the second set of operating conditions, at 2000 rpm, the model has been tested with 8 steady-state load points. In this paragraph the load will be again expressed in terms of Normalized BMEP, following the notation of Table 4-1. The normalized BMEP imposed as a target to the model will go in this case from 0.19 to 1.50. The maximum value of BMEP is higher than for the 1500 rpm case, because the load reached at higher engine speed is larger, as expected from the knowledge of the torque curve of a turbocharged engine. Also for this set of operating points, three (the highest loads) out of the eight load points refer to conditions in which the electric supercharger is applied and the electric supercharger speed is 65000 rpm for all cases.

Set Point	1	2	3	4	5	6	7	8
Electric Supercharger Speed [rpm]	0	0	0	0	0	65000	65000	65000

Table 5-1: Electric supercharger speed for the 8 steady-state load points for model validation at 2000 rpm

The comparison between the imposed target for the BMEP (from experimental results) and the value reached by the model is reported in reported in Table 5-2. It is pointless to show the comparison on a graph since the values are very close for all points: the highest relative deviation is about 0.2%.

Set Point	1	2	3	4	5	6	7	8
Normalized BMEP imposed target	0.189	0.367	0.547	0.729	1.016	1.276	1.368	1.483
Normalized BMEP reached value	0.189	0.366	0.547	0.728	1.017	1.275	1.368	1.483
Relative Deviation [%]	0.10	0.16	-0.03	0.10	-0.05	0.00	-0.01	0.00

Table 5-2: Normalized BMEP value for the load points for model validation at 2000 rpm and relative deviation of the value reached by the GT-POWER model

The EGR fraction is varying with the set point and the comparison between the imposed value (experimental) and the one reached is shown in Figure 5-10. The relative deviation is never higher than 3% for the considered 8 load points.

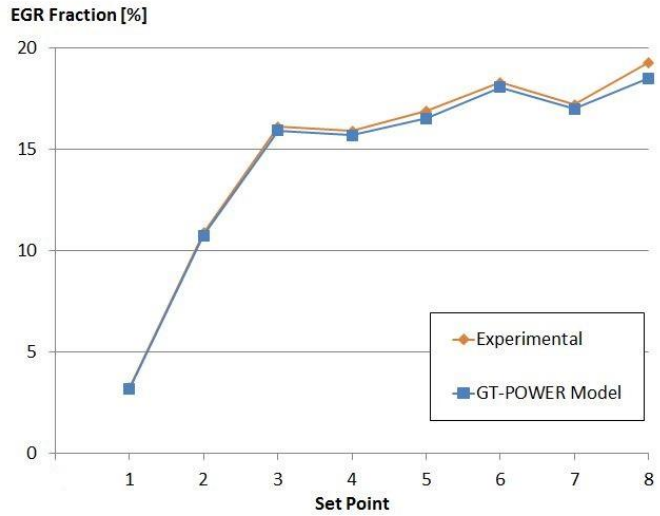

Figure 5-10: Experimental - Model comparison for EGR Fraction at 2000 rpm

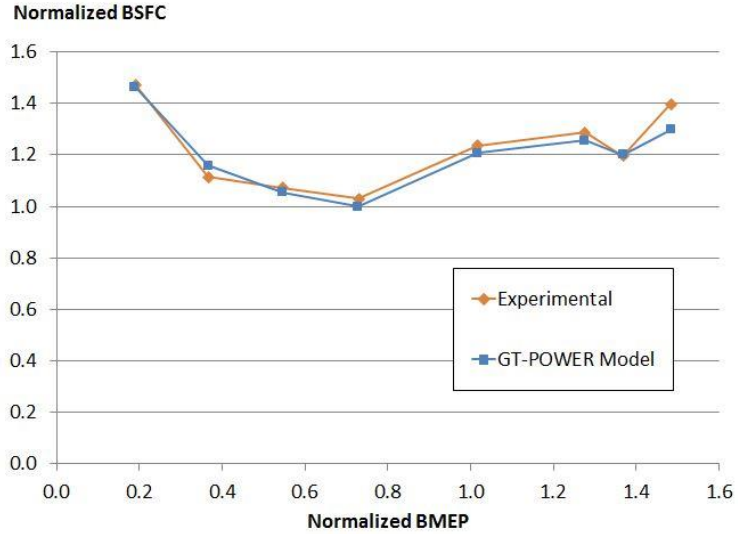

Figure 5-11: Experimental - Model comparison for Normalized Brake Specific Fuel Consumption at 2000 rpm

Figure 5-11 presents a comparison of normalized BSFC values from experimental tests and predicted by the model at 2000 rpm. As for the 1500 rpm simulations, in general the comparison shows good agreement between experimental and model results and the

maximum relative deviation, which is equal to 7.1%, occurs again at the maximum load point.

The comparison between experimental and model results at 2000 rpm for the engine air mass flow rate and the pressure at the inlet of the intake manifold is presented in Figure 5-12 and Figure 5-13 respectively. In both cases the two curves show good agreement and for both variables the highest deviations are in the high load region. The maximum relative deviation between the value given by the model and the measured one is 7.5% for the air flow rate and 8.2% for the pressure measured at the inlet of the intake manifold.

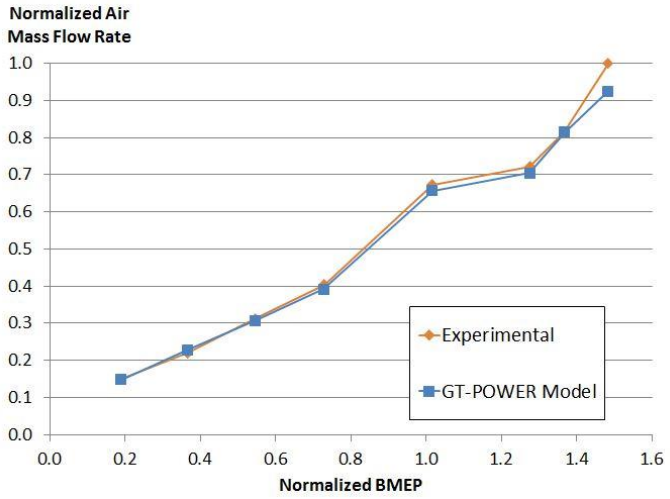

Figure 5-12: Experimental - Model comparison for Normalized Air Mass Flow Rate at 2000 rpm

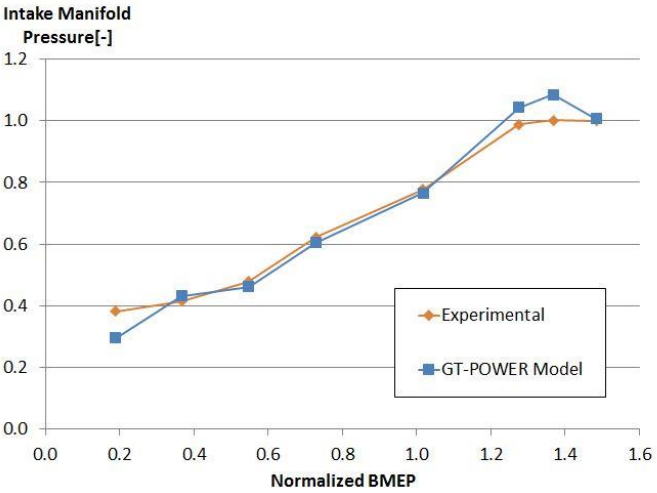

Figure 5-13: Experimental - Model comparison for Normalized Intake Manifold Pressure at 2000 rpm

The maximum deviations are slightly higher in this case than for the 1500 rpm case, but still never higher than 10%; the trends shown by all the variables still confirms the validity of the calculations of the model. Furthermore, the main application of the model in the next phases of this project will be the transient simulation and the latter will be performed at 1500 rpm.

The last compared variable is the CA50, as shown in Figure 5-14. As it happened for the 1500 rpm case, the two curves show the same trend even if, especially in the high load region, the combustion phasing predicted by the model seems to be slightly retarded. The maximum deviation of the model results with respect to the experimental one is encountered for the highest load point and is about 5.5 crank angle degrees. The same considerations made about the combustion model when presenting the model validation at 1500 rpm still apply.

The obtained level of accuracy will be considered sufficient for predicting the engine performance in the next phase of this work.

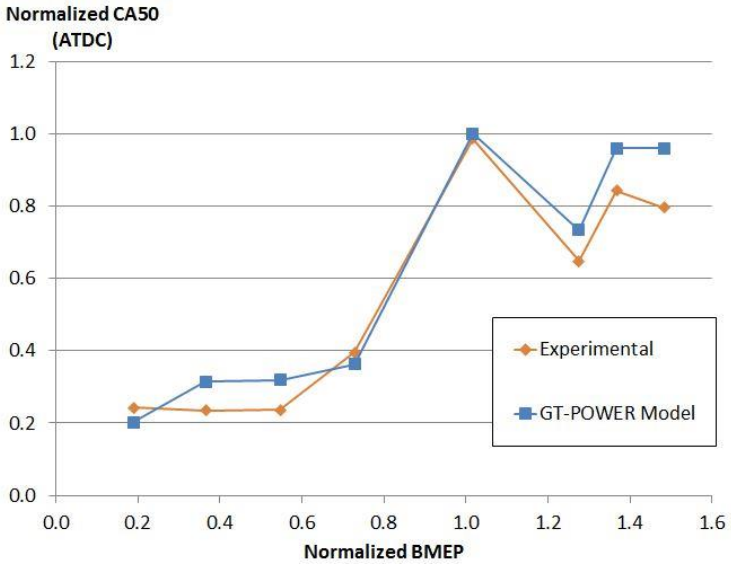

Figure 5-14: Experimental - Model comparison for 50% Burned Crank Angle (after TDC) normalized to the maximum value at 2000 rpm

5.2 Steady-state simulations for low end torque improvement estimation

Once the model validation was obtained, as reported in the previous paragraph, and before moving to transient simulations, steady-state simulations were used to quantify the torque improvement in the low speed range produced by the contribution of the electric supercharger. The estimation of the absolute maximum BMEP achievable by the engine at a given speed is not straightforward considering the high number of input variables that influence the load (spark timing, valves timing, EGR fraction, etc.) and the fact that, especially at low speed, the maximum load is usually limited by knock occurrence. As a consequence the choice was to run the model setting as the "target BMEP" the values reported in Figure 4-8 and Table 4-2. The position of these operating points with respect to the maximum load theoretically obtainable and to the maximum load imposed by knocking occurrence will be then explained. As far as the aforementioned input variables are concerned, it was chosen to keep them as close as possible to the values from the experimental data used for model validation. The values of the input variables will be reported below along with the obtained BMEP values.

The valve timing was kept fixed, even if in real application it would be optimized depending on load and speed. The reason is that the considered points are all in the low-speed high-load range. Furthermore, the optimization of those timings in real application would generally take into account also other effects, such us fuel consumption, which was not considered in this section just aimed at proving the possibility for the BMEP target to be reached. The valve timing (ICL and ECL) is the same used at 1500 rpm maximum load in the previous phase of this work. The two values can be defined recalling Figure 4-5 and Figure 4-6: the values chosen for these runs at maximum load would have 0 deg variation in that notation.

The level of EGR was kept fixed at 16%. This value was chosen because, both at 1500 and 2000 rpm, experimental data showed a similar value in the high load region.

Spark timing values were again kept close to the ones from model validation; the spark was slightly anticipated, when possible, as long as no knock occurrence was predicted.

The air-fuel ratio was imposed to be stoichiometric for all these cases.

As it is shown in Figure 5-15 the target is always reached in the case of turbocharged only engine. The area of interest in this work is the one characterized by the contribution of electric supercharger; as a consequence the trend shown by the supercharged engine will be discussed below.

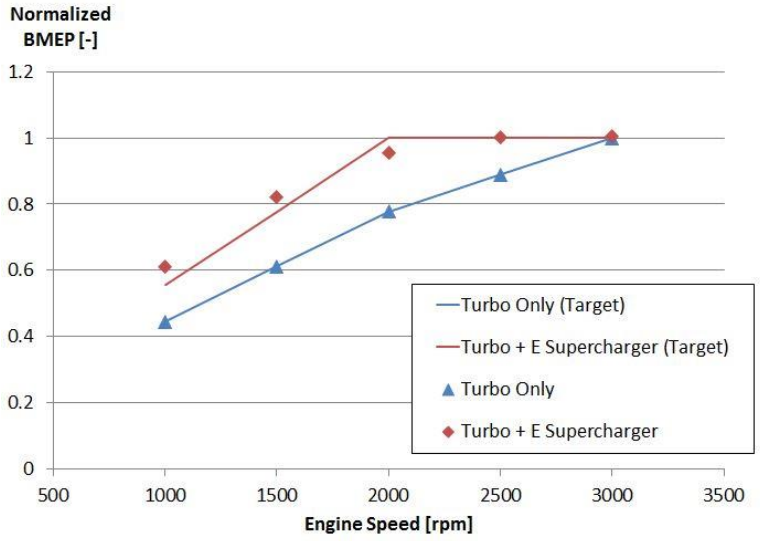

Figure 5-15: Normalized BMEP vs Engine speed, imposed target and value reached by the model

The first three points are not exactly overlapping with the BMEP target curve: below 1500 rpm the BMEP level is even exceeding the target curve.

The electric supercharger speed was imposed to be maximum (65000 rpm) in all cases except at 1000 rpm where the target is exceeded even with a lower electric supercharger speed, see Figure 5-16. In this first case, since a small mass flow rate is flowing through the intake, the electric supercharger is able to provide all the boost pressure necessary to increase the engine BMEP and even more. The wastegate valve is indeed completely open but the obtained load is still higher than the target.

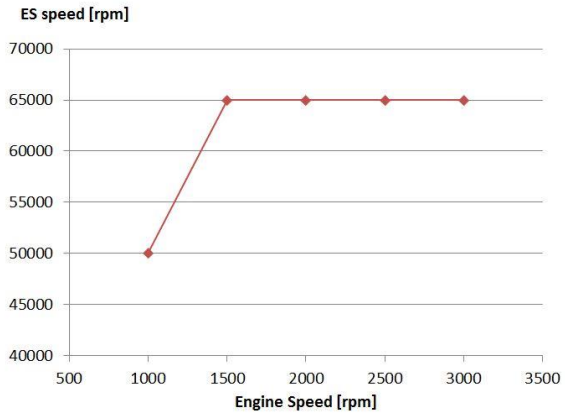

Figure 5-16: Electric Supercharger Speed for the 5 simulated maximum load operating points

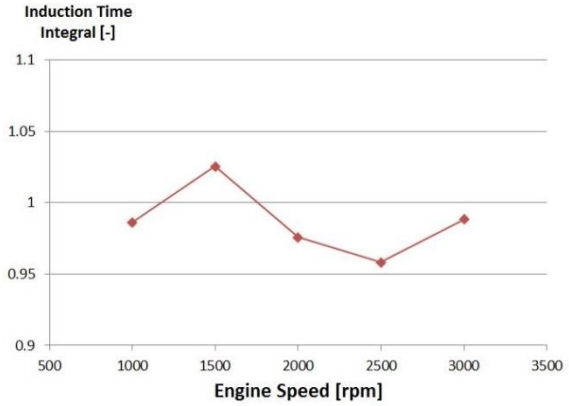

Figure 5-17: Knock model Induction time integral for the 5 simulated maximum load operating points

At 1500 rpm the maximum load is the same considered in the previous phase of this work (model validation) and the value from experimental data is higher than the target curve, as can be seen in Figure 5-15. The load is likely to be limited by engine knocking, as suggested by the fact the Induction Time Integral is in this case just exceeding the value of 1 (which means the model is actually predicting knock to occur). The value is very close to 1 and as explained in Chapter 3 will be considered acceptable. Furthermore this operating condition is derived by experimental testing and knocking was not occurring during the testing. Also in all the other cases at higher speeds the Induction Time Integral is very close to one, and the wastegate valve is never fully closed. This means the maximum engine load is again limited by the need to avoid the occurrence of knock.

Even considering the limitation imposed by engine knocking, the target is always reached or exceeded, except at 2000 rpm, where the BMEP value is just 4% lower than the target. From Figure 5-15 it is also possible to notice how the positive contribution of the electric supercharger in achieving high load is decreasing as the engine speed increases. The percent improvement in engine BMEP is reported, for the five simulated speeds, in Table 5-3.

Engine Speed [rpm]	1000	1500	2000	2500	3000
BMEP improvement [%]	0.37	0.34	0.23	0.13	0.00

Table 5-3: Maximum BMEP relative improvement due to electric supercharger action

In particular when the engine speed is equal to 3000 rpm the same BMEP is obtained considering the two different working conditions; the pressure ratio across the electric supercharger, when active, is indeed almost equal to 1; the operating condition of the engine with or without the electric boost is the same, as shown from the comparison made in Table 5-4 (in which the percent variation of some engine variables between the two boosting conditions is shown).

Given that with increasing engine speed the air mass flow rate through the intake would increase as well, it is useless to test the contribution of the electric supercharger at higher speeds. The machine is not large enough to provide positive pressure ratio for higher mass flow rates and as a consequence the activation of the electric compressor would be a waste of power.

Engine variable	Relative deviation
Intake Pressure	0.44%
BSFC	0.26%
Turbine Speed	0.81%
Induction Time Integral	0.69%

Table 5-4: Relative deviation of some engine variables between the cases with and without electric supercharger

5.3 Load step at constant engine speed

One of the main goals for the application of the electric supercharger is the improvement in the transient performance of the engine. In order to evaluate this improvement, in the last phase of this work the simulation of a load step at constant engine speed was performed. The response was evaluated with and without the application of the electric supercharger and depending on the choice of some electric supercharger operating parameters.

5.3.1 Transient response without electric supercharger

The procedure of the simulation was explained in Chapter 4. In this paragraph the evolution in time of the main engine variables following the opening of the throttle will be presented and explained.

The first presented simulation features 0% EGR and wastegate valve completely open at low load, closed during the transient. This initial condition is the more realistic and will be the one selected in all the next cases when not specified otherwise.

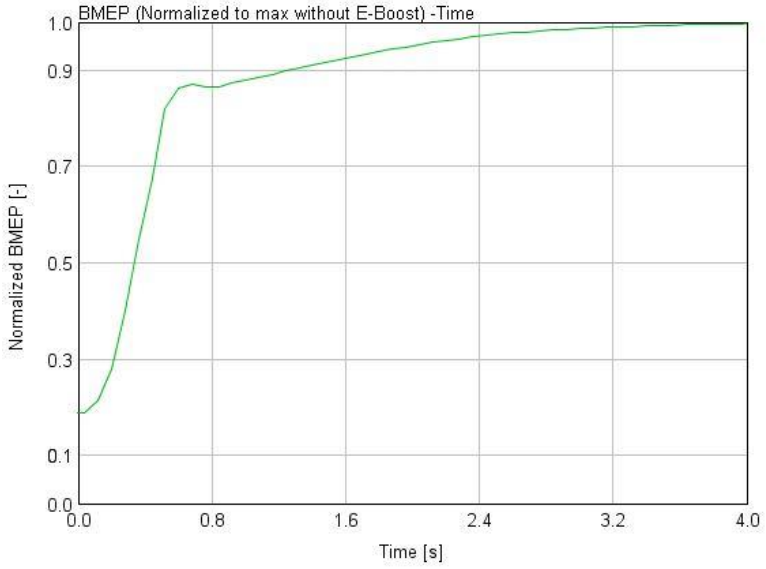

Figure 5-18: Normalized BMEP vs Time during the load step at 1500 rpm

In Figure 5-18 the evolution of the engine BMEP over time is shown. This graph represents the main output of the transient simulation because shows the behavior of the engine load after the throttle opens ($t = 0\ s$).

As anticipated in Chapter 4, the definition of the spark by means of a look up table causes the spark timing to be varied too late from the model and the occurrence of knock can be predicted.

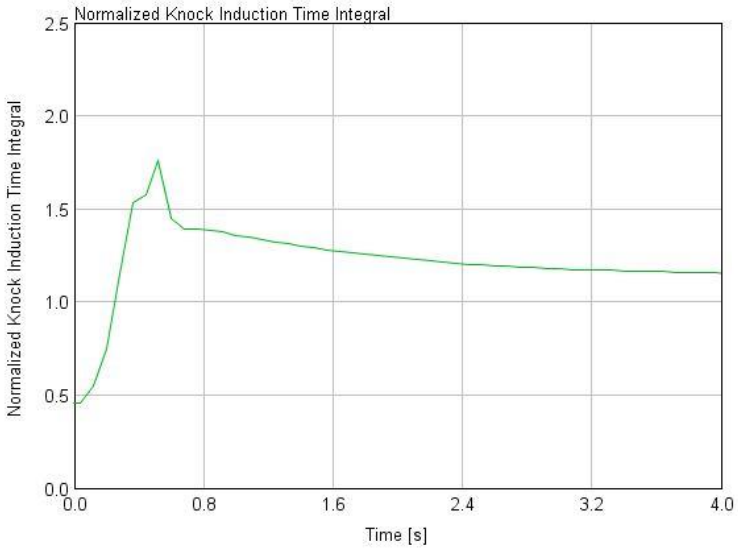

Figure 5-19: Induction Time Integral during load step normalized to the maximum admissible value

Figure 5-19 shows the value of the Induction Time Integral, defined in paragraph 3.2.4, normalized to the limit value for this variable, which is higher than 1 as explained in the same paragraph. As can be seen, during the transient the value of this variable is always higher than the limit and this indicates that knocking is likely to occur.

In order to make sure that knocking is not occurring, the spark timing has been then imposed over time, determining the needed retarding of the spark to avoid knocking by trial and error procedure progressively retarding the spark. This procedure will be used for all the following simulations.

Figure 5-20 shows the increase of the engine BMEP after the modification of the spark timing. The response is slightly slower but the occurrence of engine knocking is avoided.

It is possible to identify on this graph the two phases in the load transient defined in the literature review: the first one (from $t = 0\ s$ to about $t = 0.6\ s$) characterized by very steep slope and due mainly to the increase in the flow caused by the throttle opening; the second one during which the increase in engine load is governed by the acceleration of the turbocharger. The time required for the torque to reach 90% of the maximum value - $BMEP_{max,NO\ EB}$ - is 2.5 s.

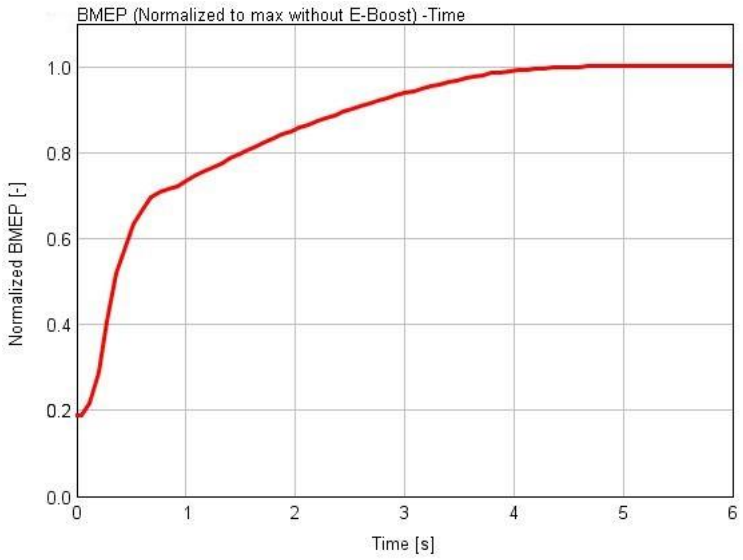

Figure 5-20: Normalized BMEP vs time during the load step at 1500 rpm with modified spark timing

This trend is explained also by the evolution of the intake pressure during the load variation, Figure 5-21. The pressure grows very fast up to a value close to the atmospheric one, as a result of the throttle valve opening; then it increases due to the boosting effect of the turbocharger. A large amount of time is needed by the turbocharger to accelerate and the required boosting pressure is obtained only 4 seconds after the beginning of the transient. This time is required because the increased energy available in the exhaust flow is not immediately exploited by the compressor: between $t = 0.6\ s$ and $t = 4\ s$ most of the energy produced by the turbine is used to accelerate the rotating parts of the turbo-compressor assembly and as a consequence is not reintroduced in the intake flow in terms of boost pressure.

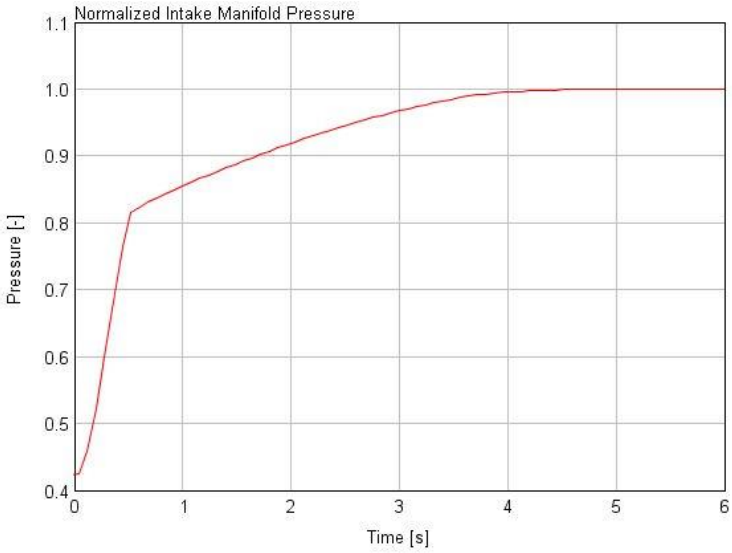

Figure 5-21: Normalized intake pressure vs time during the load step at 1500 rpm

The turbine speed is reported in Figure 5-22. It can be noted how the turbine speed is increasing until the required boost pressure is obtained, after that point the wastegate valve is open so that the turbine speed, hence the pressure ratio across the compressor, remains constant.

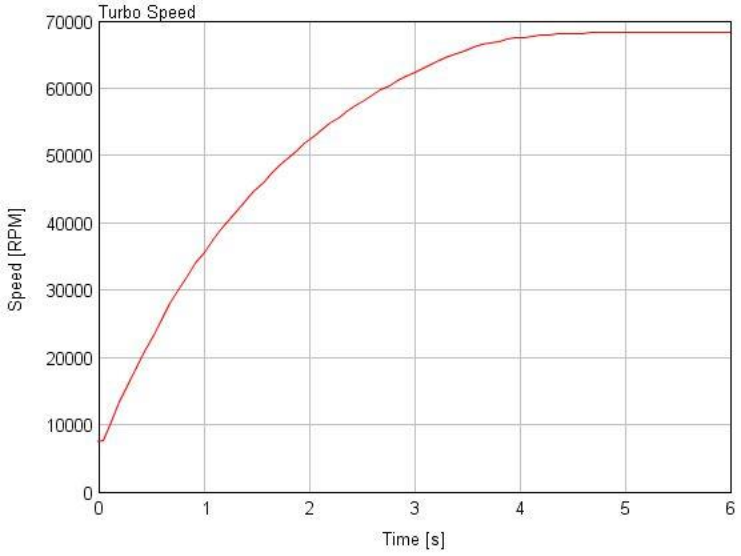

Figure 5-22: Turbocharger speed vs time during the load step at 1500 rpm

It must be clarified that the BMEP has been chosen as the main input of the transient simulation because this is the variable reprensenting the engine load in experimental data reported in the previous sections of this work. As a consequence, for the sake of clarity it was chosen to keep indicating the load in terms of BMEP.

The BMEP is actually calculated in the GT-Power model by subtracting the friction mean effective pressure (FMEP) from the IMEP, which is instead directly calculated by the pressure inside the cylinder along the thermodynamic cycle. The FMEP represents the component of engine work which is wasted due to the mechanical losses of the engine.

The FMEP can be defined in several ways in the software, in this case is defined depending on both engine speed and load through a user defined polynomial, function (already implemented in the model provided to the author). Nevertheless, the influence of the engine load is limited and the increase in BMEP and IMEP show a very similar trend, as shown by Figure 5-23.

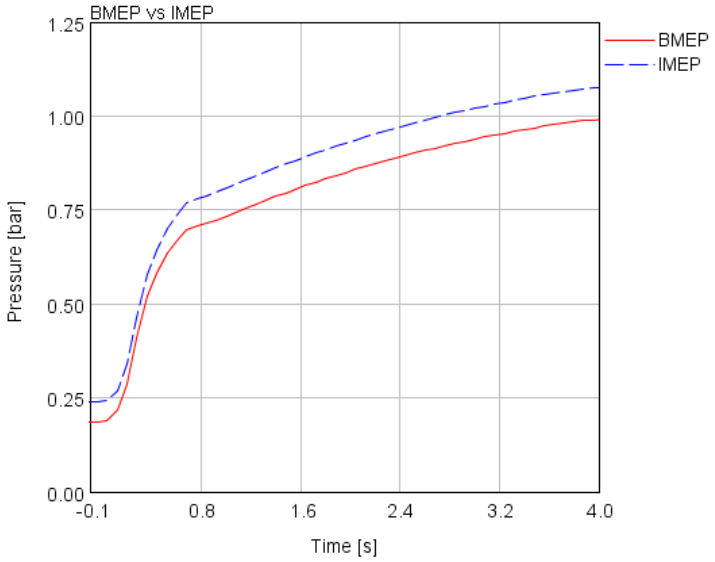

Figure 5-23: Normalized BMEP and IMEP during the load transient at 1500 rpm. Both variables are normalized to the maximum BMEP value.

5.3.2 Effect of the wastegate valve position at the beginning of the load transient

The comparison of the response to the throttle opening with two different positions of the wastegate valve at the beginning of the transient is shown in Figure 5-24. The red line represent the same case reported in the previous paragraph, the blue line corresponds to a simplified situation in which all the input parameters are defined in the same way except for the wastegate valve diameter: the latter is imposed to be 0 mm throughout the whole duration of the simulation.

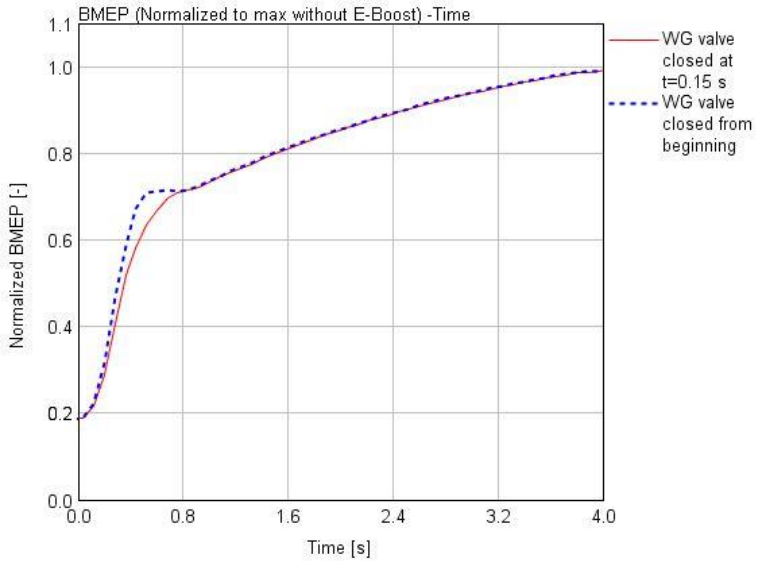

Figure 5-24: Normalized BMEP vs time during the load step at 1500 rpm for two different wastegate valve control solutions

As expected, a faster increase of the BMEP is obtained applying this modification, at least in the first phase of the response. As long as the wastegate valve is even partially open, some fraction of the exhaust gases will not flow through the turbine and the associated enthalpy will be wasted. This simplification, though, is often made in the literature [26]. The reason can be found in the behavior of the BMEP in the second phase of the transient: as can be noticed from Figure 5-24 the difference between the two curves is negligible after $t = 0.8\ s$ and the response time would not be changed.

Also the evolution of the turbine speed (reported in Figure 5-25) shows that the difference between the two simulations is minor.

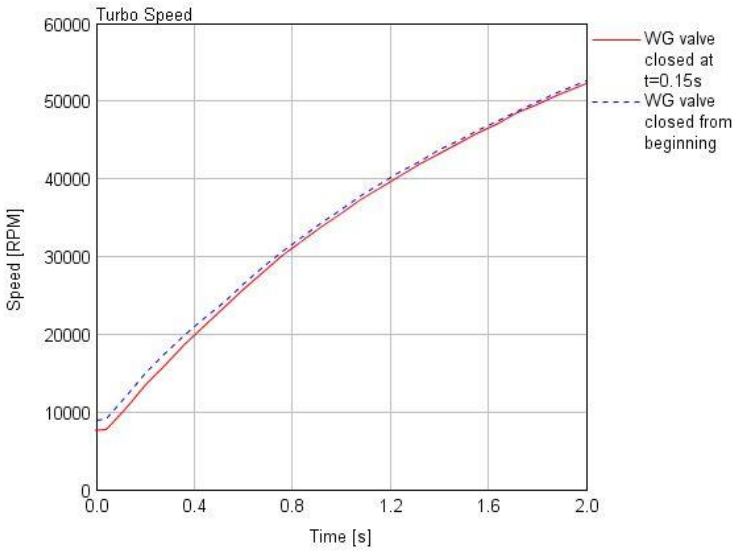

Figure 5-25: Turbocharger speed vs time during the load step for two different wastegate valve control solutions

Anyway, at least in the case of this engine, this situation is not likely to be encountered in real application: at low loads the wastegate is usually open as mentioned during the analysis of the steady-state performance. As a consequence, the case in which the wastegate is initially open will be considered in the following paragraphs.

5.3.3 Transient response with electric supercharger

The results of the simulations of the system in which the electric supercharger is working will be presented in this paragraph. As in the previous paragraph, no EGR is initially assumed. As far as the control of the electric supercharger is concerned, the electric supercharger speed is imposed to increase linearly from 0 rpm to the maximum speed of 65000 rpm in 0.5 s, as explained in Chapter 4.

The response of the engine load is shown in Figure 5-26. The BMEP is again normalized to the maximum value, it must be noted that this value is now higher than in the case without electric supercharger.

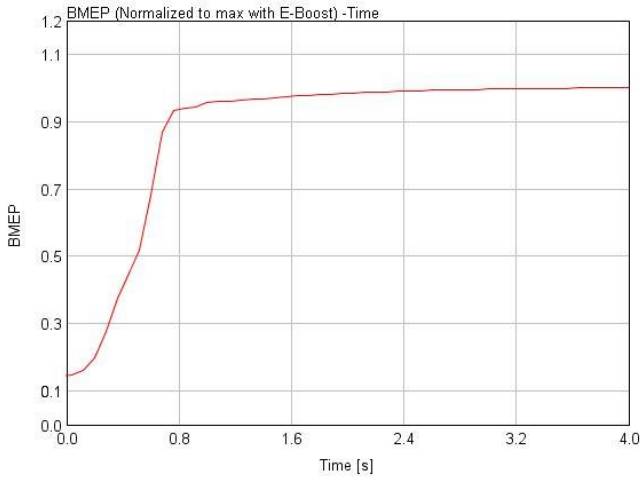

Figure 5-26: Normalized BMEP vs time during the load step at 1500 rpm with electric supercharger

The electric supercharger contribution radically changes the transient response. The load now increases directly up to the more than 90% of maximum load - $BMEP_{max,EB}$. The phase of the transient related to the slow acceleration of the turbocharger can't be identified.

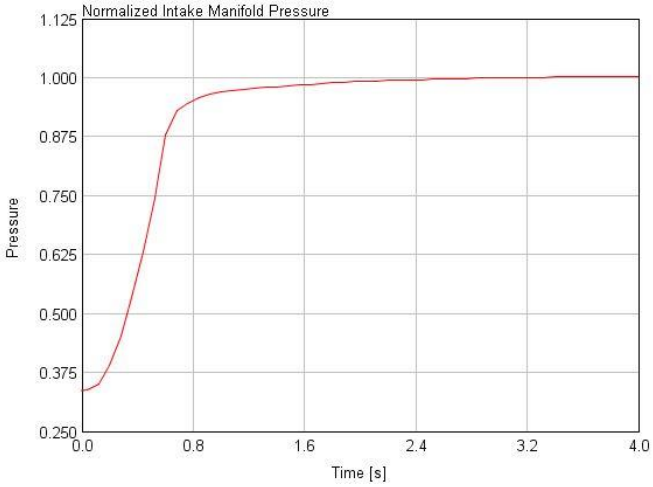

Figure 5-27: Normalized intake pressure vs time during the load step at 1500 rpm with electric supercharger

Also the intake pressure evolution during the transient, shown in Figure 5-27, confirms that the electric supercharger makes possible to provide the required boost pressure in about 1 s. This increase in intake pressure is partly due to the electric supercharger boosting action and partly to the increase in turbo speed and indeed the final value of the

turbocharger speed is lower than when the electric supercharger is not present. Furthermore, the electrically driven compressor other than reducing the amount of boost pressure required to the turbocharger compressor also speeds up the acceleration of the turbo. Also the turbine speed (Figure 5-28) rises very quickly up to a value close to the maximum load one; its acceleration in the first phase is improved by the electric supercharger work.

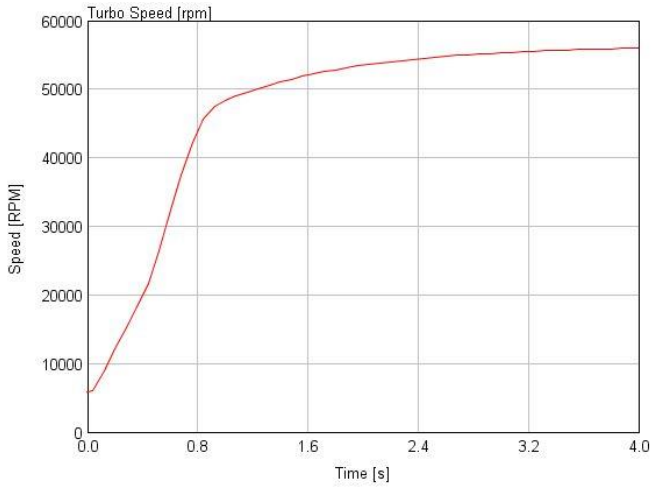

Figure 5-28: Turbocharger speed vs time during the load step at 1500 rpm with electric supercharger

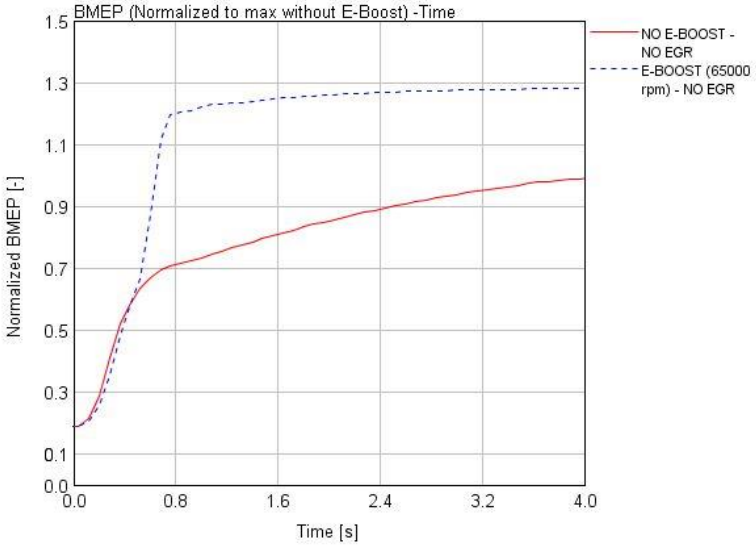

Figure 5-29: Normalized BMEP vs time during the load step at 1500 rpm with and without electric supercharger

The response of the engine depending on the boosting condition is reported in Figure 5-29. The maximum load reached by the electrically supercharged engine is obviously higher, as discussed for the simulations in steady-state conditions. In order to compare the response in the two cases, for the electrically supercharged engine both the time needed to reach 90% of $BMEP_{max,EB}$ - $t_{resp,EB}$ - and the time needed to reach 90% of $BMEP_{max,NO\ EB}$ - t_{resp} - will be considered.

Boosting condition	t_{resp} [s]	$t_{resp,EB}$ [s]
No E-boost	2.52	-
E-boost (max speed 65000 rpm)	0.62	0.71

Table 5-5: Response time depending on boosting condition

From the values of the response time reported in Table 5-5, the improvement due to the electric supercharger contribution is clear. The 90% of the maximum torque is obtained in less than 1 second even if the max BMEP is 30% higher than without e-boost.
If t_{resp} is compared, the improvement is even more evident: it decreases to 0.62 s, 25% of the time needed without electric supercharger.

5.3.4 Effect of EGR fraction

The effect of EGR fraction is evaluated by repeating the simulation with two different fixed diameters for the EGR valve flow section. The diameter is kept fixed in order for the EGR level to remain constant throughout the simulation. Actually, due to the very fast nature of the transient, is natural to observe a fluctuation in the EGR fraction. The two diameters were selected so that the EGR fraction remains within a given range during the whole simulation. In particular, for the case referred as '10% EGR' an EGR fraction in the 8-11% range has been found and considered acceptable.

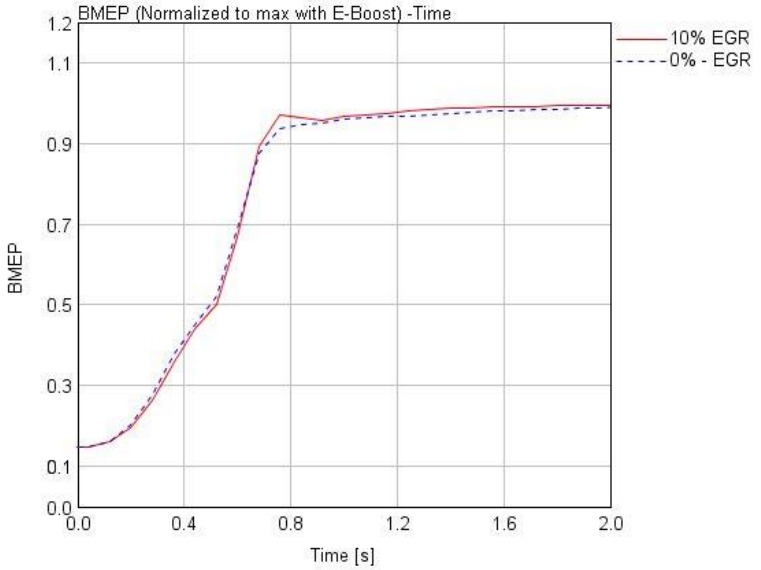

Figure 5-30: Normalized BMEP during the transient at 1500 rpm; 0 (dashed blue) and 10 (solid red) % EGR

The response of the engine is very similar in the two simulated condition (see Figure 5-30). The impact of the higher fraction of exhaust gases in the combustion chamber is balanced by the more advanced spark timing which is possible to adopt thank to the knock suppressing ability of the EGR (see Figure 5-31), as explained in section 2.5.

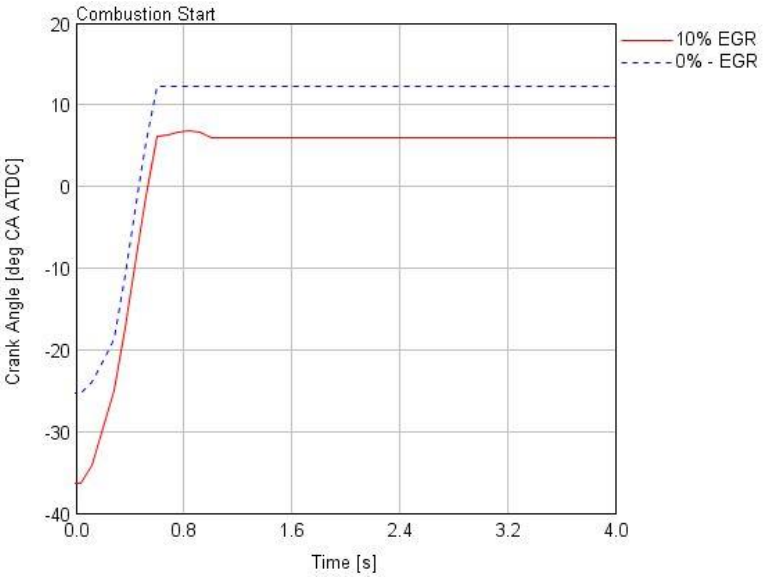

Figure 5-31: Spark timing during the load step at 1500 rpm; 0% (dashed blue) and 10% (solid red) EGR

When EGR is not applied indeed the intake pressure needs to be higher to obtain the same BMEP, see Figure 5-32.

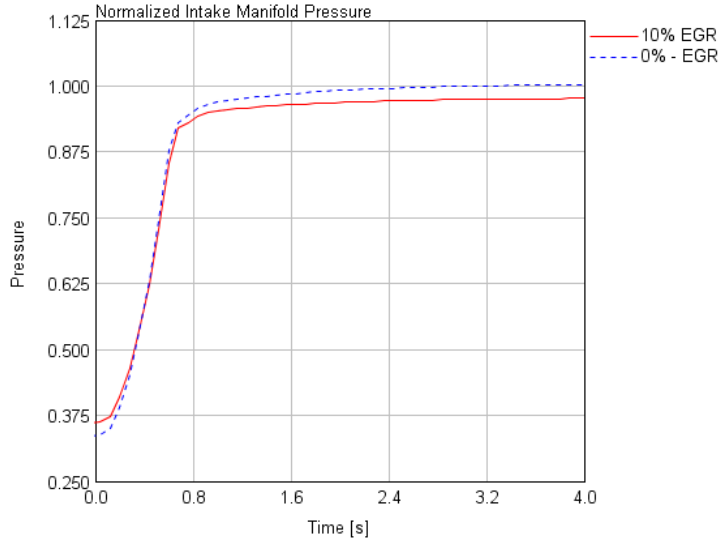

Figure 5-32: Intake pressure during the load step at 1500 rpm; 0% (dashed blue) and 10% (solid red) EGR

In order to obtain a lower intake pressure a lower turbocharger speed (in Figure 5-33) is sufficient: it is the action of the compressor to cause the rise in the intake pressure and its speed needs to rise in order for the pressure ratio across the compressor to build up.

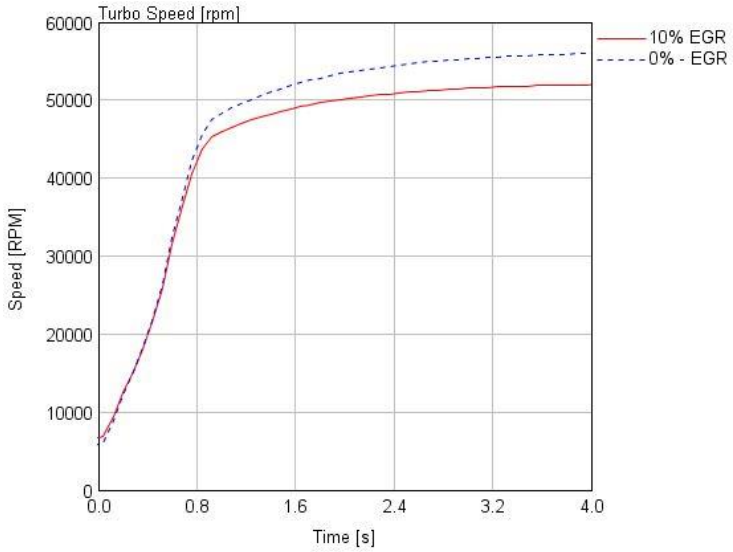

Figure 5-33: Turbine speed during the load step at 1500 rpm; 0% (dashed blue) and 10% (solid red) EGR

The response time of the engine depending on the EGR fraction is reported in Table 5-6, the values results to be very similar as suggested by Figure 5-30.

EGR fraction [%]	t_{resp} [s]	$t_{resp,EB}$ [s]
0	0.62	0.71
10	0.62	0.68

Table 5-6: Response time with 0% and 10% EGR

5.3.5 Effect of delay in electric supercharger activation

In this section the influence on transient response of a delay in the electric supercharger activation with respect to the opening of the throttle is evaluated. All the input parameters to the simulation are defined in the same way as in the previous paragraph (case without EGR) except for the electric compressor speed. The supercharger is assumed to start accelerating at t_{start} = 0.3 s and t_{start} = 0.5 s respectively in two different simulations, instead of having the start of the rise in compressor speed at t_{start} = 0 s as in the base case. The closure of the by-pass channel is shifted ahead in the same fashion.

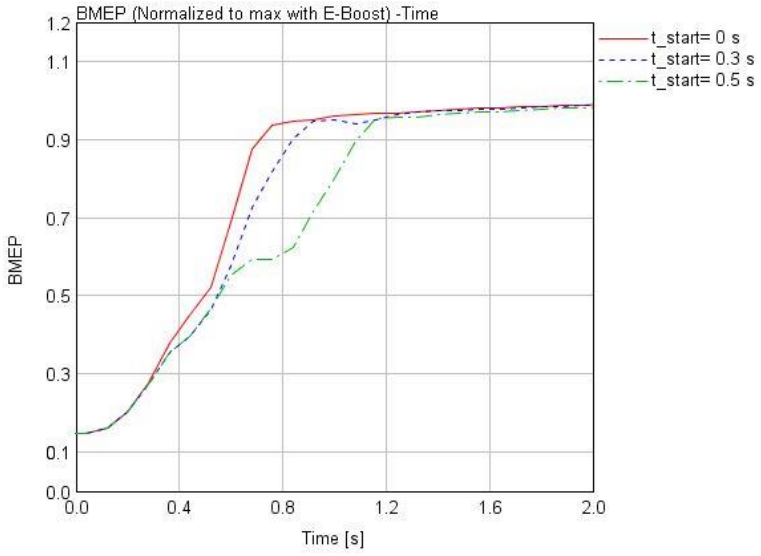

Figure 5-34: Normalized BMEP during the transient at 1500 rpm depending on e-boost activation time

Case	t_{start} [s]	t_{resp} [s] (increase from previous case)	$t_{resp,EB}$ [s] (increase from previous case)
1	0	0.62	0.71
2	0.3	0.67 (+8%)	0.84 (+18%)
3	0.5	0.92 (+37%)	1.08 (+29%)

Table 5-7: Response time at 1500 rpm depending on t_{start}

As expected, the response time increases if the electric supercharger is activated later. The delay in the response time though is smaller than the delay in the supercharger activation. This is due to the fact that in the first phase (0.5 s) of the load rise, where it is increasing rapidly thanks to the throttle opening, the influence of the electric compressor is minimal. In particular, from $t = 0\ s$ to $t = 0.3\ s$ the difference in the response in the three different cases is negligible.

On the other hand, by examining case 3, it can be noticed how the load increase is not as smooth as in the other two cases: the BMEP-Time curve gets flat between $t = 0.6\ s$ and $t = 0.8\ s$. A similar behavior is shown by the intake pressure, see Figure 5-35.

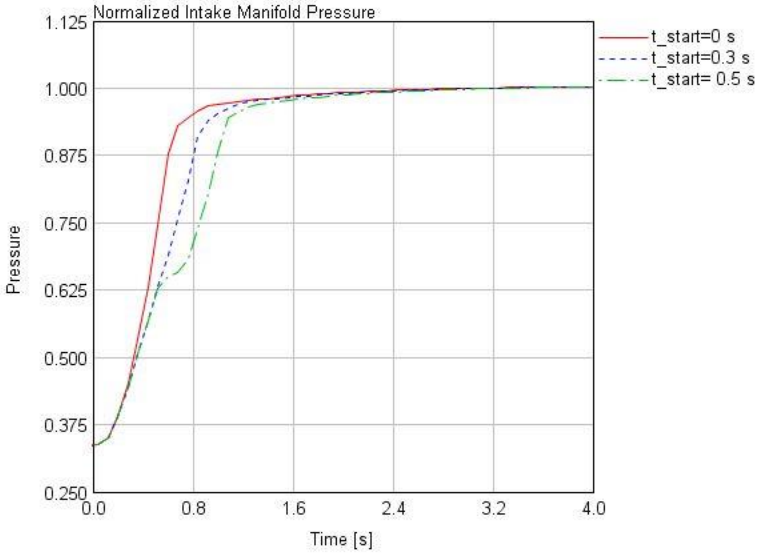

Figure 5-35: Normalized intake pressure during the transient at 1500 rpm depending on e-boost activation time

Furthermore, the relative increase both in t_{resp} and $t_{resp,EB}$ from case 2 to 3 is far higher than from case 1 to 2. As a consequence, an effective control strategy for the electric compressor should limit the delay in t_{start} in order not to waste its positive effect on the transient.

Such a control strategy, which is not to be developed in this work, may be based on the identification of a threshold in the engine load for the actuation of the supercharger. The BMEP at t_{start} for case 2 and 3 is respectively 38% and 57% of $BMEP_{max,NO\ EB}$.

The delay in the electric compressor activation has anyway no influence on the steady-state operating condition reached at the end of the transient, as can be deduced by the intake pressure and turbo speed (Figure 5-36).

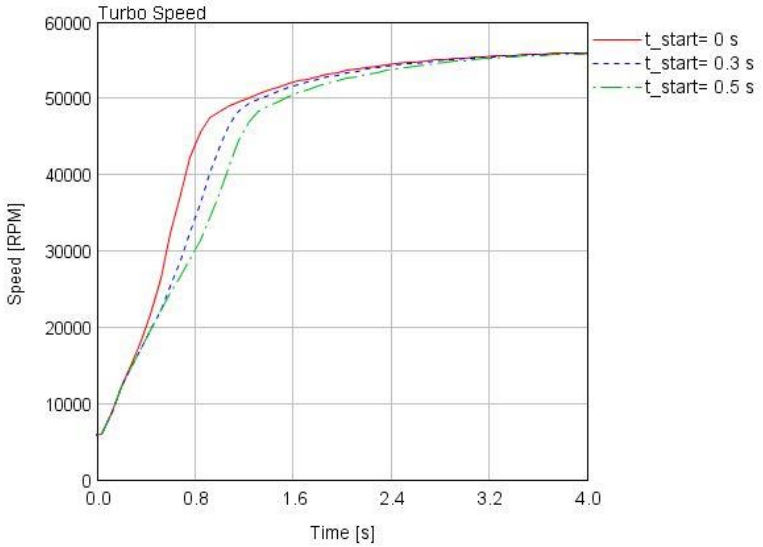

Figure 5-36: Turbocharger speed during the load transient at 1500 rpm depending on e-boost activation time

5.3.6 Effect of maximum electric supercharger speed

In this section the influence on transient response of the maximum rotational speed of the electrical compressor is evaluated. Again, the only modified input parameter is the electric compressor speed: in particular the speed is imposed to linearly increase in 0.5 s from 0 rpm to the maximum value, but the latter is changed from case to case. With reference to the previous paragraphs, t_{start} is now set to 0 s and EGR to 0%. The values of the maximum speed are reported in Table 5-8.

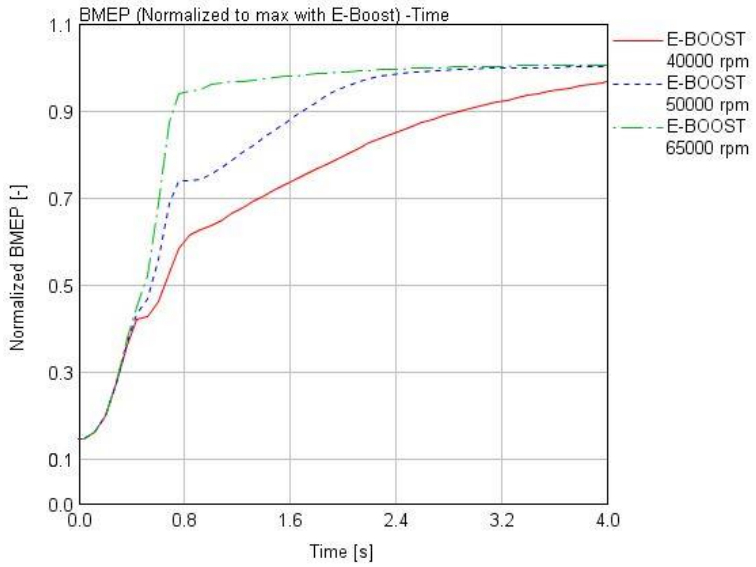

Figure 5-37: Normalized BMEP during the transient at 1500 rpm depending on maximum e-boost speed

Case	E-boost max speed [rpm]	t_{resp} [s]	$t_{resp,EB}$ [s]
1	65000	0.62	0.71
2	50000	0.71	1.70
3	40000	1.42	2.90

Table 5-8: Response time at 1500 rpm depending on maximum electric supercharger speed

In both case 2 and 3 it is clear how the boost pressure provided by the electric supercharger is not high enough to reach 90% of $BMEP_{max,EB}$. A second phase of slower increase of the load can be identified in the transient response, Figure 5-37; this is especially evident in case 3: at $t = 4\ s$ the BMEP is reaching the maximum value but not yet stabilized. The response times are reported in Table 5-8: in case 3 the $t_{resp,EB}$ is much higher than 2 s; hence, even if this speed allows the steady-state torque to reach $BMEP_{max,EB}$, the advantage on the transient response over the conventionally boosted engine is null.

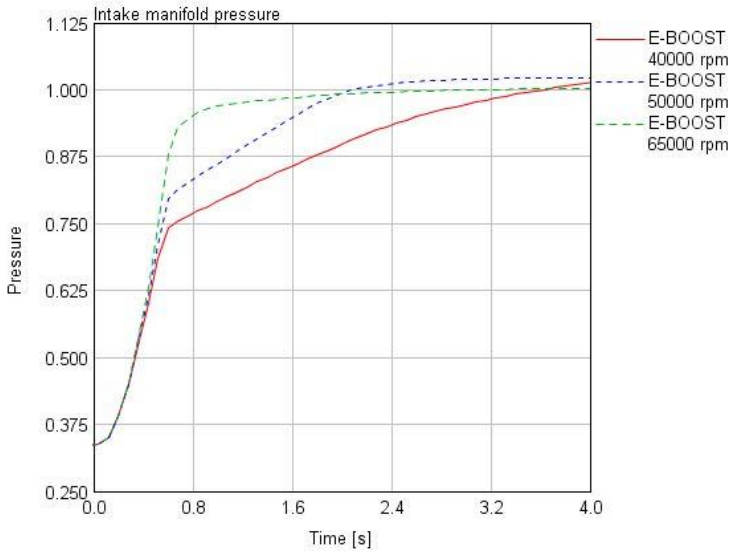

Figure 5-38: Normalized intake pressure during the transient at 1500 rpm depending on maximum e-boost speed

Engine load rise is driven by the intake pressure evolution, which shows indeed a similar behavior (Figure 5-38). The pressure rise is not influenced by the supercharger speed until $t = 0.5\ s$; as mentioned earlier, during this phase the opening of the throttle causes the intake manifold pressure to reach the value upstream of the throttle body almost instantaneously. After this phase, the increase in intake pressure is related to the pressure ratio provided by the two compressors and the fraction of the boost pressure related to the work of the turbocharger grows indeed from case 1 to case 3.

While the value reached by the intake pressure at the end of the simulation is very close in the three cases, the associated turbocharger speed indeed changes noticeably (Figure 5-39);

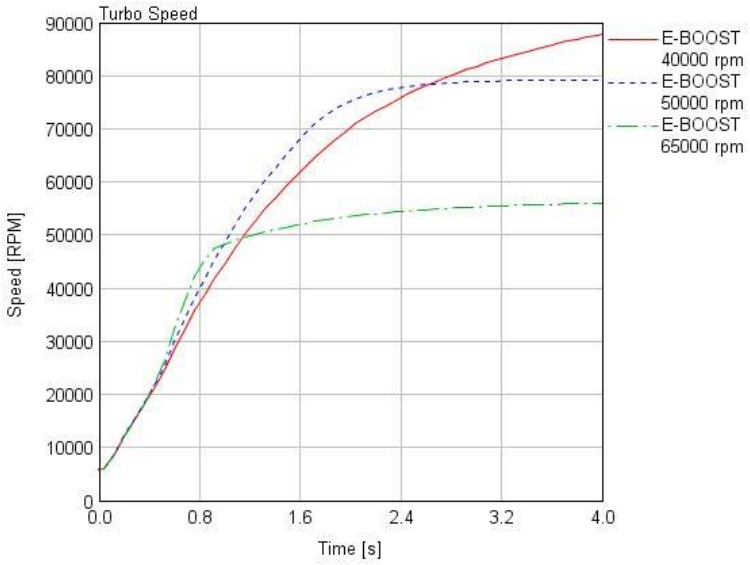

Figure 5-39: Turbocharger speed during the load transient at 1500 rpm depending on maximum e-boost speed

5.3.7 Remarks about electric power requirements

In chapter 3, the modelling of compressors in GT-SUITE by means of performance maps was explained. As far as the electric compressor is concerned, the model is able to calculate the power required to obtain the imposed speed profile. This is done by extrapolating the efficiency from the map and thus computing the enthalpy rise across the compressor. The power is obtained from Equation (3.11). The maximum required power for the three cases considered in paragraph 5.3.6 is reported in Table 5-9.

Case	E-boost max speed [rpm]	Max Power [kW]
1	65000	2.25
2	50000	1.07
3	40000	0.62

Table 5-9: Maximum electric compressor power depending on supercharger speed

Even if the model is not taking into account the efficiency of the electric motor which should drive the compressor, it is possible to compare the power requirements with the available energy storage solutions for automotive applications at least qualitatively.

Considering the configuration of the examined system, it must be noted that this power requirement is likely to be limited in time. Even though at low speed the maximum steady-state torque is obtainable only by activating the electric compressor, the latter is bypassed when the engine speed increases; in real applications the engine revolutions would indeed increase as the power is demanded by the user acting on the throttle pedal.

As already highlighted in the literature, ultracapacitors seem to be the most suitable alternative to batteries when short-term peak power is required. Ultracapacitors indeed feature a much higher power density than batteries. For UCs it goes up to 5 kW/kg for several manufacturers, while for batteries the highest values are shown by Li-ion batteries and they are not higher than 2 kW/kg [46]. As a consequence UCs would allow some extent of weight reduction when compared to any type of batteries.

Moreover, most types of batteries are quite sensitive to abuse such as deep discharges and, additionally, the cyclical behavior of batteries is quite poor in comparison to ultracapacitors. Batteries can only withstand a few thousand cycles and in the case of Li-Ion batteries their life is shortened by deep discharges, while an UC can withstand hundreds of thousands of cycles.

Furthermore, it must be noticed that in this work the energy to drive the electric compressor was assumed to be free energy, which in real application could be provided by some kind of regenerative system. Most automotive manufacturers have already developed prototypes that use UCs instead of batteries to store braking energy in order to improve driveline efficiency.

Finally, in order to simultaneously meet requirements of power density and energy density, UCs could be combined with batteries to achieve the maximum efficiency for the power system.

6 CONCLUSIONS AND RECOMMENDATIONS

6.1 Conclusions

This thesis has investigated the performance in both steady-state and transient conditions of a gasoline engine featuring an advanced boosting system: a conventional twin-scroll turbo is combined with an electrical supercharger, located upstream of the turbocharger compressor, in order to overcome some of the drivability issues usually associated with a downsized gasoline engine.

An engine model developed with the software GT-Power Version 7.4, by Gamma Technologies, was provided by FCA at the beginning of the project. Thanks to the calibration work done on the model before this project and to some further tweaking operated by the author, the results of the model show good agreement with the available experimental data, for all the mean engine values compared as a function of speed and load. As a consequence, the model can be used to consistently predict the engine performance, at least in the low speed range where it is validated.

The model has been used to estimate the improvement in maximum low-end torque obtainable thanks to the supercharger in steady-state conditions at different engine speeds:

1. The maximum improvement is obtained at very low engine speed; it is higher than 30% below 1500 rpm.
2. The supercharger contribution is null at speeds higher than 3000 rpm. The air flow rate is too high for the electric compressor to be effective and provide additional boost pressure.

Moreover, the model has been used to investigate the effect of the electric supercharger on transient performance of the engine. In order to do so, a load step at fixed engine speed (1500 rpm) has been simulated considering several possibilities for the control of the boosting system:

1. When the electric supercharger is not active, the transient response shows the typical delay of turbocharged engines referred as turbo-lag. The response time (time needed to reach 90% of the maximum BMEP) is higher than 2 seconds.
2. With the contribution of the electric supercharger the transient response is much faster. Even though the BMEP level reached is higher by about 30%, the response time is lower than 1 s: a reduction in response time of about 70% is obtained.
3. This response time is obtained even if about 10% EGR is introduced in the simulated condition. The response time is indeed even slightly shorter thanks to the more advanced spark timing allowed by the EGR.
4. If a small delay is introduced in the activation of the electric compressor with respect to the throttle opening, the same delay does not result in the response time. In particular, if the delay is 0.3 s the transient response is 0.13 s longer only. The supercharger can be then effective even in real world application, where it would not be possible to activate it in the exact same instant of the throttle valve opening.
5. The maximum supercharger speed, which is related to the available electrical power, has a strong impact on the transient performance of the engine. The maximum value for the speed allowed by the technical specifications of the compressor, 65000 rpm, gives the better transient performance. In this case, the load increases directly to its maximum value, as it would do in a naturally aspirated engine, and the response time is very short (as mentioned in the previous points). A slower speed for the compressor introduces a delay in the response: the load step looks like a turbocharged engine one. When 40000 rpm is the maximum speed the response time is higher than 2 seconds, thus no improvement in transient response is obtained with respect to the base engine.

6.2 Recommendations and future works

The considered engine is still in the research stage; bench testing has been carried out by FCA throughout the duration of this project and will be continued in the future. It is indeed common practice for several car makers to conduct in parallel engine testing and simulation in order to speed up the research and development phase.

In order to improve the model used in this project further testing would be beneficial, especially for simulations in transient conditions. In particular the combustion and heat transfer sub-models could require further tuning to closely reproduce the operating conditions occurring during the load step. With a proper validation of the model in transient conditions, it would possible to use it to quantitatively assess the effect of substantial modifications to the boosting system, such as the utilization of a different turbocharger or supercharger. Nevertheless, the model was validated in steady-state conditions both with and without the electric supercharger: thus the results obtained from the simulations should be regarded as valid for the considered conditions.

The obtained results could be used to select operating conditions to be tested for the considered engine and can be considered a useful tool aimed at the development of control strategies for the electric supercharger.

Furthermore, the results obtained in this work are limited to the performance of the engine alone. The natural continuation of this research would be the assessment of the performance of the considered engine when applied to a vehicle. In particular the following points should be addressed:

- The feasibility of the application of such an electric device to the vehicle. Even if the power requirements are limited and should be possible to address them considering the state of the art technologies, issues could be encountered in terms of energy storage solutions, packaging and cost.
- The performance of the engine in terms of fuel consumption and pollutant emissions should be analyzed and compared to that of similar engines. Only in this way it could be proved that the benefit usually associated with downsizing applies to this engine.

REFERENCES

[1] J. D. Miller and C. Façanha, "THE STATE OF CLEAN TRANSPORT POLICY - A 2014 SYNTHESIS OF VEHICLE AND FUEL POLICY DEVELOPMENTS," ICCT, 2014. [Online]. Available: http://www.theicct.org/state-of-clean-transport-policy-2014. [Accessed 17 04 2015].

[2] E. Kasseris and J. Heywood, "Comparative Analysis of Automotive Powertrain Choices for the Next 25 Years," *SAE Technical Paper 2007-01-1605,* 2007.

[3] "The Downsizing Agenda," 2014. [Online]. Available: http://turbo.honeywell.com/turbo-basics/the-downsizing-agenda/. [Accessed 20 04 2015].

[4] S. Shahed and K. Bauer, "Parametric Studies of the Impact of Turbocharging on Gasoline Engine Downsizing," *SAE Int. J. Engines,* vol. 2, no. 1, pp. 1347-1358, 2009.

[5] N. Ito, T. Ohta, R. Kono and S. Arikawa, "Development of a 4-Cylinder Gasoline Engine with a Variable Flow Turbo-charger," *SAE Technical Paper 2007-01-0263,* 2007.

[6] D. Han, S. Han, B. Han and W. Kim, "Development of 2.0L Turbocharged DISI Engine for Downsizing Application," *SAE Technical Paper 2007-01-0259,* 2007.

[7] F. Steinparzer, "The new BMW 2.0-l four-cylinder gasoline engine with turbocharger," *AutoTechnology,* pp. 44-51, June 2011.

[8] N. Merdes, C. Enderle, G. Vent and R. Weller, "The New Four-Cylinder Gasoline Engines From Mercedes-Benz," *MTZ worldwide,* vol. 72, pp. 16-23, 2011.

[9] N. Fraser, "Challenges for increased efficiency through gasoline engine downsizing," *SAE technical paper 2009-01-1053,* 2009.

[10] J. Turner, A. Popplewell, R. Patel and T. Johnson, "Ultra Boost for Economy: Extending the Limits of Extreme Engine Downsizing," *SAE Int. J. Engines,* vol. 7, no. 1, pp. 387-417, 2014.

[11] H. Kleeberg, D. Tomazic, O. Lang and K. Habermann, "Future Potential and Development Methods for High Output Turbocharged Direct Injected Gasoline Engines," *SAE Technical Paper 2006-01-0046,* 2006.

[12] R. Stone, Introduction to Internal Combustion Engines, SAE International, 2012.

[13] J. Heywood, Internal Combustion Engine Fundamentals, McGraw-Hill Education, 1988.

[14] "How a Turbo System Works," Garret, 2015. [Online]. Available: http://www.turbobygarrett.com/turbobygarrett/basic. [Accessed 25 04 2015].

[15] T. Uhlmann, D. Lückmann, R. Aymanns, J. Scharf, B. Höpke, M. Scassa, N. Schorn and H. Kindl, "Development and Matching of Double Entry Turbines for the Next Generation of Highly Boosted Gasoline Engines," in *Internationales Wiener Motorensymposium*, 2013.

[16] P. Pallotti, E. Torella, J. New, M. Criddle and J. Brown, "Application of an Electric Boosting System to a Small, Four-Cylinder S.I. Engine," *SAE Technical Paper 2003-32-0039,* 2003.

[17] P. Divekar, B. Ayalew and R. Prucka, "Coordinated Electric Supercharging and Turbo-Generation for a Diesel Engine," *SAE Technical Paper 2010-01-1228,* 2010.

[18] S. Birch, "Testing Audi's new e-booster reveals turbocharging's future," 04 08 2014. [Online]. Available: http://articles.sae.org/13421/. [Accessed 25 04 2015].

[19] B. An, H. Suzuki, M. Ebisu and H. Tanaka, "Development of two-stage turbocharger system with electric supercharger," *Proceedings of the FISITA 2012 World Automotive Congress,* pp. 147-155, 2013.

[20] J. King, D. Boggs, M. Heaney, J. Andersson, M. Keenan, N. Jackson and N. Owen, "HyBoost - An intelligently electrified optimized gasoline engine concept," in *Global Automotive Management Council - Emissions 2012, Papers - Proceedings*, Ypsilanti, 2012.

[21] S. Birch, "Volvo "triple boost" engine uses twin turbos plus e-compressor," 23 10 2014. [Online]. Available: http://articles.sae.org/13626/. [Accessed 20 04 2015].

[22] W. Hannibal, R. Flierl, L. Stiegler and R. Meyer, "Overview of current continuously variable valve lift systems for four-stroke spark-ignition engines and the criteria for their design ratings," *SAE Technical Paper 2004-01-1263,* 2004.

[23] A. Elrod and M. Nelson, "Development of a Variable Valve Timed Engine to Eliminate the Pumping Loses Associated with Throttled Operation," *SAE Technical Paper 860537,* 1986.

[24] M. Grohn and K. Wolf, "Variable Valve Timing in the new Mercedes-Benz Four-Valve Engines," *SAE Technical Paper 891990,* 1989.

[25] "Valvetronic.," 2015. [Online]. Available: http://www.bmw.com/com/en/insights/technology/technology_guide/articles/mm_valvetronic.html?source=index&article=mm_valvetronic. [Accessed 24 03 2015].

[26] F. Bozza, V. D. Bellis, A. Gimelli and M. Muccillo, "Strategies for Improving Fuel Consumption at Part-Load in a Downsized Turbocharged SI Engine: a Comparative Study," *SAE Technical Paper 2014-01-1064,* 2014.

[27] L. Tie, G. Yi, W. Jiasheng and C. Ziqian, "The Miller cycle effects on improvement of fuel economy in a highly boosted, high compression ratio, direct-injection gasoline engine: EIVC vs. LIVC," *Energy Conversion and Management,* pp. 59-65, March 2014.

[28] E. Galloni, "Analyses about parameters that affect cyclic variation in a spark ignition engine," *Appl Therm Eng,* vol. 29, pp. 1131-1137, 2009.

[29] D. Takaki, H. Tsuchida, T. Kobara, M. Akagi, T. Tsuyuki and M. Nagamine, "Study of an EGR System for Downsizing Turbocharged Gasoline Engine to Improve Fuel Economy," *SAE Technical Paper 2014-01-1199,* 2014.

[30] B. Grandin and H. Ångström, "Replacing Fuel Enrichment in a Turbo Charged SI Engine: Lean Burn or Cooled EGR," *SAE Technical Paper 1999-01-3505,* 1999.

[31] J. Miller, J. Taylor, P. Freeland and M. Warth, "Future Gasoline Engine Technology and the Effect on Thermal Management and Real World Fuel Consumption," *SAE Technical Paper 2013-01-0271,* 2013.

[32] Y. Kawabata, T. Sakonji and T. Amano, "The Effect of NOx on Knock in Spark-ignition Engines," *SAE Technical Paper 1999-01-0572,* 1999.

[33] M. Zheng, G. T. Reader and J. G. Hawley, "Diesel engine exhaust gas recirculation - A review on advanced and novel concepts," *Energy Conversion and Management,* vol. 45, no. 6, pp. 883-900, April 2004.

[34] A. Albrecht, O. Grondin, F. L. Berr and G. L. Solliec, "Towards a stronger

simulation support for engine control design: a methodological point of view," *Oil Gas Sci. Technol. 62,* vol. 4, pp. 437-456, 2007.

[35] A. Albrecht, G. Corde, V. Knop and B. H., "1D Simulation of Turbocharged Gasoline Direct Injection Engine for Transient Strategy Optimization," *SAE Technical Paper 2005-01-0693*, 2005.

[36] L. Zhong, M. Musial, W. Resh and K. Singh, "Application of Modeling Technology in a Turbocharged SI Engine," *SAE Technical Paper 2013-01-1621*, 2013.

[37] F. Millo, G. Di Lorenzo, E. Servetto and A. Capra, "Analysis of the Performance of a Turbocharged S.I. Engine under Transient Operating Conditions by Means of Fast Running Models," *SAE Int. J. Engines,* vol. 6, no. 2, 2013.

[38] A. Lefebvre and S. Guilain, "Modelling and Measurement of the Transient Response of a Turbocharged SI Engine," *SAE Technical Paper 2005-01-0691,* 2005.

[39] V. Bevilacqua and G. Grauli, "Potential of turbocharging in SI Engines: a 1D CFD based analysis," in *GT-Suite User Conference*, Frankfurt, 2009.

[40] A. Lefebvre and S. Guilain, "Transient Response of a Turbocharged SI Engine with an electrical boost pressure supply," *SAE Technical Paper 2003-01-1844*, 2003.

[41] E. Spessa, *Design of engine and control system, course material*, Torino: Politecnico di Torino, 2015.

[42] Gamma Technologies, *GT-Suite: Flow Theory Manual,* 2013.

[43] Gamma Technologies, *GT-Suite: Engine Performance Application Manual*, 2013.

[44] A. Douaud and P. Eyzat, "Four-Octane-Number Method for Predicting the Anti-Knock Behavior of Fuels and Engines," *SAE Technical Paper 780080,* 1978.

[45] Gamma Technologies, *GT-Suite Help Navigator Version 7.4*, 2013.

[46] G. Ren, G. Ma and N. Cong, "Review of electrical energy storage system for vehicular applications," *Renewable and Sustainable Energy Reviews,* no. 41, p. 225–236, 2015.

VITA AUCTORIS

NAME:	Ivan Filidoro
PLACE OF BIRTH:	Torino, Italy
YEAR OF BIRTH:	1992
EDUCATION:	Politecnico di Torino, B.Sc. in Automotive Engineering, Torino, Piemonte, Italy, 2010 – 2013. Politecnico di Torino, Master in Automotive Engineering, Torino, Piemonte, Italy, 2013 - 2015. University of Windsor, International M.A.Sc. in Mechanical Engineering, Windsor, ON, Canada, 2014 – 2015